Axon Guidance in Human Neurons and

Tuberous Sclerosis: Caveat mTOR

By
Timothy S. Catlett

A dissertation submitted in partial fulfillment of
the requirements for the degree of

Doctor of Philosophy
(Cellular and Molecular Biology)

at the
UNIVERSITY OF WISCONSIN-MADISON
2019

Date of final oral examination: 12/13/2019

The dissertation is approved by the following members of the Final Oral Committee:
Timothy Gomez, Professor, Neuroscience
William Bement, Professor, Integrative Biology
Erik Dent, Associate Professor, Neuroscience
David Gamm, Associate Professor, Ophthalmology and Visual Sciences
David Wassarman, Professor, Medical Genetics

Table of Contents

Acknowledgments

Graduate school is a unique challenge, and I could not and would not have completed the journey without these people. I cannot adequately thank them here and can only express my gratitude in clichés, nonetheless they follow in brief.

Thank you to my advisor and mentor, Timothy Gomez. You are the best supervisor I've had the pleasure of working with. Your enthusiasm is infectious, and I will try to emulate your unflappability, open door, and flexible, individualized mentorship style going forward. I'm very proud to consider you a friend.

Thank you to my committee, Bill Bement, Erik Dent, David Gamm, and David Wassarman, for your invaluable insight, support, and example.

Thank you to the Dent lab. Your lab makes us better in ways large and small, and I appreciate you. Thanks also to the other members of the Neurodevelopmental Group, especially the constancy, intelligence, and good humor of our neighbors Zhen Huang, Kate Kalil, and their labs.

I've had extraordinary fortune in lab colleagues during my time here. Miguel Santiago-Medina, Patrick Kerstein, and Robert Nichol IV deserve special mention. I joined the Gomez lab in large part due to my respect and admiration for you three and am lucky to know you as scientists and friends. Also special thanks to current lab mates Caitlin Warlick-Short and Sarah Rempel for your scientific insight and advice, wit, kindness, and friendship. Thank you also to numerous others who have contributed to our lab through the years.

Thank you to Alec McCann, my first undergraduate colleague. Mentoring you helped put me on track in my second and third years of graduate school, and I will always remember

what I owe you for that. Thank you to Massimo Onesto, my current undergraduate colleague, whose ship will sail much further than mine. I am excited to watch your career wherever it takes you and support you however I can.

Thanks to the Neuroscience department administrative staff for your support and to my graduate program CMB for the opportunity to research and study at UW-Madison. Thanks to Christina Hull and MBTG for support and advice.

Thanks to many friends in CMB, especially my cohort. The retreats, Friendsgivings, the Terrace, or to the Library and Rathskeller when the Wisconsin winter drove us indoors, kept me balanced. Ryan Kessens deserves special mention—when this is all over I'm going to play pool fourteen hours a day. Thanks to neighbors and friends in the UW Housing community for making our family feel like we belonged, especially to the Clos and Montemayor families.

Thanks to my friends and colleagues at MEB, WiSolve, and in the UW-Business school.

Thanks to my undergraduate research mentors at WSC, Barbara Hayford and Gustavo Zardeneta, and academic advisor Douglas Christensen. Without you all I would not have had the opportunity to do research nor the confidence to apply to graduate school.

Thanks to the many friends who visited over the past several years and reminded us of home, especially to Derek and Mike & Laurie, thank you.

Love and thanks to my family. Dad, Mom & Paul, Grandma C and Grandma M, Uncle Tim, Aunt Lisa, Tali & Nate and family, Aric & Jen and family, the Bryan & Joy Davidson family, uncles and aunts and cousins. Brother, thanks for watching the Badgers with me as they cheated us over and over again. We'll get them next year, 63-12.

Thank you to my children. Jack, Silas, and Benjamin - I love you. You can do anything you want to do, but you must work very hard with no excuses. Watching you grow in strength, intelligence, and empathy is my greatest joy.

Thank you to my wife, Rose. Day after day you put yourself last to “do the thing that needs to be done”, including a new career path to support us during our new adventure. The hardest things to do are those that have to be done every day, and are thus the easiest for others to take for granted. Your love and support made our time here one of joy and gratitude for our growing family. I love you and admire you. For whatever it may be worth, I dedicate this work to you.

Abstract

Animal models have served to answer many questions of axon guidance mechanisms *in vitro* and *in vivo*, and to provoke speculation as to their conservation in human development. Now, human induced pluripotent stem cell (iPS)-derived neurons allow us to further our understanding of axon guidance during normal human development and within a neurodevelopmental disease context. We utilized iPS and ES lines to differentiate human forebrain and motor neurons and show these cells respond to canonical guidance cues via growth promotion, inhibition, and guidance. Moreover, utilizing an iPS disease model of Tuberous Sclerosis Complex (TSC) with a mutation in TSC2, a key negative regulator of protein synthesis within growth cones, we show defects in axon outgrowth and guidance downstream of cues. Investigating these pathways, pharmacological mTOR inhibition failed to rescue these phenotypes, suggesting an mTOR-independent role for TSC2 in growth cone dynamics. Investigating these pathways further, we uncovered a role for TSC2-dependent cytoskeletal modulation of RhoA downstream of guidance cues. In addition, cytoplasmic HDAC6 inhibition rescued some mTOR-independent phenotypes, suggesting post-translational acetylation regulation as a potential mechanism of TSC2-dependent guidance.

Our results suggest that neural network connectivity defects in patients with TSC, an autism spectrum disorder, may result from defects in direct RhoA regulation of the cytoskeleton. Contra some animal model systems, local protein synthesis was not required for a collapse response to canonical guidance cues in human growth cones.

Our work shows *in vitro* axon guidance in a human model system and axon guidance deficits in an iPS-derived human disease model, and furthermore demonstrates that in

some respects human neurodevelopmental mechanisms may diverge from other model organisms, and thus we hope these studies will promote further investigation into these questions.

Chapter 1: Introduction to Guidance Pathways and Tuberous Sclerosis

Introduction

Axon guidance is the central developmental event of the nascent embryonic nervous system. Neuron-neuron and neuron-target connections allow for the rapid and efficient communication of the information required of the complex organism to survive in a complex environment[1]. Imaging advances have allowed a window into the intricate *in vivo* neural network, one that can appear at first glance random and chaotic[2,3]. Principles of axon guidance, yet poorly understood, are revealing that the trillions of synaptic interactions are in fact highly choreographed and subject to robust stereotypy: a stereotypy which when disturbed leads to abnormality and disease[4].

The study of axon guidance has benefited from a host of model organisms, each carrying with it unique benefits that have pushed the field forward remarkably over the past couple of decades[5]. However, the nature of animal models has left the field hampered in fully understanding human neurological disorder. Human stem cell technology carries the potential of bridging the gap between animal models and human patients with cognitive abnormalities such as the Autism Spectrum Disorders (ASD)[6,7]. With the advent of induced Pluripotent Stem Cells (iPSCs), these studies can even take place within the unique genetic milieu of the diseased individual.

To date, basic axon guidance mechanisms in human cells have not been well studied. This is curious, as previous research has shown often unexpected divergence in pathways between *Xenopus laevis*, chick, and mouse axon guidance pathways[8–10]. It is thus crucial to basic and translational research that canonical axon guidance pathways be determined specifically in human neurons.

The central character in axon guidance is the growth cone: a motile, highly dynamic amoeboid-like structure tipping the axon and leading its path to its synaptic destination. The growth cone senses its environment via filopodia and transduces multiple substrate-bound and soluble cues simultaneously via molecular cascades converging at the cytoskeleton and leading to extension or retraction, as well as attractive or repulsive turning[11]. These decisions take place within minutes of cue encounters and hundreds of microns from the axon soma[12]. While I largely focus upon axon guidance in the following pages, it is worth remembering that the growth cone has another, equally important function: laying down and structuring the microtubules and other components of the nascent axon, which will later serve to propagate action potentials in the mature neuron.

The cytoskeleton is the substrate of guidance

Axon guidance is the process of external signal convergence through the individual neuron's complement of effectors and onto the growth cone cytoskeleton to arrange and rearrange the actin and microtubule building blocks to provoke directed motility. The growth cone structure is divided into three zones; the peripheral, transitional, and central domains[12]. Globular actin monomers polymerize into helical, filamentous actin (F-actin) and branch extensively within the peripheral domain to form a dense meshwork that, to a first approximation, provides the raw substrate for force production and ultimately the directionality of growth cone movement[12]. Eliminating this meshwork does not prevent neurite outgrowth per se, but growing microtubules within an extending neurite are otherwise slow to extend and rudderless, unable to respond to cues in the absence of actin[13]. Continual turnover of the actin mesh provides the mechanism for directional movement via a combination of 1) actin polymerization through proteins such as the

formins and the branching-mediator Arp2/3, and 2) depolymerization by severing proteins such as cofilin towards the transitional zone. The actin motor protein non-muscle myosin II also provides force driving actin polymers backward towards the transitional zone[14,15]. This continuous movement of filaments, called ‘actin treadmilling’, is selectively coupled to substrate adhesions via integrins and adaptor proteins to push the polymerizing meshwork against the outer plasma membrane and promote forward motion[16]. Protrusive dynamics at the leading edge of the growth cone are thus the cumulative product of actin polymerization and depolymerization rates, adhesion dynamics, and myosin motor contractile activity, which together tightly coordinate the actin dynamics crucial to motility. Downstream of external signals, Rho GTPase regulation overlays this cytoskeletal network and contributes a mechanism for spatiotemporal control of growth cone dynamics[17].

Rho GTPases

The Rho GTPases are members of the Ras superfamily of small GTPases, and the best studied members are RHOA, RAC1, and CDC42. Classically referred to as “molecular switches”, Rho GTPase activation is regulated by GDP-GTP cycling[18]. The “on”, active conformation is bound to GTP, promoting conformational change in two switch regions - switch I and switch II - which expose an effector-binding domain. Rho GTPases exhibit intrinsic GTPase activity, and the “off” conformation is triggered via auto-hydrolysis of GTP to GDP, with a consequent conformational change in the switch regions and concealment of the effector protein binding site.

However, the intrinsic kinetics of this process are not favorable, and the Rho GTPase activation state is manipulated by a variety of upstream regulators[19]. Guanine nucleotide

exchange factors (GEFs) activate Rho GTPases by catalyzing the exchange of GDP for GTP, and GTPase activating proteins (GAPs) stimulate intrinsic GTPase activity to inactivate Rho GTPases. Many GEFs and GAPs have tunable affinities for multiple Rho GTPases partly based on post-translational modifications (PTMs)[20], complicating studies of their function. Rho GTPases are active only at the membrane via a C-terminal prenylation site, which provides proximity to regulatory GEFs, GAPs, and their effectors. Rho GDP disassociation inhibitors (RhoGDIs) also play a regulatory role by extracting Rho GTPases from the membrane and preventing the exchange of their bound guanine nucleotides[20]. Each of these act upon Rho GTPases to facilitate their activation or inactivation in localized areas of the cell at physiologically relevant time scales[21], and many studies have found a role for GEFs and GAPs in Rho GTPase regulation within growth cones to direct actin cytoskeletal dynamics in polarization, outgrowth, and guidance.

RHOA

Many of the pathways of the various Rho GTPases converge on similar effectors, and effects on the growth cone cytoskeleton can differ markedly depending upon which GEFs/GAPs and effectors are present. RHOA, associated with cell contractility, activates Rho-associated coiled-coil containing kinase (ROCK), which both phosphorylates myosin light chain kinase (MLCK) and inhibits myosin light chain phosphatase (MLCP) to activate the myosin light chain (MLC) of myosin-2 and contract the actin cytoskeleton[22]. Myosin-2 forms a hexamer via pairs of its three subunits, an essential light chain, regulatory light chain, and heavy chain. Each essential and regulatory light chain combines to form a globular head which both binds actin and contains an ATPase motor domain. The globular

head connects to the heavy chain, which itself forms a coiled-coil with the heavy chain from another trimeric subunit. Myosin-2 is then a heterohexameric protein complex, and residues within the regulatory chain are phosphorylated, thought to release the native autoinhibitory binding of the heavy chain to the light chain and facilitate the latter's interaction with another myosin-2 heavy chain in opposition. Thus myosin-based contractility involves binding of multiple actin filaments at its opposing globular domains and acting upon them in an anti-parallel fashion. RHOA activation is strongly correlated with decreased extension and collapse in growth cone transduction pathways downstream of guidance cues. A Rho GEF Ephexin -> RHOA -> ROCK -> MLCK -> myosin-2 cascade contracts the actin cytoskeleton to effect collapse and turning in response to the repulsive guidance cue ephrin, detailed below[17,23]. However, cell-type specific alternative pathways can predominate depending upon the effectors present and degree of pathway activation. For example, downstream of low concentrations of SDF-1, RHOA activates mDia to promote linear actin polymerization[24]. It has been proposed that RHOA-dependent linear actin polymerization downstream of cues provides a substrate for myosin-2 based contractility and collapse, even as RAC1 activity decreases and branched actin dissipates.

RAC1

RAC1 is associated with both an increase in polymerization of lamellipodial actin and cue-dependent endocytosis. Work in the McLoon lab showed in a chick retinal model that RAC1 was transiently downregulated in response to ephrin-A2 and semaphorin 3A, concurrent with increasing RhoA activity, and then returned to basal levels in a manner which correlated with an increase in endocytosis[25]. Blocking RAC1 activity did not alter

actin depolymerization downstream of ephrins but blocked the enhanced endocytosis and collapse. Michael Greenberg's group examined the GEFs involved in RAC1 response, showing ephrin-collapse resistance and guidance defects in a GEF Vav2 knockout model[26]. Other studies show RAC1 actin polymerization activity antagonizing macropinocytosis[27], possibly by either keeping endocytic maturation machinery from the plasma membrane, or via the properties of polymerizing actin meshwork at the cortex. These studies may suggest cell type and condition dependence in the relationship between RAC1 and actin polymerization and endocytosis.

Growth cone collapse

Growth cone collapse is generally characterized by four interconnected events: 1) depolymerization of the cortical actin meshwork at the peripheral zone with accompanying loss of lamellipodia and most filopodia, 2) increased myosin-based contractility, 3) increased endocytosis or macropinocytosis, and 4) loss of adhesion to the underlying substrate[12]. Thus, collapse can be viewed as a coordinated event downstream of inhibitory cues and with many molecular players. While all of these processes are associated with collapse events, researchers have also observed growth cone collapse in the absence of one or more of these conditions[28,29]. Collapse is difficult to measure *in vivo* and is considered in some situations to be an *in vitro* artifact. For example, *in vivo* cues may provide directional information to the growth cone which lead to highly localized responses on the side of the growth cone receiving the cue, such that actin depolymerization and endocytosis on the cue side of the structure leads to a repulsive turning. This may differ qualitatively from the total collapse seen in bath applications in our studies and others. Similarly, bath applications may reflect a more concentrated dose

than is seen *in vivo*, which again may saturate the signal transduction system and lead to a more robust response than is necessary in the developing organism. To avoid this, researchers often use “turning” or “puffing assays” to apply acute directional cues to individual growth cones, which often results in turning behaviors toward or away from attractive or repulsive cues, respectively[30]. So while *in vivo* growth cone collapse has also been reported[31], it is thought that generally *in vivo* repulsive substrates or cue concentrations will provoke sufficient repulsive response without fully collapsing the structure. Regardless, *in vitro* collapse and guidance assays are sensitive, reliable, and corroborated by *in vivo* axon tract studies.

Local protein synthesis

The paradigm-shifting development in the understanding of molecular mechanisms of axon guidance in the past twenty years was the discovery of protein synthesis localized at the growth cone[8]. By regulating mRNA at the translational level, the growth cone can rapidly synthesize the proteins needed for navigation decisions without a retrograde signal to the distant nucleus and anterograde transport of protein all the way to the growth cone, providing an additional mechanism for precise spatial and temporal control of response to cues. Recently, next-generation RNA sequencing techniques have enabled researchers to distinguish these unique mRNA populations within neurons of differing subtype and age[32]. Studies have shown that some signaling molecules require local protein synthesis in order to stimulate an appropriate cue response[33] for turning behavior and neuronal survival. Reciprocally, degradation also plays a crucial regulatory role[34].

As illustrated in Figure 1, the mammalian Target of Rapamycin (mTOR) pathway is one such hub of protein synthesis at the growth cone[35], and has been linked to guidance in

response to multiple cues in animal models[36–38]. Downstream of ligand-receptor complexes promoting extension or retraction are MAPKs including ERK1/2 and the p38 MAPK families, long known as regulators of cell motility, translation, and stress responses. PI3K-Akt signaling and AMPK are also key regulators of mTOR signaling. Activation of the serine/threonine kinase mTOR Complex 1 (mTORC1) is associated with phosphorylating activation of key translation initiators leading to on-site translation. TSC1/2 is a negative regulator of mTORC1 through the GTPase-activating domain of TSC2. This enzyme inactivates the Ras family GTPase Rheb. Rheb-GTP activates mTORC1[39]. TSC is thus an important protein complex through which several intracellular guidance cascades must travel in order to fully activate or inactivate the mTOR pathway.

Tuberous Sclerosis

Tuberous Sclerosis is an autosomal dominant disorder classically characterized by hamartomas in multiple organ systems; the most commonly affected include the brain, skin, heart, lungs, and kidneys[40]. Affecting 1:6000 live births in the United States, individuals with TSC are commonly afflicted with epilepsy (80%), and mental retardation and/or Autism Spectrum Disorder (ASD) in approximately half of cases[41]. The disease is caused by loss of function mutations in either TSC1 (hamartin) or TSC2 (tuberin). Impairment of these proteins leads to overactive mTOR signaling and excessive protein synthesis and cell growth[42]. While other functions are being explored, mTOR regulation is the canonical role of the TSC proteins.

In the TSC brain, hamartomas manifest in adults as sclerotic gyri, and developmentally are combinations of dysplastic neurons and glia which calcify over time[40]. Subependymal nodules (SEN) at the border of the ventricular zone are also common in TSC[43]. SENs

occasionally continue their growth into subependymal giant astrocytomas (SEGA, in upwards of 20% of cases)[43], which may occlude the flow of cerebrospinal fluid through the ventricles. TSC neurological symptoms are highly variable and together were classically attributed to these focal malformations, but recent evidence from various angles indicates a more complicated etiology as detailed below.

Structure-function:

The Tuberous Sclerosis proteins are tumor suppressors comprised of a heterotrimeric complex of TSC1, TSC2, and the comparatively recently discovered TBC1D7[44]. TSC2 is an 1807 amino acid sequence encoding a 198kD protein. Showing little overall homology to other proteins, TSC2 carries a GTPase-activating protein (GAP) domain near its C-terminus which was shown in early studies to exhibit some activity towards Rab5[45] and Rap1[46] *in vitro*, but has since been shown to specifically activate the GTPase activity of the small G-protein Rheb upstream of mTOR[42]. TSC2 also bears a nuclear localization signal near the carboxyl terminus, a leucine zipper, and multiple HEAT domains, indicating a potential role for transcriptional regulation[47]. TSC2 binds TSC1 at the former's N-terminus[48,49]. Occupying a 40kB stretch of gDNA, several TSC2 splice variants have been detected but are yet understudied and poorly understood[50,51].

TSC1 is a 1163 amino acid sequence encoding a 130 kD protein and like TSC2 shares little homology with other proteins. TSC1 binds TSC2 between aa 302-430[52]. TSC1 exhibits no enzymatic activity on its own but serves to stabilize TSC2; in the absence of TSC1, TSC2 is preferentially ubiquitinated and degraded, impairing mTOR regulation[42,53]. While individual phenotypes are highly variable, TSC1 mutations are associated with less severe outcomes[41]. TSC1 also exhibits both a putative RhoA binding domain overlapping

the TSC2 binding domain, an Ezrin-Radixin-Moesin (ERM) binding domain at aa 881-1084[54], and a predicted coiled-coil sequence at aa 719-998[55].

TBC1D7 is also reported to bind and further stabilize the TSC complex and contribute to its function, but the contribution of this third partner is yet being explored[44]. Dysfunction in the protein has been linked to macrocephalies/megalencephalies, although mutations in the TBC protein have not yet been causally linked to Tuberous Sclerosis[56].

TSC patients exhibit missense mutations concentrating in the TSC2 GAP domain and TSC1-TSC2 binding domains, although others have been reported[41]. TSC1 deleterious mutations are generally nonsense in origin, although there are a few missense mutation clusters elsewhere[41], and TSC disease-causing mutations in TBC1D7 have yet to be identified[56].

mTOR pathway and upstream pi3k, mapk, gsk3, ampk

A functional mechanistic Target of Rapamycin complex (mTORC) is composed of the mTOR serine/threonine kinase core and associated proteins forming one of two complexes, known as mTORC1 and mTORC2[57]. mTORC1, the better studied of the two complexes, is defined by associated Raptor and LST8. Downstream of mTORC1 are two directly phosphorylated branches: S6K1 and S6K2, and 4E-BP1 and 4E-BP2 (eukaryotic translation initiation factor 4E-binding proteins). Phosphorylated S6K itself phosphorylates and activates translation activators ribosomal protein S6 and eIF4B to stimulate protein synthesis. Active 4E-BP resides in an inhibitory complex with eIF4E at the mRNA 5’ cap, and mTOR-dependent phosphorylation of the binding protein facilitates its release from eIF4E and is necessary for initiation of translation of 5’ TOP mRNAs. As the name indicates, mTOR gets its name from its susceptibility to the protein synthesis-

suppressing effects of rapamycin, a compound originally discovered during a scientific expedition to the island of Rapa Nui in 1964[58]. Rapamycin binds FK506 binding protein 12 (FKBP12), forming a complex that allosterically inhibits mTOR[59]. Rapamycin inhibits protein translation downstream of mTORC1 acutely, a tool which has greatly facilitated understanding of the mTOR protein's function in cells.

TSC proteins function by activating the intrinsically unfavorable GTPase activity of Rheb, stimulating conversion of GTP to GDP[42,53]. A corresponding guanine nucleotide exchange factor (GEF) for Rheb is speculated but not yet identified, and while Rheb-mTOR activation is well attested, its mechanism of action is an active area of research[60].

In its role as a protein synthesis positive regulator, and given the energetic cost of new protein synthesis, mTOR is a major nexus of a variety of cell signaling pathways. Cellular decision-making for growth must integrate information about nutrient availability, external growth factor stimuli, stress pathways, and energy levels. Thus it is unsurprising that mTOR signaling is critical for key developmental milestones within the growing brain, including cell fate specification, proliferation, migration, axon guidance, synaptogenesis, and synaptic maintenance[61,62].

What has also become clear from many investigations is the central role of the TSC proteins in integrating disparate cellular signals to permit or obstruct mTOR activity. Kinase-mediated cell signaling converges upon TSC2 protein downstream of PI3K-Akt and MAPK-Erk signaling, and multiple specific inhibitory TSC2 phosphorylation sites downstream of Akt and Erk have been identified, in addition to activating sites downstream of GSK-3β and AMPK[63,64]. Phosphorylation does not appear to meaningfully impact TSC2 *in vitro* GAP activity towards Rheb, although this has been disputed in some

earlier studies[65]. While some research has suggested modulation of TSC1-TSC2 binding as a mechanism of mTOR regulation, currently it is thought that in some cases TSC2 phosphorylations instead regulate its localization within the cell. Evidence from the Manning and Sabatini labs suggest a model in which mTOR activity is dependent upon its activation at the lysosome[66,67]. Addition or subtraction of amino acids or growth factors to serum starved HEK293T or MEFs could alter the localization of mTOR and TSC2. In this model, unfavorable cell growth conditions lead to TSC2 phosphorylation and disengagement from the lysosome, and cytosolic TSC2 is unable to trigger Rheb GTPase activity. Idiosyncrasies of the cell types utilized and the serum state of the system are important caveats to consider in evaluating these studies, as shown in Averous and colleagues 2014[68]. In addition, TSC1 phosphorylation sites are also reported, but their possible roles in signaling have not been deeply investigated[69,70].

mTORC2 is composed of mTOR, Rictor, SIN1, Protor, and LST8[57]. mTORC2 phosphorylates Akt at residue T427, and this phosphorylation site has been used as a readout for its relative activity level[71]. Otherwise, few definitive outputs for mTORC2 have been identified, but Protein Kinase Cα and Rho GTPases upstream of the actin cytoskeleton are reported downstream targets[72,73]. The acute resistance of mTORC2 to rapamycin is partially responsible for the lag in understanding, although some reports have suggested that chronic rapamycin treatment may inhibit mTORC2 by sequestering mTOR and preventing complex assembly[74]. Rictor is an obligate cofactor of mTORC2, and neurological abnormalities were reported in a rictor mutant mouse model[75], but there are no rigorous mechanistic studies of mTORC2 function in developing neurons. The question of TSC regulation on mTORC2 has been reported but is yet controversial, as

multiple groups report both mTORC1-dependent and independent functions of this signaling pathway[76,77]. Crosstalk between the mTOR complexes, cell-type dependent interactions, and the extensive feedback mechanisms within the mTOR pathway likely explain these discrepancies.

Observation of hamartoma formation in Tuberous Sclerosis was the original example in the formation of Knudson's influential Two-Hit Hypothesis[78]. According to Knudson, heterozygous mutation in a tumor suppressor was insufficient to cause formation of the hamartoma. However, sporadic mutations in the second allele, more likely in a heterozygous background, could trigger the tumor. DNA sequencing of TSC-associated pulmonary cysts (lymphangioleiomyomatosis, LAM) and renal angiomyolipomas have confirmed Knudson's hypothesis via some "second-hit" mutated cells, and likely also cell non-autonomous effects on nearby heterozygous cells[79]. These lesions exhibiting enhanced mTOR signaling are often responsive to treatment with rapamycin or its derivatives, rapalogs. Interestingly, cortical tuber etiology is less tractable to the Two-Hit Hypothesis, as these cells often do not exhibit mutations in the second allele[80]. There are several potential explanations for this. One possibility is other mutations in the mTOR pathway that were not identified in the tuber model, although it is unclear why this would apply to cells within the brain and not commonly elsewhere. Alternatively, sequencing may not yet be sensitive enough to detect TSC mutations in only a single cell or a few cells which had unusually large non-cell autonomous effects. mTOR signaling and apoptotic mechanisms are closely aligned, and second-hit mutations may have led to increased likelihood of cell death in a null cell at an earlier developmental stage. Finally,

other yet unknown mechanisms may contribute to tuber occurrence in a TSC heterozygous background.

While TSC proteins have been well studied since their discovery and linking to mTOR signaling, much is yet unknown about their function and studying their putative roles is challenging. Direct binding of either TSC1 or TSC2, or both, has been reported for over fifty proteins[52]. As noted above, the lack of homology to other proteins provides little insight via domain comparisons. In addition, because TSC1/2 are negative regulators of mTOR-dependent protein synthesis, eliminating both copies of either TSC1 or TSC2 is sufficient to markedly dysregulate protein synthesis levels of a substantial portion of the proteome. Transcriptional regulation is also markedly aberrant in TSC2 knockout neurons[81], while haploinsufficiency in TSC reveals much milder proteomic changes and few if any transcriptional changes. Because of the dysregulation of large numbers of functional proteins within the cell in the knockout models, the few studies examining non-canonical TSC1 or TSC2 functions are difficult to parse from their role in mTOR regulation. Even so, a few groups have examined the interactions between TSC and Rho GTPases, in both an mTOR-dependent and independent manner. Alan Hall's group first reported a role for TSC1-mediated RhoA activation, showing that TSC1 immunoprecipitated with Ezrin-Radixin-Moesin (ERM) proteins, and TSC1 transfection increased RhoA activity with focal adhesion and stress fiber formation in a HUVEC line[54]. Hall's group also showed that TSC1 knockdown abrogated cytoskeletal rearrangements in response to lysophosphatidic acid (LPA), a known potent RhoA activator. Hall's study also found increased activation of the adhesion protein FAK upon TSC2 transfection, but only in the epithelial cells. Another group found a complex with Ezrin, TSC1, and the Rho

GEF Dbl were necessary for the latter's activation of Rho GTPases downstream of LPA[82]. Elizabeth Henske's group used TSC2$^{-/-}$ uterine leiomyoma cell lines (ELT3) derived from the Eker rat, which harbors a germline TSC2 mutation, and MLCK epithelial cells to examine TSC2's role in Rho activation[83]. Henske's group also found increased RhoA activity and migration dysfunction in both epithelial cell stable TSC2 overexpression and in ELT3 TSC2 re-expression. Finally, Vera Krymskaya's lab has published multiple studies on TSC1-TSC2 and Rho GTPases, and showed results opposite that of Henske's group[84,85]. Focusing on transient expression, Krymskaya's studies have found TSC1 alone promotes RhoA activity at the expense of Rac1, while transfection of the TSC1-binding domain of TSC2 was sufficient to block this Rac1 inactivation and downregulate RhoA activity. This group also conducted experiments in the presence of rapamycin and with TSC2 GAP-dead mutants, concluding that actin rearrangement was independent of mTOR activation.

From a clinical standpoint, heterozygous TSC animal model phenotypes which are tractable via rapamycin are a non-issue, but isolating mTOR-independent functions in rapamycin-resistant phenotypes is challenging. This challenge is to be embraced, because TSC patients with neurological abnormalities generally carry heterozygous mutations in the vast majority of their brain cells and stand to benefit from a more complete understanding of TSC function and dysfunction within a heterozygous background.

TSC and axon guidance

Is TSC an axon guidance disease? Multiple lines of evidence suggest connectivity abnormalities, which may be due in part to defects attributable to this aspect of

neurodevelopment. Diffusion tensor imaging (DTI) studies are a form of MRI which measure the free diffusion properties of polar water molecules within cells to visualize the axon tracts within the brain, which is possible due to the tract's unique morphology relative to other brain structures. DTI abnormalities have been documented in people with a variety of cognitive deficits, including Autism Spectrum Disorders[86]. Indeed, several studies in human TSC patients show varying defects in white matter diffusivity relative to controls. TSC with associated autism shows marked decreases in fractional anisotropy (FA), a measurement of directional diffusivity of the tract[87–89]. DTI can only resolve the grossest of axon tracts as present at the corpus collosum, and defects can arise from a variety of mechanisms, including enhanced cell death of neurons or supporting cells, neural proliferation defects, or inappropriate de-myelination of the tracts. Thus while significant guidance defects are likely to be detectable via DTI, defects do not by themselves conclusively determine underlying axon guidance defects. Furthermore, brain imaging studies often show a high degree of variation between patients. For example, a DTI study of individuals with ASD showed decreases in axon tract robustness relative to healthy controls, but within the ASD group there were marked differences in which specific tracts and brain areas were affected[90]. Conclusions from pooled DTI samples should thus be interpreted with caution, but corroborate the hypothesis that axon tract defects are present in TSC patients.

As noted above, TSC phenotypes were classically attributed to cortical tubers[40]. These abnormalities appear randomly in the gyri of the cerebral cortex, and a robust literature has explored the relationship between tubers and epileptic foci[39]. While the tubers themselves are electrically silent, the normal-appearing peritubular tissue is commonly—

though not always—associated with foci. Excision of these peritubular areas has met with some success in treating intractable epilepsy[91]. Epilepsy is perhaps the most debilitating comorbidity of TSC, and neurological outcomes in TSC patients are strongly correlated with seizure control. Certainly tubers play a role in TSC pathology, but evidence suggests that other mechanisms likely play a role in the disease. For example, multiple studies have pointed out a poor correlation between tuber load and some neurocognitive pathologies[39]. In multiple studies, TSC patients showed significant axon tract abnormalities in otherwise grossly normal tissue relative to healthy controls[87], and work in rodent models has shown substantial behavioral and cognitive abnormalities despite the general absence of epilepsy phenotypes and tubers[92,93]. Rarely, TSC patients with neurocognitive deficits do not exhibit tubers[94].

Most compelling, a few groups have examined axon guidance within TSC animal models. Eye-specific TSC1 loss in rodent retinal progenitors resulted in extensive impairment of eye development, including increased apoptosis and aberrant projections of retinal ganglion neurons[95]. Scott Selleck's group also found guidance errors in a TSC1 Drosophila model of photoreceptor development[96]. While knockout models are useful, heterozygous TSC models are likely most relevant to axon guidance due to the rarity of second-hit mutations, although as noted above, non-cell autonomous effects may magnify the effects of the latter. Accordingly, the Mustafa Sahin group studied the disease in a heterozygous mouse model and found aberrant targeting of retinal ganglion cells to the brain and a reduced ability of cultured axons to respond to ephrin-A stimulation[37]. The Sahin group proposed a model in which mTOR suppression via TSC downstream of ERK downregulation may be required for guidance in response to ephrin-A, and heterozygous

loss of TSC may be sufficient to impair its suppression ability and lead to guidance failures. The *in vitro* phenotype was mimicked by Rheb transfection, although rescue via mTOR inhibition was not shown.

Multiple studies also show varying effects of TSC loss on neuronal outgrowth and polarity more generally, suggesting an important role for the TSC proteins in axonal dynamics[97,98]. Animal models and other organism-based evidence provide compelling evidence for TSC-dependent neurodevelopmental defects. As noted above, the factors that contribute to neuronal connectivity are myriad; because of the many steps leading to functional networks and the conserved molecular players guiding these various processes, it is not trivial to deconstruct the pathways contributing specifically to neurodevelopmental events such as axon guidance. iPS technology provides an opportunity for this deconstruction via several virtues: allowing for 1) the generation of large numbers of 2) fate-specific individual neurons with 3) patient-specific genotypes and amenable to examination at 4) the developmental time point in question. In the following pages, I used ES and iPS cells from healthy control lines and a patient with Tuberous Sclerosis to both establish a human stem cell model of axon guidance, which can be used to study human-specific basic mechanisms, and also to examine the role of TSC2 in axon guidance.

References

1. Kolodkin, A. L. & Tessier-lavigne, M. Mechanisms and Molecules of Neuronal Wiring : A Primer. 1–14 (2011).

2. Wilt, B. A. *et al.* Advances in Light Microscopy for Neuroscience. *Annu. Rev. Neurosci.* **32**, 435–506 (2009).

3. Fornasiero, E. F. & Opazo, F. Super-resolution imaging for cell biologists: Concepts, applications, current challenges and developments Prospects & Overviews E. F. Fornasiero and F. Opazo. *BioEssays* **37**, 436–451 (2015).

4. Battum, E. Y. Van, Brignani, S. & Pasterkamp, R. J. Axon guidance proteins in neurological disorders. *Lancet Glob. Heal.* **4422**, (2015).

5. Dudanova, I. Integration of guidance cues : parallel signaling and crosstalk. **36**, 295–304 (2013).

6. Bakos, J., Bacova, Z., Grant, S. G., Castejon, A. M. & Ostatnikova, D. Are Molecules Involved in Neuritogenesis and Axon Guidance Related to Autism Pathogenesis? *NeuroMolecular Med.* **17**, 297–304 (2015).

7. Sterneckert, J. L., Reinhardt, P. & Schöler, H. R. Investigating human disease using stem cell models. *Nature Reviews Genetics* **15**, 625–639 (2014).

8. Campbell, D. S. & Holt, C. E. Chemotropic responses of retinal growth cones mediated by rapid local protein synthesis and degradation. *Neuron* **32**, 1013–1026 (2001).

9. Roche, F. K., Marsick, B. M. & Letourneau, P. C. Protein Synthesis in Distal Axons Is Not Required for Growth Cone Responses to Guidance Cues. *J. Neurosci.* **29**, 638–652 (2009).

10. Luo, Y., Raible, D. & Raper, J. A. Collapsin: A protein in brain that induces the collapse and paralysis of neuronal growth cones. *Cell* **75**, 217–227 (1993).

11. Dent, E. W. *et al.* The Growth Cone Cytoskeleton in Axon. (2011). doi:10.1101/cshperspect.a001800

12. Lowery, L. A. & Vactor, D. Van. The trip of the tip : understanding the growth cone machinery. **10**, (2009).

13. Marsh, L. & Letourneau, P. C. Growth of neurites without filopodial or lamellipodial activity in the presence of cytochalasin B. *J. Cell Biol.* **99**, 2041–2047 (1984).

14. Lin, C. H. & Forscher, P. Growth cone advance is inversely proportional to retrograde F-actin flow. *Neuron* **14**, 763–771 (1995).

15. Lin, C. H., Espreafico, E. M., Mooseker, M. S. & Forscher, P. Myosin drives retrograde F-actin flow in neuronal growth cones. *Neuron* **16**, 769–782 (1996).

16. Gomez, T. M. & Letourneau, P. C. Actin dynamics in growth cone motility and navigation. *Journal of Neurochemistry* **129**, 221–234 (2014).

17. Hall, A. & Lalli, G. Rho and Ras GTPases in axon growth, guidance, and branching. *Cold Spring Harb. Perspect. Biol.* **2**, a001818 (2010).

18. Bishop, A. L. & Hall, A. Rho GTPases and their effector proteins. *Biochemical Journal* **348**, 241–255 (2000).

19. Hennig, A., Markwart, R., Esparza-Franco, M. A., Ladds, G. & Rubio, I. Ras activation revisited: Role of GEF and GAP systems. *Biological Chemistry* **396**, 831–848 (2015).

20. Hodge, R. G. & Ridley, A. J. Regulating Rho GTPases and their regulators. *Nature Reviews Molecular Cell Biology* **17**, 496–510 (2016).

21. Pertz, O. & Fritz, R. D. The dynamics of spatio-temporal Rho GTPase signaling: Formation of signaling patterns. *F1000Research* **5**, (2016).

22. Amano, M., Nakayama, M. & Kaibuchi, K. Rho-kinase/ROCK: A key regulator of the cytoskeleton and cell polarity. *Cytoskeleton* **67**, 545–554 (2010).

23. Wahl, S., Barth, H., Ciossek, T., Aktories, K. & Mueller, B. K. Ephrin-A5 Induces Collapse of Growth Cones by Activating Rho and Rho Kinase. **149**, 263–270 (2000).

24. Arakawa, Y. *et al.* Control of axon elongation via an SDF-1α/Rho/mDia pathway in cultured cerebellar granule neurons. *J. Cell Biol.* **161**, 381–391 (2003).

25. Jurney, W. M., Gallo, G., Letourneau, P. C. & McLoon, S. C. Rac1-mediated endocytosis during Ephrin-A2- and semaphorin 3A-induced growth cone collapse. *J. Neurosci.* **22**, 6019–6028 (2002).

26. Cowan, C. W. *et al.* Vav family GEFs link activated Ephs to endocytosis and axon guidance. *Neuron* **46**, 205–217 (2005).

27. Fujii, M., Kawai, K., Egami, Y. & Araki, N. Dissecting the roles of Rac1 activation and deactivation in macropinocytosis using microscopic photo-manipulation. *Sci. Rep.* **3**, (2013).

28. Zhou, F. Q. & Cohan, C. S. Growth cone collapse through coincident loss of actin bundles and leading edge actin without actin depolymerization. *J. Cell Biol.* **153**, 1071–1083 (2001).

29. Bashaw, G. J., Hu, H., Nobes, C. D. & Goodman, C. S. A novel Dbl family

RhoGEF promotes Rho-dependent axon attraction to the central nervous system midline in Drosophila and overcomes Robo repulsion. *J. Cell Biol.* **155**, 1117–1122 (2001).

30. Murray, A. J., Peace, A. G., Tucker, S. J. & Shewan, D. A. Mammalian growth cone turning assays identify distinct cell signalling mechanisms that underlie axon growth, guidance and regeneration. *Methods Mol. Biol.* **846**, 167–178 (2012).

31. Knobel, K. M., Jorgensen, E. M. & Bastiani, M. J. Growth cones stall and collapse during axon outgrowth in Caenorhabditis elegans. *Development* **126**, 4489-4498 (1999).

32. Kar, A. N., Lee, S. J. & Twiss, J. L. Expanding Axonal Transcriptome Brings New Functions for Axonally Synthesized Proteins in Health and Disease. *Neurosci.* **24**, 111–129 (2018).

33. Holt, C. E. & Schuman, E. M. The central dogma decentralized: New perspectives on RNA function and local translation in neurons. *Neuron* **80**, 648–657 (2013).

34. Deglincerti, A. *et al.* Coupled local translation and degradation regulate growth cone collapse. *Nat. Commun.* **6**, 1–12 (2015).

35. Laplante, M. & Sabatini, D. M. MTOR signaling in growth control and disease. *Cell* **149**, 274–293 (2012).

36. Piper, M. *et al.* Signaling mechanisms underlying Slit2-induced collapse of Xenopus retinal growth cones. *Neuron* **49**, 215–228 (2006).

37. Nie, D. *et al.* Tsc2-Rheb signaling regulates EphA-mediated axon guidance. *Nat. Neurosci.* **13**, 163–172 (2010).

38. Wu, K. Y. *et al.* Local translation of RhoA regulates growth cone collapse. *Nature* **436**, 1020–1024 (2005).

39. Han, J. M. & Sahin, M. TSC1/TSC2 signaling in the CNS. *FEBS Letters* **585**, 973–980 (2011).

40. Gomez, M. R., Sampson, J. & Whittemore, V. *Tuberous Sclerosis Complex*. (Oxford University Press, 1999).

41. Van Eeghen, A. M., Black, M. E., Pulsifer, M. B., Kwiatkowski, D. J. & Thiele, E. A. Genotype and cognitive phenotype of patients with tuberous sclerosis complex. *Eur. J. Hum. Genet.* **20**, 510–515 (2012).

42. Inoki, K., Li, Y., Xu, T. & Guan, K. L. Rheb GTpase is a direct target of TSC2 GAP activity and regulates mTOR signaling. *Genes Dev.* **17**, 1829–1834 (2003).

43. Grajkowska, W., Kotulska, K., Jurkiewicz, E. & Matyja, E. Brain lesions in

tuberous sclerosis complex. Review. *Folia Neuropathologica* **48**, 139–149 (2010).

44. Dibble, C. C. *et al.* TBC1D7 Is a Third Subunit of the TSC1-TSC2 Complex Upstream of mTORC1. *Mol. Cell* **47**, 535–546 (2012).

45. Xiao, G. H., Shoarinejad, F., Jin, F., Golemis, E. A. & Yeung, R. S. The tuberous sclerosis 2 gene product, tuberin, functions as a Rab5 GTPase activating protein (GAP) in modulating endocytosis. *J. Biol. Chem.* **272**, 6097–6100 (1997).

46. Wienecke, R., König, A. & DeClue, J. E. Identification of tuberin, the tuberous sclerosis-2 product: Tuberin possesses specific Rap1GAP activity. *J. Biol. Chem.* **270**, 16409–16414 (1995).

47. Lou, D., Griffith, N. & Noonan, D. J. The tuberous sclerosis 2 gene product can localize to nuclei in a phosphorylation-dependent manner. *Mol. Cell Biol. Res. Commun.* **4**, 374–380 (2001).

48. Plank, T. L., Yeung, R. S. & Henske, E. P. Hamartin, the product of the tuberous sclerosis 1 (TSC1) gene, interacts with tuberin and appears to be localized to cytoplasmic vesicles. *Cancer Res.* **58**, 4766–70 (1998).

49. van Slegtenhorst, M. Interaction between hamartin and tuberin, the TSC1 and TSC2 gene products. *Hum. Mol. Genet.* **7**, 1053–1057 (1998).

50. Xu, L. *et al.* Alternative splicing of the tuberous sclerosis 2 (TSC2) gene in human and mouse tissues. *Genomics* **27**, 475–480 (1995).

51. Ekong, R. *et al.* Variants Within *TSC2* Exons 25 and 31 Are Very Unlikely to Cause Clinically Diagnosable Tuberous Sclerosis. *Hum. Mutat.* **37**, 364–370 (2016).

52. Rosner, M., Hanneder, M., Siegel, N., Valli, A. & Hengstschläger, M. The tuberous sclerosis gene products hamartin and tuberin are multifunctional proteins with a wide spectrum of interacting partners. *Mutation Research - Reviews in Mutation Research* **658**, 234–246 (2008).

53. Castro, A. F., Rebhun, J. F., Clark, G. J. & Quilliam, L. A. Rheb binds tuberous sclerosis complex 2 (TSC2) and promotes S6 kinase activation in a rapamycin- and farnesylation-dependent manner. *J. Biol. Chem.* **278**, 32493–32496 (2003).

54. Lamb, R. F. *et al.* The TSC1 tumour suppressor hamartin regulates cell adhesion through ERM proteins and the GTPase Rho. *Nat. Cell Biol.* **2**, 281–287 (2000).

55. Van Slegtenhorst, M. *et al.* Identification of the tuberous sclerosis gene TSC1 on chromosome 9q34. *Science (80-.).* **277**, 805–808 (1997).

56. Capo-Chichi, J. M. *et al.* Disruption of TBC1D7, a subunit of the TSC1-TSC2 protein complex, in intellectual disability and megalencephaly. *J. Med. Genet.* **50**,

740–744 (2013).

57. Saxton, R. A. & Sabatini, D. M. mTOR Signaling in Growth, Metabolism, and Disease. *Cell* **168**, 960–976 (2017).

58. VÉZINA, C., KUDELSKI, A. & SEHGAL, S. N. Rapamycin (AY-22,989), a new antifungal antibiotic. I. Taxonomy of the producing streptomycete and isolation of the active principle. *J. Antibiot. (Tokyo).* **28**, 721–726 (1975).

59. Sabatini, D. M., Erdjument-Bromage, H., Lui, M., Tempst, P. & Snyder, S. H. RAFT1: A mammalian protein that binds to FKBP12 in a rapamycin-dependent fashion and is homologous to yeast TORs. *Cell* **78**, 35–43 (1994).

60. Yang, H. *et al.* Mechanisms of mTORC1 activation by RHEB and inhibition by PRAS40. *Nature* **552**, 368–373 (2017).

61. Lee, D. Y. Roles of mTOR Signaling in Brain Development. *Exp. Neurobiol.* **24**, 177 (2015).

62. Costa-Mattioli, M. & Monteggia, L. M. mTOR complexes in neurodevelopmental and neuropsychiatric disorders. *Nature Neuroscience* **16**, 1537–1543 (2013).

63. Mendoza, M. C., Er, E. E. & Blenis, J. The Ras-ERK and PI3K-mTOR pathways: Cross-talk and compensation. *Trends in Biochemical Sciences* **36**, 320–328 (2011).

64. Sengupta, S., Peterson, T. R. & Sabatini, D. M. Regulation of the mTOR Complex 1 Pathway by Nutrients, Growth Factors, and Stress. *Molecular Cell* **40**, 310–322 (2010).

65. Kwiatkowski, D. J. & Manning, B. D. Tuberous sclerosis: A GAP at the crossroads of multiple signaling pathways. *Human Molecular Genetics* **14**, (2005).

66. Menon, S. *et al.* Spatial control of the TSC complex integrates insulin and nutrient regulation of mTORC1 at the lysosome. *Cell* **156**, 771–785 (2014).

67. Zoncu, R. *et al.* mTORC1 senses lysosomal amino acids through an inside-out mechanism that requires the vacuolar H+-ATPase. *Science (80-.).* **334**, 678–683 (2011).

68. Averous, J. *et al.* Requirement for lysosomal localization of mTOR for its activation differs between leucine and other amino acids. *Cell. Signal.* **26**, 1918–1927 (2014).

69. Li, Z. *et al.* Plk1-mediated phosphorylation of tsc1 enhances the efficacy of rapamycin. *Cancer Res.* **78**, 2864–2875 (2018).

70. Astrinidis, A., Senapedis, W., Coleman, T. R. & Henske, E. P. Cell Cycle-

regulated Phosphorylation of Hamartin, the Product of the Tuberous Sclerosis Complex 1 Gene, by Cyclin-dependent Kinase 1/Cyclin B. *J. Biol. Chem.* **278**, 51372–51379 (2003).

71. Huang, J. & Manning, B. D. D. A complex interplay between Akt, TSC2 and the two mTOR complexes: Figure 1. *Biochem. Soc. Trans.* **37**, 217–222 (2009).

72. Sarbassov, D. D. *et al.* Rictor , a Novel Binding Partner of mTOR , Defines a Rapamycin-Insensitive and Raptor-Independent Pathway that Regulates the Cytoskeleton. **14**, 1296–1302 (2004).

73. Jacinto, E. *et al.* Mammalian TOR complex 2 controls the actin cytoskeleton and is rapamycin insensitive. *Nat. Cell Biol.* **6**, 1122–8 (2004).

74. Sarbassov, D. D. *et al.* Prolonged Rapamycin Treatment Inhibits mTORC2 Assembly and Akt/PKB. *Mol. Cell* **22**, 159–168 (2006).

75. Carson, R. P., Fu, C., Winzenburger, P. & Ess, K. C. Deletion of Rictor in neural progenitor cells reveals contributions of mTORC2 signaling to tuberous sclerosis complex. **22**, 140–152 (2013).

76. Pezze, P. D. *et al.* A Dynamic Network Model of mTOR Signaling Reveals TSC-Independent mTORC2 Regulation. **5**, 1–18 (2012).

77. Huang, J., Dibble, C. C., Matsuzaki, M. & Manning, B. D. The TSC1-TSC2 Complex Is Required for Proper Activation of mTOR Complex 2. *Mol. Cell. Biol.* **28**, 4104–4115 (2008).

78. Knudson, A. G. Mutation and cancer: statistical study of retinoblastoma. *Proc. Natl. Acad. Sci. U. S. A.* **68**, 820–823 (1971).

79. Hino, O. & Kobayashi, T. Mourning Dr. Alfred G. Knudson: the two-hit hypothesis, tumor suppressor genes, and the tuberous sclerosis complex. *Cancer Science* **108**, 5–11 (2017).

80. Martin, K. R. *et al.* The genomic landscape of tuberous sclerosis complex. *Nat. Commun.* **8**, (2017).

81. Winden, K. D. *et al.* Biallelic mutations in TSC2 lead to abnormalities associated with cortical tubers in human iPSC-derived neurons. *J. Neurosci.* 0642–19 (2019). doi:10.1523/jneurosci.0642-19.2019

82. Ognibene, M. *et al.* The tumor suppressor hamartin enhances Dbl protein transforming activity through interaction with ezrin. *J. Biol. Chem.* **286**, 29973–29983 (2011).

83. Astrinidis, A. *et al.* Tuberin, the tuberous sclerosis complex 2 tumor suppressor gene product, regulates Rho activation, cell adhesion and migration. *Oncogene*

21, 8470–8476 (2002).

84. Goncharova, E., Goncharov, D., Noonan, D. & Krymskaya, V. P. TSC2 modulates actin cytoskeleton and focal adhesion through TSC1-binding domain and the Rac1 GTPase. *J. Cell Biol.* **167**, 1171–1182 (2004).

85. Goncharova, E. A., James, M. L., Kudryashova, T. V., Goncharov, D. A. & Krymskaya, V. P. Tumor suppressors TSC1 and TSC2 differentially modulate actin cytoskeleton and motility of mouse embryonic fibroblasts. *PLoS One* **9**, 1–10 (2014).

86. Qiu, A., Mori, S. & Miller, M. I. Diffusion Tensor Imaging for Understanding Brain Development in Early Life. *Annu. Rev. Psychol.* **66**, 853–876 (2015).

87. Widjaja, E. *et al.* Diffusion tensor imaging identifies changes in normal-appearing white matter within the epileptogenic zone in tuberous sclerosis complex. *Epilepsy Res.* **89**, 246–53 (2010).

88. Im, K. *et al.* Altered Structural Brain Networks in Tuberous Sclerosis Complex. *Cereb. Cortex* **26**, 2046–2058 (2016).

89. Peters, J. M. *et al.* Loss of White Matter Microstructural Integrity Is Associated with Adverse Neurological Outcome in Tuberous Sclerosis Complex. *Acad. Radiol.* **19**, 17–25 (2012).

90. Walker, L. *et al.* Diffusion tensor imaging in young children with autism: Biological effects and potential confounds. *Biol. Psychiatry* **72**, 1043–1051 (2012).

91. Shahid, A. Resecting the epileptogenic tuber: What happens in the long term? *Epilepsia* **54**, 135–138 (2013).

92. Goorden, S. M. I., van Woerden, G. M., van der Weerd, L., Cheadle, J. P. & Elgersma, Y. Cognitive deficits in Tsc1+/- mice in the absence of cerebral lesions and seizures. *Ann. Neurol.* **62**, 648–55 (2007).

93. Waltereit, R., Japs, B., Schneider, M., De Vries, P. J. & Bartsch, D. Epilepsy and Tsc2 haploinsufficiency lead to autistic-like social deficit behaviors in rats. *Behav. Genet.* **41**, 364–372 (2011).

94. Giannantoni, N. M., Restuccia, D., Della Marca, G., Alfano, R. M. & Vollono, C. A novel TSC2 mutation causing tuberless tuberous sclerosis. *Seizure* **23**, 580–582 (2014).

95. Jones, I. *et al.* A novel mouse model of tuberous sclerosis complex (TSC): eye-specific Tsc1-ablation disrupts visual-pathway development. *Dis. Model. Mech.* **8**, 1517–1529 (2015).

96. Knox, S. *et al.* Mechanisms of TSC-mediated Control of Synapse Assembly and

Axon Guidance. *PLoS One* **2**, e375 (2007).

97. Choi, Y. J. *et al.* Tuberous sclerosis complex proteins control axon formation. *Genes Dev.* **22**, 2485–2495 (2008).

98. Umegaki, Y. *et al.* Palladin is a neuron-specific translational target of mtor signaling that regulates axon morphogenesis. *J. Neurosci.* **38**, 4985–4995 (2018).

Figure 1: The Canonical TSC-mTOR pathway – a role in axon guidance? TSC1/2 is a complex which acts as a hub upon which growth/guidance promoting or inhibitory signals may converge to effect growth cone motility. In the absence of inhibitory phosphorylations by Akt or Erk (and/or in the presence of stimulatory phosphorylations via GSK-3β or AMPK), active TSC1/2 stimulates intrinsic Rheb GTPase activity via the GAP domain on TSC2. Rheb is upstream of mTOR complexes mTORC1 and mTORC2. In the presence of active TSC2, Rheb is unable to activate mTORC1, a complex defined by various co-effectors such as Raptor. mTORC1 phosphorylating activation of S6K is decreased, followed by a decrease in S6K activating phosphorylation of ribosomal protein S6. mTORC1 is also located upstream of the translation regulator eIF-4EBP1. Upon phosphorylation, 4EBP1 releases its inhibitory association with the translation initiation factor eIF-4E, stimulating the latter's translational activity. Thus, multiple mTORC1 phosphorylations direct protein translation and decreases in mTORC1 activity lead to rapid decreases in protein translation. As noted in the text, local protein synthesis of individual transcripts has been linked to attractive cue response downstream of mTOR-dependent protein synthesis, and at least one group has reported mTOR-dependent decreases in LPS downstream of a cue.

mTORC2, defined by association of mTOR with proteins such as Rictor, is poorly defined in neurons. Downstream effectors include PKC, Akt, and RhoA. In the canonical model, mTORC2 activation downstream of TSC2 may increase RhoA dependent contractility and repulsive activity at the growth cone.

Some studies in non-neuronal cells have posited a TSC -> RhoA axis, which may influence growth cone motility via an mTOR-dependent or -independent mechanism.

Figure 1: The TSC Pathway

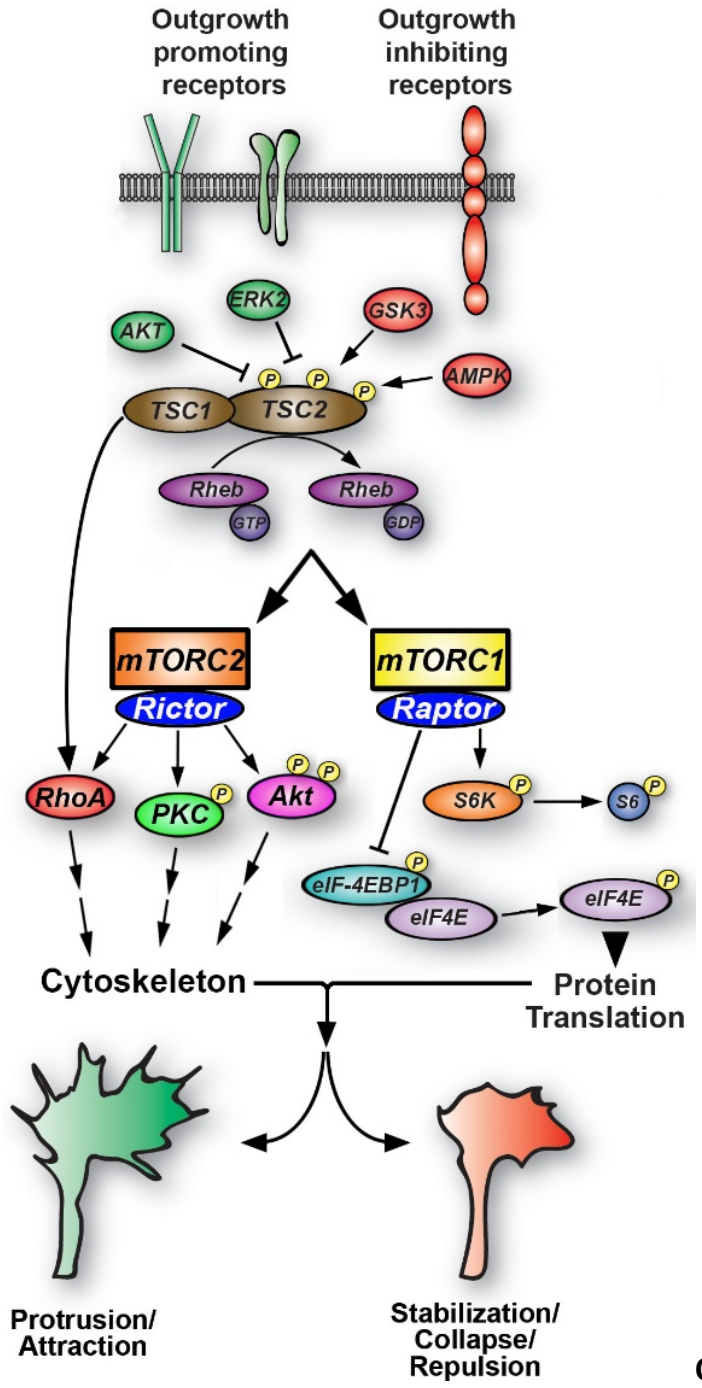

Credit: Timothy Gomez

Chapter 2: Abnormal axon guidance of human tuberous sclerosis neurons is due to mTOR-independent defects in RhoA

Timothy Catlett and Timothy Gomez designed the study; Timothy Catlett, Massimo Onesto, Alec McCann and Sarah Rempel performed the research and analyzed the data; Jennifer Glass and David Franz provided the patient samples. Timothy Catlett and Timothy Gomez wrote the paper.

SUMMARY

Growing evidence suggests that patients with Tuberous Sclerosis Complex (TSC), like other neuro-developmental disorders, have mis-wiring of neuronal connections that form during development. These defects in neuronal connectivity likely contribute to symptoms of TSC, such as intellectual disabilities, autism, and epilepsy. However, defective axon guidance by human neurons has only been suggested from brain imaging studies and models to study the molecular basis for misguidance of developing human neurons have not been developed. To directly address these fundamental questions, we generated human induced pluripotent stem cells (hiPSC) from patient-derived cells, as well as several genetically engineered counterparts and control hiPSCs. By differentiating hiPSCs into both dorsal forebrain (FB) and motor neurons (MNs), we first show that normal human neurons respond to permissive and repulsive canonical guidance cues through proper regulation of axon extension and guidance. On the other hand, neurons with heterozygous loss of TSC2 function exhibit severely reduced responses to several repulsive cues and show defective axon guidance. Interestingly, while TSC2 is known to be a key negative regulator of mTOR-dependent protein synthesis, we find that axon guidance cues also signal through TSC2 in growth cones through modulation of RhoA independent of mTOR. Our results suggest that neural network connectivity defects in patients with TSC may result from abnormal RhoA regulation of the cytoskeleton.

INTRODUCTION

Accurate guidance of developing axons is a critical early process necessary for correct assembly of neural circuits. The tips of these axonal projections, growth cones, follow patterns of chemical and mechanical cues to extend along pathways to reach specific synaptic partners. Each growth cone expresses receptors to these various cues, and integrates multiple discrete signals to ultimately effect axon extension and guidance through cytoskeletal rearrangements[1–3]. This guidance cue-to-cytoskeleton signaling axis involves numerous intermediaries, which have been shown in animal model neurons to include both the Rho family GTPases and local protein synthesis (LPS) within the growth cone[4,5]. While defects in signal transduction have been linked to abnormal neural network wiring in animal models, few human neural development disorders have yet been attributed to specific growth cone signaling abnormalities[6–8].

Tuberous sclerosis complex (TSC) is an autosomal dominant neurodevelopmental disorder affecting approximately one million people worldwide. Most TSC patients have some degree of neurological symptoms including mild to profound intellectual disability (50%), autism spectrum disorders (ASDs) (50%), and up to 90% develop seizures[9]. Pathological variants in the TSC1 (hamartin) or TSC2 (tuberin) genes cause TSC, which is best characterized by benign tumors called hamartomas that form within multiple organ systems, including the central nervous system (CNS)[10,11]. While neurological symptoms were classically attributed to the formation of cortical tubers during embryonic development, recent research indicates there is a poor correlation between CNS tubers and severity of epilepsy and intellectual disability. While the formation of

tumors in TSC has long been attributed to the contribution of a "second-hit" loss of the normal TSC1/2 allele, recent research has shown that many tumors, especially cortical tubers, lack a second-hit, raising the possibility of an alternate pathway for tumorigenesis that depends on monoallelic inactivation of TSC1/2[12]. In addition, TSC patients with severe intellectual disabilities may have defects in neural network wiring due to abnormal axon guidance and synaptogenesis during development. Consistent with this notion, diffusion tensor imaging (DTI) studies show abnormal axon tract development in patients with mutations in TSC1 or TSC2[13–15]. Neural connectivity abnormalities are also likely responsible for some learning and behavioral abnormalities in TSC animal models that typically lack tubers[16,17]. Moreover, one group reported both retinotectal axon guidance abnormalities and guidance cue insensitivity in a heterozygous TSC2 mutant mouse model[18].

Here we demonstrate that developing human neurons derived from unaffected and disease-corrected iPSCs are sensitive to and can be guided by several canonical axon guidance cues, including ephrin-A1, ephrin-A5, slit2, netrin, and semaphorin3F. In contrast, TSC patient-derived neurons from $TSC2^{+/-}$ mutant iPSCs exhibit enhanced basal axon extension and severe insensitivity to several guidance cues. Interestingly, basal mTOR activity and mTOR-mediated protein synthesis modulation in response to cues is normal in $TSC2^{+/-}$ mutant neurons, suggesting that defective mTOR signaling may not account for abnormal axon growth and guidance phenotypes. In contrast, basal and cue-activated RhoA was diminished in $TSC2^{+/-}$ neurons, suggesting that TSC1/2 signaling through RhoA is necessary for proper axon extension and response to guidance cues in

these neurons. Consistent with this notion, we find that mTORC1 and mTORC2 inhibitors neither significantly impact control neuron outgrowth nor rescue axon growth and guidance defects in $TSC2^{+/-}$ neurons. Therefore, contrary to reports in some animal model systems, we find that human neurons do not require rapid TSC2-dependent modulation of protein synthesis to regulate outgrowth and cue responses. Instead neurons require direct modulation of RhoA signaling downstream of TSC1/TSC2 for proper axon development.

METHODS

IPSC generation and characterization

Dermal fibroblast samples from normal tissue and an identified hypomelanotic macule (”ash leaf spot”) were collected from an individual with Tuberous Sclerosis (TSC). The patient presented with high tuber load, epilepsy, autism spectrum disorder, and expressive language delay. Cells were reprogrammed into iPSCs using non-integrating Sendai viruses expressing C-MYC, KLF4, OCT3/4, and SOX2 as described in Ban et al., 2011[19]. Lines reprogrammed from each tissue type were verified for the heterozygous nonsense TSC2 pathogenic mutation at base pair c.972C>G. Characterization was performed utilizing immunofluorescence staining for NANOG, OCT4, and SOX2 with specific antibodies. Mycoplasma testing was provided by WiCell (WiCell, Madison, WI).

CRISPR-Cas9 gene editing

In addition to IMR90 iPS and WA09 (H9) ES cell lines, CRISPR-Cas9 single-strand oligonucleotide (ssODN) method of gene editing was utilized in the heterozygous TSC

patient line to correct the nonsense mutation and create isogenic control lines as in Yang et al., 2013 and Chen, et al., 2015[20,21]. Briefly, DNA fragment 5'-CACACAGAAACCGCCTTACCTGG-3' was inserted into a plasmid downstream of the U6 promoter (Addgene #52961; http://www.addgene.org/52961/) for sgRNA expression targeting exon 9 of TSC2. 200bp homology arms surrounding the mutation site were constructed by Integrated DNA Technologies (IDT). Constructs were electroporated into patient cells followed by puromycin selection, expansion, and sequencing. Off-target analysis was performed via Q5-polymerase PCR for the 5 highest-likelihood off-target sites as predicted by crispr.mit.edu algorithms. All generated lines were verified and characterized as noted above.

IPSC maintenance

IPSCs and WA09 (H9) cells were cultured on feeder-free substrate vitronectin (Thermofisher) with Essential 8 Flex media (ThermoFisher) as described (https://assets.thermofisher.com/TFS-Assets/LSG/manuals/Essential_8_Flex_Medium_UG.pdf).

Neural differentiation and culture

hFBs were differentiated as previously described in Doers et al., 2014. At 60-80% confluency, stem cell colonies were lifted with 1mg/mL Dispase II (Sigma) and cultured in suspension in embryoid body medium (EB) consisting of DMEM/F12 (ThermoFisher), KnockOut Serum (1:4; Thermofisher), MEM NEAA (1:100; ThermoFisher), and Glutamax supplement (1:100; Thermofisher). Over the following three days whole media exchanges

were performed with EB and Neural Induction Medium (NIM) consisting of DMEM/F12, MEM NEAA, Glutamax, and heparan sulfate (2µg/mL; Stem Cell Technologies) in a ratio of 3:1, 1:1, 1:3. On days 4-7 whole media exchanges were made with NIM media. On day 7, cells were plated on laminin (25µg/mL; Sigma-Aldrich) coated plates and allowed to adhere for 48 hours; then half media exchanges of NIM every other day until day 17-18 upon which cells were lifted manually and kept in suspension as neurospheres in Maintenance media consisting of DMEM/F12, MEM NEAA, Glutamax, and B27 supplement minus Vitamin A (1:100; ThermoFisher). Characterization was performed at 10-15DIV via immunostaining for PAX6 (1:20; DSHB) and SOX2 (1:100; R&D Systems), and at 25-30DIV via immunostaining for OTX2 (1:100; R&D Systems) and FOXG1 (1:100; Abcam). Motor neurons were differentiated according to established protocols following Du et al., 2015 and characterized via immunostaining for Islet-1 (1:250; DSHB).

Neurons were cultured as neurospheres on acid-washed coverslips coated with poly-D-lysine (PDL, 50µg/mL; Sigma-Aldrich) and laminin (LN, 25µg/mL; Sigma-Aldrich) in Neurobasal (ThermoFisher) media with B27 supplement and Glutamax (NB) for 1- 14DIV with half media changes every third day as needed. For experiments with dissociated neurons, neurospheres were incubated at RT for 15 minutes in Accumax (Stem Cell Technologies) prior to quenching in neurobasal medium, centrifugation at 100xg, and plating at $3x10^4$ - $1x10^5$ densities. Cells were cultured 3-5 DIV.

Live and fixed immunofluorescent cell imaging

For live phase contrast or differential interference contrast (DIC) microscopy, images were acquired using either a 10x/0.3, 20x/0.5, or 40x/1.3 numerical aperture (NA)

objective lens on a Nikon TE2000 inverted microscope with a Coolsnap HQ2 camera (Roper Scientific) with no binning (pixel size = 155 nm). Fixed immunostained images were acquired using either a 60x/1.45 NA objective lens at 2-2.5x zoom on an Olympus Fluoview 500 laser-scanning confocal system mounted on an AX-70 microscope or using a 63x/1.4 NA objective lens at 2-2.5x zoom on a Zeiss LSM800 Airy-disc scanning confocal system mounted on an Axio Observer Inverted Microscope. Live images of fluorescent neurons were acquired using the Nikon TE2000 or Zeiss microscopes.

Immunofluorescence staining and outgrowth analyses

Immunofluorescence (IF) staining was performed as previously described[24]. Measurements of fluorescence intensity of proteins of interest were made within growth cones by creating an image mask from a thresholded F-actin (AlexaFluor (AF)-phalloidin, ThermoFisher) channel and measuring the average pixel intensity of immunolabeling within the selected area. Measurements of fixed neurite lengths were made by tracing from the end of the neurite as determined by acetylated-tubulin (Sigma-Aldrich) labeling to the edge of the neurosphere using the Simple Neurite Tracer plug-in[25] and Fiji/ImageJ[26–28]. Image stacks of live neurons were stabilized as needed prior to analysis using the ImageStabilizer plug-in[29].

Live DIC outgrowth analysis was performed by taking consecutive measurements at the furthest edge of the growth cone lamellipodia opposite the central domain; retraction distances were capped at three times growth cone length or 30 microns to account for skewing of single very large retractions. Collapse was quantified via disassembly of the lamellipodial veil and ≤ 2 filopodia of <10 microns in length.

All other data analysis was performed on raw images; the Unsharp Mask filter (ImageJ) was utilized in some instances for display purposes only. Gaussian blur background subtraction was similarly utilized in DIC images as needed for background shading correction for display purposes.

Western Blot

Immunoblotting performed as in Basu et al., 2019 using lysates collected as in Kerstein et al., 2013. Briefly, cell lysates were collected as neurosphere suspensions or as cultured cells incubated in RIPA buffer (ThermoFisher) supplemented with PhoSTOP (Roche) and Compleat protease inhibitor (Roche) followed by protein concentration evaluation (BCA Assay, Pierce/ThermoFisher) via a NanoDrop 2000 spectrophotometer (ThermoScientific). Approximately 20µg of protein were run for each lane on a Biorad 4-15% SDS-PAGE gel (Biorad). Primary antibodies were used as follows: TSC2, phospho-S6, S6 (1:1000; Cell Signaling Technologies), and Actin (1:1000; Sigma-Aldrich). Horseradish peroxidase-conjugated secondary antibodies (Jackson Immunoresearch) were used at 1:10000 and blots visualized via Pierce ECL and Pierce Femto ECL kits (ThermoFisher).

Puromycin Translation Assay

Assay was performed as in Schmidt, Clavarino, Ceppi, & Pierre, 2009. Briefly, cultures were incubated in 10µg/mL puromycin (ThermoFisher) for 10 minute increments concurrent with or following treatment with Slit2 (200ng/mL), netrin-1 (100ng/mL), or ephrin-A1 (200ng-2µg/mL) (R&D) and pharmacological agonists/antagonists as noted in

the results, including rapamycin (Calbiochem) and anisomycin (MP Biomedicals). Puromycin-containing media was rinsed 2x with NB media before fixation. Growth cones were fixed and stained with anti-puromycin primary antibody (1:1000, Developmental Studies Hybridoma Bank) and AF488 secondary (ThermoFisher) with AF-conjugated phalloidin (ThermoFisher) counterstain and analyzed as described above. Some experiments also utilized succinimidyl ester-AF647 (1:1000, ThermoFisher) as a total protein control (data not shown).

G-LISA Assay for RhoA activity

Neurospheres were stimulated with ephrin-A1 for 15 min, then rinsed immediately in ice-cold phosphate buffered saline (PBS, Sigma) prior to lysate collection. Cells were stored in G-LISA lysis buffer with manufacturer's protease and phosphatase inhibitors (Cytoskeleton). Protein concentrations were determined using Precision Red Advanced Protein Assay Reagent with absorbance at 600nm measured using a NanoDrop 2000 spectrophotometer. Lysates were incubated in wells for 1 hr at 4° C with shaking, then rinsed and sequentially incubated with primary antibodies to RhoA followed by HRP secondary antibodies (Cytoskeleton) and colorimetric reaction was performed for 15 min at 37°C, which was measured using a Molecular Devices SpectraMax 250.

iPSC nucleofection protocol

IPSC neurons were transfected as described in the Amaxa Primary Mammalian Neuron protocol (https://bioscience.lonza.com/lonza_bs/US/en/download/product/asset/21464) using whole or dissociated neurospheres, as described above. Cells were immersed in

transfection solution with 1-5µg of plasmid DNA and transfected using an Amaxa Nucleofector II, program settings O-O5 for dissociated cultures, and B-016 for neurospheres (kit VPI-1003, Amaxa). We utilized both Amaxa's commercial solution and a lab prepared solution[33], noting no significant differences in performance between them in our hands. Cells were allowed to recover in suspension for 24 hrs before culturing on PDL-LN coated coverslips or on stripes (below).

FRET assay

To measure basal RhoA activity in growth cones, acceptor photo-bleaching was performed on neurons expressing a RhoA FRET sensor as described[34,35]. Briefly, CFP (donor, excited with 440 nm diode laser) and YFP (acceptor, excited with 514 nm argon laser) images of live hFB neurons expressing a RhoA FRET sensor were collected before bleaching. Next, YFP fluorescence was locally bleached by repetitive fast scanning 520 nm light at 100% power for 5s. Immediately after YFP bleaching, post-bleaching CFP and YFP images were collected with the same detector settings as used for original images. CFP emission typically increases when the acceptor (YFP) is bleached and FRET efficiency is recorded as the change in CFP/YFP.

Stripe Guidance assay

Stripe molds produced by Dr. Martin Bastmeyer at Karlsruhe Institute of Technology were purchased or provided by Paul Letourneau. Acid washed coverslips were first coated in PDL (50µg/mL) for 45 minutes and rinsed extensively with ddH2O before drying. Molds were affixed and 50µL of guidance cue plus LN (25µg/mL) and dextran conjugated to

tetramethylrhodamine (TMR) or AF647 (500µg/mL; ThermoFisher) diluted in PBS was vacuum fed through the mold and allowed to incubate for one hour at RT, with one solution exchange. After extensive rinsing with PBS, molds were removed and the patterns were rinsed further with PBS. The cue-patterned coverslips were next flooded with LN (25µg/mL) for one hour at RT followed by final PBS rinses. Cues utilized in stripe assay included ephrin-A1 (10µg/mL; R&D Systems), ephrin-A5 (10µg/mL; R&D), netrin1 (100ng/mL; R&D), and hSlit2 (1µg/mL; R&D). Cue binding was independently confirmed with antibodies to His (Netrin and Slit2) or Fc (ephrin-A5 and ephrin-A1) and visualization with appropriate AF-conjugated secondary. Ephrin-A5 stripe preparation required pre-clustering with anti-Fc antibody incubated under mild agitation at RT for 30 minutes before application. Unclustered ephrin-A5 stripes were utilized as a control.

Neurons on patterned cues were labeled AF-Phalloidin and neurite orientation and length within quadrants were quantified using a Sholl analysis plug-in[36]. In addition, image thresholding of the F-actin channel was used to measure the area of neurites on versus off stripes. Sampled image analysis was confined to areas corresponding to the parallel quadrants and a minimum 100 microns away from the neurosphere. Data were normalized to the mean neurite area occupying LN stripes.

RESULTS

Generation and gene editing of iPSC lines from a TSC patient.

Fibroblasts were isolated from skin biopsies from an 18-year-old male TSC patient at the Tuberous Sclerosis Clinic at Cincinnati Children's Hospital Medical Center. This patient has a history of complex partial seizures, autism and expressive language delay, intellectual disability, as well as a large tuber burden. Genomic sequencing confirmed a

heterozygous C>G point mutation at bp 972, which results in a premature stop at codon 324 (of 1843). Patient-derived fibroblasts were reprogrammed into iPSCs using non-integrating Sendai virus-containing genes for the transcription factors Oct4, Sox2, Klf4 and Myc (Invitrogen CytoTune™-iPS 2.0 Sendai Reprogramming Kit.) by the Waisman Center iPSC service core (UW-Madison). This service includes verification of stem cell marker expression, chromosome karyotyping, and short Tandem Repeat (STR) analysis to confirm that the somatic cells and derived iPSCs are from the same individual and each line is a unique clone without contamination (not shown). Subsequently, we edited the point mutation in $TSC2^{+/-}$ iPSCs to generate corrected isogenic control $TSC2^{+/+}$ iPSCs and also introduced the same mutation in the unaffected allele to create null $TSC2^{-/-}$ iPSCs via CRISPR-Cas9. Six clones of each respective genotype were generated and stem cell colonies were morphologically normal and divided at similar rates (Supplemental Fig. 1a, data not shown). Western blotting confirmed that this early stop codon results in reduced protein levels in $TSC2^{+/-}$ iPSCs and complete loss of protein in $TSC2^{-/-}$ iPSCs (not shown) compared to corrected $TSC2^{+/+}$ iPSCs, as well as IMR90 iPSCs and WA09 (H9) embryonic stem cell lines.

TSC2 haploinsufficiency does not alter basal mTOR activity in hFB neurons

Excitatory glutamatergic dorsal human forebrain neurons (hFB) of each TSC2 genotype were differentiated using established protocols[37,38] and plated as neurospheres for 24 hrs before fixation and immunolabeling. Developing neurospheres were positive for the neuroectoderm marker Pax6 and the neural stem cell marker Sox2. (Supplementary Figure 1). Next we used TSC2-specific antibodies to assess TSC2 expression within

growth cones of each genotype. We found that control neurons differentiated from corrected TSC2$^{+/+}$ iPSCs (as well as IMR90 and WA09 control neurons, not shown) exhibit intense staining for TSC2 within growth cones and throughout neurites, while TSC2$^{+/-}$ growth cones showed approximately 50% less fluorescence signal and TSC2$^{-/-}$ growth cones were devoid of labeling (Figure 1A-B). Similarly, neurosphere lysates immunoblotted for TSC2 showed a reduction and absence of protein in heterozygous and null hFB neurons compared to control, respectively (Figure 1C). To determine the effects of TSC2 loss on mTOR activity, we immunolabeled growth cones for ribosomal protein phospho-S6 (Ser235/236), a well-known marker for mTOR activation and protein synthesis[39,40]. Interestingly, while TSC2$^{-/-}$ growth cones showed significant upregulation of p-S6 levels, TSC2$^{+/-}$ growth cones appeared similar to TSC2$^{+/+}$ growth cones (Figure 1D-E). These immunofluorescence findings were corroborated by immunoblotting (Figure 1C). Therefore, heterozygous loss of TSC2 does not appear to impact basal mTOR activity within growth cones nor within neurospheres, which is consistent with other studies performed in rodent and iPS neuronal models[41–43].

Basal rates of neurite outgrowth are enhanced in TSC2 mutant hFB neurons.

We first tested the effects of TSC2 loss on process extension by hFB neurons. Initially we examined how partial and complete loss of TSC2 expression affected neurite outgrowth in fixed neurosphere cultures. Culturing neurons within neurospheres is advantageous, as greater numbers of neurons generate axons compared to dissociated neurons with significantly less cell death[44]. hFB neurospheres were plated and allowed to grow for 24 hrs and then fixed and immunostained for tubulin to assay neurite lengths. Neurite

extension is profuse and rapid from neurospheres, as some neurites were observed to extend more than one millimeter after one day *in vitro* (DIV) (Figure 2A). At 24 hrs the twenty longest neurites projecting from each sphere were measured and compared between cell lines (Figure 2B). hFB $TSC2^{+/-}$ neurites were found to grow significantly longer than multiple lines of $TSC2^{+/+}$ neurons, including isogenic control neurons. $TSC2^{-/-}$ axons were also longer than control $TSC2^{+/+}$ axons, although null neurons were significantly more variable between spheres (F-test, P<.0001, n=900) (Figure 2A-B). Neurite lengths of hMNs differentiated from $TSC2^{+/-}$ iPSCs were also significantly longer than control neurons (Supplemental Figure 2A-C).

To confirm these results, we also measured the rates of neurite outgrowth by time-lapse imaging of live hFB neurons from each genotype, which eliminates potential bias that may result from measuring longest axons in our previous analysis. Representative differential interference contrast (DIC) images of live $TSC2^{+/+}$ and $TSC2^{+/-}$ growth cones over thirty-minute time periods shows that $TSC2^{+/-}$ axons extend nearly two times faster than control neurons from several different iPSC lines (Figure 2C). Consistent with increased variability of fixed $TSC2^{-/-}$ neurite lengths, the average rate of outgrowth by null neurons was more variable and on average slower compared to $TSC2^{+/-}$ neurons. Similar results were obtained with hMNs (Supplemental Figure 2D). Given the canonical role of TSC2 as a negative regulator of mTOR, we sought to investigate whether the enhanced neurite outgrowth by $TSC2^{+/-}$ neurons could be attributed to upregulated mTOR signaling. However, to our surprise, acute pharmacological inhibition of mTORC1 with rapamycin had little effect on axon extension rates of $TSC2^{+/+}$ or $TSC2^{+/-}$ neurons (Figure 2E). As

previous reports have also implicated mTORC2 upstream of cytoskeletal dynamics in other cell types[45], we tested the mTORC1/C2 inhibitor torin-1[46] and the mTORC2-specific inhibitor JR-AB2-011[47]. Again, neither of these manipulations significantly affected the baseline outgrowth of $TSC2^{+/+}$ neurites or enhanced outgrowth of $TSC2^{+/-}$ neurites (Figure 2E). Additionally, we tested whether longer treatment with mTORC1 or mTORC2 inhibitors normalized $TSC2^{+/-}$ neurite outgrowth, since TSC2 haploinsufficiency is known to induce proteomic changes[41,48]. Again, we found that neither 24 hr treatment with rapamycin or torin-1, nor long term treatment with rapamycin for up to 21 days during neuronal differentiation, reversed the enhanced extension rates exhibited by $TSC2^{+/-}$ neurons (Figure 2F). Note that we confirmed that these pharmacological treatments effectively inhibited mTORC1 and mTORC2 in growth cones (Supplemental Figure 3). These data are consistent with the normal levels of S6 phosphorylation observed in $TSC2^{+/-}$ growth cones (Figure 1D-E), and with rodent and some human studies[49,50]. Together, these surprising findings suggest that TSC2 has mTOR-independent targets within growth cones that reduce neurite outgrowth, since TSC2 haploinsufficiency results in enhanced axon extension.

$TSC2^{+/-}$ neurons are less sensitive to inhibitory axon guidance cues.

Next we tested the effects of several canonical axon guidance cues on TSC2 mutant and control hFB neuron axon extension. While stem cell-derived human neurons have been widely used for over two decades, few studies have tested whether developing human neurons are sensitive to classic axon guidance cues[51–53] and none have determined whether neurons carrying mutations in ASD-related genes respond as typically

developing neurons. Given that neural network connectivity abnormalities may be responsible for some TSC2 pathologies[13–15], we hypothesized that TSC2$^{+/-}$ growth cones may be less sensitive to canonical guidance cues. Here we focused on heterozygous neurons, both because these neurons exhibit robust neurite extension phenotypes (Figure 2) and because the vast majority of TSC patient neurons are heterozygous compared to a minority of cells in some brain tubers that may carry a second-hit mutation[12]. We initially tested control and TSC2$^{+/-}$ neuron sensitivities to bath applied Ephrin-A1, which is an inhibitory axon guidance cue previously shown to signal through TSC2 in mouse cortical neurons[18]. Corrected TSC2$^{+/+}$ control neurons, as well as unrelated control neurons (see Supplemental Figure 5), rapidly and robustly collapsed in response to 2 µg/ml ephrin-A1 (high dose) (Figure 3A). Most control growth cones collapsed, and many axons retracted in response to high dose ephrin-A1 (Fig 3B), while a ten-fold lower dose of ephrin-A1 (0.2 µg/ml) decreased extension rates proportionally less (Figure 3C). In contrast, TSC2$^{+/-}$ hFB neurites were modestly inhibited by high dose ephrin-A1 (Figure 3A-C) and showed little change in extension rate upon exposure to a low dose of ephrin-A1 (Figure 3C). While control growth cones robustly retracted in response to a high dose of ephrin-A1, TSC2$^{+/-}$ neurons were frequently observed to transiently pause or lose some growth cone area without retracting (Figure 3A-B). The dose-dependent effect of ephrin-A1 suggests that TSC2$^{+/-}$ growth cones retain EphA receptors, which we confirmed to be at similar expression levels by immunolabeling for EphA2 and EphA4 (Supplemental Figure 4). The extent of growth cone collapse was also measured in fixed hFBs and hMNs after ephrin-A1 treatment (see Methods). Consistent with live imaging, we found that both isogenic control and unrelated control hFB neurons

(Figure 3D, Supplemental Figure 5), as well as hMNs (Supplemental Figure 2E), were significantly more sensitive to ephrin-A1 compared to $TSC2^{+/-}$ neurons.

To determine whether observed insensitivity of $TSC2^{+/-}$ growth cones was unique to ephrin-A1, we assayed additional canonical inhibitory cues (Figure 3D and Supplemental Figure 5). As with ephrin-A1, hSlit2 (200ng/mL) elicited a robust collapse response in control hFB neurons but had little effect on $TSC2^{+/-}$ neurons. Similarly, lysophosphatidic acid (LPA), a G-protein coupled receptor ligand and potent activator of RhoA, strongly collapsed control neurons at 100nM, but had no effect on $TSC2^{+/-}$ neurons at this dose. However, 1 μM LPA did collapse $TSC2^{+/-}$ growth cones, suggesting that these mutant neurons are intrinsically capable of collapsing, but are less sensitive to multiple inhibitory ligands (Figure 3D). This latter result is in agreement with previous work in a mouse model showing that $TSC2^{+/-}$ neurons were sensitive to a high dose of LPA[18]. Finally, while control hMNs were highly sensitive to Semaphorin-3F, $TSC2^{+/-}$ hMN growth cones were less sensitive (Supplemental Figure 2E).

To determine if either mTORC1 or mTORC2 complexes function downstream of TSC2 to regulate guidance cue sensitivity, we tested the effects of pharmacological inhibitors of each mTOR complex on ephrin-mediated growth cone collapse. Consistent with results described above, we found that acute treatment of $TSC2^{+/+}$ or $TSC2^{+/-}$ hFB neurons with mTORC1/C2 inhibitors neither prevents, nor restores ephrinA1-mediated collapse by control or heterozygous TSC2 neurons, respectively (Figure 3E). These results suggest that acute signaling downstream of EphA does not require mTORC1/C2 activity.

However, while pre-treatment of hFB neurons with mTOR inhibitors for 24 hr before stimulation with ephrin-A1 does partially block ephrinA1 collapse of $TSC2^{+/+}$ hFB axons, it does not restore sensitivity of $TSC2^{+/-}$ hFB neurons (Fig 3F). Loss of sensitivity of control neurons to ephrin-A1 may be due to mTORC1-dependent proteomic changes, but this appears unrelated to changes caused by loss of TSC2 function. These surprising results suggest that hyperactive mTORC1/C2 signaling does not account for the dramatic phenotypes we observe in developing $TSC2^{+/-}$ axons.

Ephrin-mediated changes in local protein synthesis are unaffected in $TSC2^{+/-}$ neurons

In rodent neurons, ephrin-mediated growth cone collapse is correlated with inhibition of protein synthesis[18]. To test whether similar mechanisms may operate in human neurons, we first assayed protein synthesis within growth cones of control and TSC2 mutant neurons. Given that control and $TSC2^{+/-}$ growth cones showed similar levels of mTOR activity (Fig 1), we hypothesized that constitutive translation would not differ between these groups but may be elevated in $TSC2^{-/-}$ neurons. To assess rates of protein synthesis within growth cones we utilized the SUnSET technique, which uses an anti-puromycin antibody to detect puromycin-labeled nascent peptides[32] and has been used successfully to assay LPS in growth cones[54]. Briefly, the antibiotic puromycin serves as a cell-permeable tRNA analogue which binds translating polypeptides but does not substantially impact general translation when used at low dose. Initially we assessed whether the basal rates of protein synthesis differed between genotypes by adding puromycin to cultured neurons for ten minutes to provide a readout of local translation within the growth cones.

As hypothesized, the rate of local translation was not different between control and $TSC2^{+/-}$ growth cones (Figure 4A-B). However, in agreement with our ribosomal protein activation results (Figure 1D-E), constitutive translation was markedly upregulated $TSC2^{-/-}$ growth cones. This suggests that under basal conditions, mTOR-dependent protein synthesis is normal in $TSC2^{+/-}$ growth cones. To verify that mTOR was active in hFB growth cones, we treated neurons with rapamycin, which decreased basal rates of LPS within control and $TSC2^{+/-}$ growth cones and normalized LPS within $TSC2^{-/-}$ growth cones (Figure 4B). As an additional control, co-treatment with the protein synthesis inhibitor anisomycin also decreased basal LPS within control growth cones (Figure 4B). It is important to note that these experiments were performed on growth cones that were a minimum of 300 microns from their cell bodies which, coupled with brief puromycin incubation times, ensures that the nascent proteins were locally synthesized within growth cones.

Several groups have reported in amphibian and rodent animal models that a variety of axon guidance cues affect growth cone motility and guidance by modulating mTOR-dependent LPS[18,55,56], but similar findings have not been reported in human neurons. To first test whether guidance cues regulate LPS in human neuronal growth cones, we exposed control growth cones to puromycin at defined intervals before and after cue stimulation (Figure 4B-D). EphrinA1 has been shown to decrease protein synthesis in a variety of cell types, including developing neurites and growth cones[18,57]. We found this to be true in human neurons as well, as ephrin-treated growth cones showed significantly reduced puromycin incorporation (Figure 4C-D). Since we found that $TSC2^{+/-}$ neurons

only weakly respond to several cues, we considered that mTOR-dependent regulation of LPS in response to these cues may be defective, even though basal P-S6 (Fig 1D-E) and rates of protein synthesis are unaffected (Figure 4A-B). However, ephrin-A1 treatment reduced protein synthesis in $TSC2^{+/-}$ growth cones to a similar degree (Figure 4C-D). Furthermore, ephrin-A1 treatment also decreased puromycin incorporation in $TSC2^{-/-}$ growth cones, suggesting that protein synthesis regulation in response to this cue is independent of TSC2-mTOR. While Slit2 stimulation also leads to growth cone collapse (Figure 3D, Supplemental Figure 5), in contrast to ephrins, Slit2 increases protein synthesis in growth cones[56], which we confirmed in human neurons (Figure 4E). However, while $TSC2^{+/-}$ growth cones do not collapse in response to Slit2 (Figure 3D), they still exhibit increased protein synthesis in response to Slit2 (Figure 4E). To test whether LPS in response to Slit2 required mTOR, we co-treated neurons with rapamycin, which suppressed the increase in protein synthesis in both $TSC2^{+/+}$ and $TSC2^{+/-}$ neurons (Figure 4E and Supplemental Figure 6), suggesting that while mTOR promotes LPS in response to Slit2, this pathway is normal in a TSC2 haploinsufficiency background. We also found that $TSC2^{+/+}$ and $TSC2^{+/-}$ neurons increased protein synthesis in response to Netrin-1 (Supplemental Figure 6), a growth promoting guidance cue, in agreement with previous work[55,58,59]. Together, these results suggest that growth cones modulate LPS in response to guidance cues, and that this modulation is grossly normal in $TSC2^{+/-}$ growth cones.

$TSC2^{+/-}$ neurons are not guided by patterned inhibitory cues.

Considering that $TSC2^{+/-}$ hFB neurons are less sensitive to acute stimulation with guidance cues, we asked whether mutant hFB axons may also show improper repulsive guidance. To begin to test this notion, we first needed to determine whether normal developing hFB neurons could be guided through growth cone interactions with discontinuous patterns of inhibitory cues, which has yet to be demonstrated using iPSC-derived human neurons. hFB neurospheres were plated onto alternating stripes of LN (25µg/mL) and pre-clustered ephrin-A5-Fc (10µg/mL) or LN (control) (see Methods). After three DIV, neurons were fixed and immunolabeled for Fc to visualize ephrin and axons (cross-reactive), as well as phalloidin to label F-actin. As seen in Figure 5A, control axons are guided along stripes of pure LN and are robustly repelled from stripes of ephrin-A5. On the other hand, $TSC2^{+/-}$ neurons have long axons that crossed ephrin-A5 stripes repeatedly. We measured guidance along stripes using a modified Sholl analysis[36] by dividing each neurosphere into four quadrants (Figure 5B, inset), then pooling intersecting axons as they traveled parallel or perpendicular to the stripes. From Sholl analysis, it is clear that $TSC2^{+/+}$ control neurons extend further parallel to stripes compared to perpendicular (Figure 5B), while $TSC2^{+/-}$ neurons extend long axons across ephrin-A5 stripes quite indiscriminately (Figure 5A) and showed little preference for perpendicular versus parallel orientation (Figure 5B).

The total area of axons extending upon LN versus ephrin stripes was also measured to assess substratum preference (Figure 5C-E). Corrected control neurons showed robust avoidance of both ephrin-A5 and ephrin-A1 stripes (Figure 5C-D), while $TSC2^{+/-}$ neurons were not significantly repelled from stripes of either ephrin (Figure 5C-D). To confirm that

ephrin was responsible for avoidance behaviors, control neurons were plated upon stripes of unclustered ephrin-A5, since pre-clustering of ephrin-A5, but not ephrin-A1, is required for response to this cue in other model systems[60,61]. Indeed, we observed that control neurons showed no preference on unclustered ephrin-A5, confirming that ephrin protein itself was responsible, rather than discontinuous LN or Fc conjugate.

Next we used pharmacologic manipulations as described previously to test whether mTORC1/C2 inhibition could disrupt hFB axon guidance. Stripe assays were performed as described (Figure 5), with the addition of rapamycin at time of cell culture. Note that chronic rapamycin treatment inhibits both mTORC1 and mTORC2[62,63]. Consistent with our results with collapse assays (Figure 3), we found that chronic rapamycin treatment prevented guidance of control $TSC2^{+/+}$ hFB neurons on ephrin-A1 stripes (Figure 6A-B), suggesting either that active mTOR is necessary for guidance or that chronic proteomic changes disrupt guidance. Importantly, rapamycin treatment did not restore guidance of $TSC2^{+/-}$ neurons on patterned ephrin-A1 (Figure 6C-D), suggesting that misguidance is not due to hyper-active mTORC1/C2. We previously showed that Slit2 treatment activated protein synthesis (Figure 4) and caused growth cone collapse in $TSC2^{+/+}$ hFB neurons and that collapse was reduced in $TSC2^{+/-}$ neurons (Figure 3). To test whether hFB neurons can also be guided by Slit2, and if this requires normal TSC2 function and mTOR signaling, we performed Slit2 stripe assays on neurons +/- rapamycin. We show for the first time that control hFB neurons are effectively guided by patterned Slit2 (Figure 6C-D). However, similar to ephrin-A, $TSC2^{+/-}$ neurons are poorly guided by patterned Slit2 (Figure 6C-D). Moreover, while chronic rapamycin treatment blocks guidance of $TSC2^{+/+}$

neurons to Slit2 (Figure 6E-F), it does not restore guidance of $TSC2^{+/-}$ neurons (Figure 6K-L), similar to observations made with ephrin-A1. Guidance to the positive cue netrin-1 was also inhibited by rapamycin treatment (not shown). Together, these findings indicate that chronic mTORC1 activity is likely necessary downstream of ephrin-A, Slit2, and netrin-1, but that TSC2 functions independently of mTORC1 to regulate guidance by these cues.

RhoA signaling is reduced in $TSC2^{+/-}$ hFB neurons and growth cones.

Considering our results showing that basal neurite extension rates, as well as sensitivity to guidance cues, are abnormal in $TSC2^{+/-}$ neurites, while mTOR signaling appears unaffected, we looked to other possible downstream targets of TSC2. Studies in $TSC2^{-/-}$ cells have shown that RhoA, a Ras family small G protein, is regulated downstream of TSC1/TSC2 independent of mTOR complexes[64,65]. RhoA controls F-actin contractility within growth cones, which modulates both axon extension rate[66,67] and is required for collapse in response to several inhibitory axon guidance cues, including ephrin-A, Slit2, Semaphorins, and LPA[4,67,68]. To begin to test whether basal RhoA signals are altered in $TSC2^{+/-}$ growth cones, we first used a RhoA fluorescence resonance energy transfer (FRET) biosensor[35] to measure RhoA activity within $TSC2^{+/+}$ and $TSC2^{+/-}$ hFB growth cones. By performing acceptor photobleaching (i.e. donor-dequenching)[69], we found that FRET efficiency was lower in $TSC2^{+/-}$ compared to $TSC2^{+/+}$ growth cones, indicating lower baseline RhoA activity (Fig 7A), which may account for faster neurite extension rates by $TSC2^{+/-}$ neurons (Figure 2). To corroborate FRET results, we measured active RhoA from whole neurosphere cell lysates using a modified enzyme-linked immunosorbent assay (ELISA) for active RhoA (G-LISA, Cytoskeleton) and found that active RhoA also

appeared lower in $TSC2^{+/-}$ neurospheres compared to control neurospheres (Figure 7C). However, while basal RhoA activity was only modestly lower in $TSC2^{+/-}$ neurons, differences were more pronounced in response to ephrin-A1 treatment. Live neurosphere cultures were lysed after 5 min treatment with 2 µg/ml ephrin-A1 and RhoA was measured using G-LISA. Here we found that control $TSC2^{+/+}$ neurons showed robust activation of RhoA, while $TSC2^{+/-}$ neurons showed no activation (Figure 7B). These results suggest that basal levels of TSC2 are necessary for RhoA activation in human neurons downstream of ephrin-A1.

RhoA promotes actomyosin contractility by activating Rho-associated kinase (ROCK), which phosphorylates myosin light chain (MLC) directly and inactivates myosin light chain phosphatase (MLCP) to further elevate phospho-MLC (p-MLC)[70]. Therefore, the intensity of p-MLC immunolabeling provides a useful readout of RhoA activity and the strength of actomyosin contractility. Consistent with RhoA measurements, we found that basal p-MLC immunolabeling was lower in $TSC2^{+/-}$ compared to $TSC2^{+/+}$ growth cones (Figure 7D, F). To determine if TSC2 is necessary for acute activation of MLC by ephrin-A1, we treated $TSC2^{+/+}$ and $TSC2^{+/-}$ hFB neurons for 5 min with 2 µg/ml Ephrin-A1 prior to immunolabeling. Similar to RhoA activity measurements (Figure 7C), we observed strong activation of MLC in $TSC2^{+/+}$ hFB neurons after 5 min treatment with ephrin-A1, but little change in $TSC2^{+/-}$ hFB neurons (Figure 7E, F).

RhoA-ROCK-myosin regulates axon extension and guidance downstream of TSC2

Since RhoA and MLC activity appear lower in $TSC2^{+/-}$ hFB growth cones compared to control (Figure 7A-D), we hypothesized that inhibition of this pathway may differentially

affect axon extension by $TSC2^{+/+}$ compared to $TSC2^{+/-}$ neurons. To test this possibility, we treated neurons with RhoA-ROCK-myosin inhibitors and evaluated the effects on basal axon outgrowth and response to ephrin-A1. Interestingly, acute treatment of control $TSC2^{+/+}$ neurons with either ROCK (Y-27632) or myosin II (blebbistatin) inhibitors stimulated the rate of axon outgrowth to rates comparable with $TSC2^{+/-}$ neurites but had no significant effect on already rapid $TSC2^{+/-}$ neurite outgrowth (Figure 8A, B). These results suggest that the RhoA/ROCK/myosin II axis is minimally active in $TSC2^{+/-}$ growth cones so inhibition cannot further lower myosin activity, which is consistent with our direct measurements of this pathway (Figure 7A-D). To directly activate myosin II to test how this may affect axon extension by $TSC2^{+/+}$ and $TSC2^{+/-}$ neurons, we tested the effects of CalyculinA (CalyA). CalyA is a potent inhibitor of protein phosphatase 1 (PP1), which is the catalytic subunit of myosin light chain phosphatase[71]. Five min treatment with 200 pM CalyA increases p-MLC in $TSC2^{+/+}$ and $TSC2^{+/-}$ growth cones (Supplemental Figure 7) and inhibits axon extension by both genotypes (Figure 8B), suggesting that MLC-mediated actomyosin contractility can be activated in TSC2 mutant neurons and is sufficient to slow axon extension.

Next we tested how blocking the RhoA/ROCK/myosin II pathway affected ephrin-A1 induced collapse in $TSC2^{+/+}$ compared to $TSC2^{+/-}$ neurons. Pre-treatment of control hFB neurons with RhoA, ROCK or myosin II inhibitors prevented ephrin-A1 dependent collapse, confirming that ephrin-A1 signals through the RhoA pathway in human neurons (Figure 8C). However, $TSC2^{+/-}$ neurons, which are largely insensitive to ephrin-A1, are not further inhibited by blocking the RhoA pathway, suggesting this pathway is already

largely inactive in $TSC2^{+/-}$ neurons (Figure 8C). In contrast, activation of MLC with low dose CalyA, which slows outgrowth (Figure 8B), but does not collapse growth cones (not shown), sensitizes $TSC2^{+/-}$ neurons to ephrin-A1 mediated collapse (Figure 8C).

Finally, we tested whether RhoA signaling was necessary for guidance on ephrin-A1 stripes. $TSC2^{+/+}$ and $TSC2^{+/-}$ neurons were cultured in presence of Y-27632 on stripes of ephrin-A1. Control neurons with ROCK chronically inhibited showed no significant substratum preference (Figure 8D, E) and overall neuron lengths were increased (not shown). $TSC2^{+/-}$ hFB neurites, which normally are not guided by ephrin-A1 (Figure 4), showed no apparent effects from this treatment (Figure 8D, E). These data indicate that the RhoA/ROCK/myosin II pathway regulates axon extension and response to ephrin-A1, and loss of RhoA signaling phenocopies defects exhibited by $TSC2^{+/-}$ neurons.

Discussion

In this paper we show for the first time that hFB neurons differentiated from TSC patient-derived iPSCs exhibit several severe developmental abnormalities compared to their isogenic control counterparts. Axon extension by hFB neurons with heterozygous loss of TSC2 is two times faster than control neurons and $TSC2^{+/-}$ neurons are less sensitive to several inhibitory axon guidance cues (Figures 2 and 3). However, while $TSC2^{+/-}$ neurons show severe growth and axon guidance defects (Figure 5 and 6), mTOR signaling appears normal in $TSC2^{+/-}$ neurons but is robustly upregulated in $TSC2^{-/-}$ neurons (Figure 1). This result suggests that axon extension phenotypes may be due to mTOR-independent activities downstream of TSC2 (Figure 2 and 3). While

mTOR signaling is normal in TSC2$^{+/-}$ neurons, RhoA-ROCK-mediated actomyosin contractility is reduced in TSC2$^{+/-}$ growth cones (Figures 7 and 8). Together, our results suggest that TSC patients may have neural network connectivity abnormalities due to mTOR-independent TSC2 regulation of RhoA signaling.

TSC is a neurodevelopmental disorder characterized by cortical tubers and neural network connectivity defects[10]. While cortical tubers and lesions in other organ systems likely result from hyperactive mTORC1-mediated protein synthesis[72], the effects of TSC2 loss of function causing neuronal connectivity defects are less well understood. However, a number of studies using different animal model systems have established roles for local protein synthesis (LPS) downstream of axon guidance cues[73], suggesting that TSC2 may also regulate LPS within growth cones to control neural network wiring. If true, neural network abnormalities in TSC patients could be due to dysregulation of LPS within growth cones. In support of this notion, it was reported in rodent model neurons that activation of TSC2 downstream of EphrinA decreased mTOR-dependent LPS and that TSC2$^{+/-}$ neurons exhibited axon guidance defects *in vivo*[18]. Other reports showed that some guidance cues activate mTOR-dependent LPS in growth cones[74], leading us to hypothesize that defects in human neuron axon guidance in TSC patients were due to abnormal regulation of mTOR signaling. However, we were surprised to discover that the axon outgrowth and guidance defects we observed in TSC2$^{+/-}$ neurons were not due to abnormal mTOR signaling.

While many reports demonstrate that abnormal mTORC1 signaling is responsible for developmental defects associated with TSC pathogenic variants, we find in neuronal growth cones that TSC2 has mTOR-independent targets. Our surprising findings raise the important question: What downstream targets of TSC2 are responsible for abnormal axon developmental phenotypes exhibited by human neurons? There are several reports in the literature of mTOR-independent targets of TSC1/TSC2 in a variety of cell types[75]. However, interpretation of these studies is complicated, as many utilize homozygous null TSC1 or TSC2 cells, which express global proteomic changes from hyperactive mTOR. Nonetheless, potential TSC-associated targets that may affect outgrowth and guidance include FAK[76], HDACs[30], and p53[77], as well as the GTPase Rheb. A recent study utilizing a farnesylation-defective Rheb mutant observed mTORC1-independent enhanced axonal extension rates, consistent with our observations[78]. WT Rheb transfection in mouse RGCs also showed increased resistance to Ephrin-A1 induced collapse, suggesting Rheb may mediate TSC-dependent axon phenotypes[18]. Another potential downstream target of TSC1/2 is activation of Rho family GTPases. For example, TSC1 binds Ezrin-Radixin-Moesin (ERM) family proteins and activates RhoA to promote cell adhesion[79]. Consistent with these findings, homozygous knockout of TSC1 resulted in unstable TSC2 and a decrease in RhoA activity in a mouse fibroblast model[80]. On the other hand, the Krymskaya lab showed that stable transfection of TSC2 upregulated Rac1 at the expense of RhoA activity[64]. This group suggests a model in which TSC1 bound to TSC2 increases Rac1 activity at the expense of RhoA activation. It is possible that TSC2 has cell type specific activities, as well as unique targets within neuronal growth cones.

We observed robust phenotypes using heterozygous TSC2 mutant neurons, which is important for several reasons. First, while a minority of cells in some TSC patient tubers may be $TSC2^{-/-}$ due to a second hit mutation, in familial TSC patients with neuropathology, a vast majority of their neurons are $TSC2^{+/-}$, as well as most neurons in TSC patients that acquired early sporadic mutations[12]. Second, complete loss of TSC2 results in profound mTOR-dependent proteomic changes in cells[48], which confounds mechanistic interpretations. While heterozygous TSC2 neurons likely also exhibit some mTOR-dependent proteomic differences compared to wild type neurons, we show that we cannot rescue axon extension or guidance cue sensitivities even with chronic inhibition of mTOR. This result strongly suggests that proteomic changes do not account for the developmental phenotypes we observe in $TSC^{+/-}$ neurons. However, it is important to note that we do find that chronic mTOR inhibition substantially impacted the ability of normal neurons to be guided *in vitro*. Given the complex and overlapping roles of mTOR signaling in neurodevelopment, more studies are needed to inform clinical decisions with regard to pharmacological interventions in patient care.

Acknowledgments

We thank Erik Dent, Christopher Gomez, Kate Kalil, and members of the Gomez lab for comments on the manuscript. Thanks to the Dent, Huang, Kalil, and Roopra labs for reagents and advice. This work was supported, in part, by NIH Grant R21088477 and R01NS099405 (to TMG). TSC received support from grant T32 GM007215. AJM and

MMO were supported in part by University of Wisconsin-Madison Hilldale

Undergraduate Research Fellowships.

References

1. Gallo, G. & Letourneau, P. C. Regulation of Growth Cone Actin Filaments by Guidance Cues. *J. Neurobiol.* **58**, 92–102 (2004).

2. Lowery, L. A. & Vactor, D. Van. The trip of the tip : understanding the growth cone machinery. **10**, (2009).

3. Dent, E. W. *et al.* The Growth Cone Cytoskeleton in Axon. (2011). doi:10.1101/cshperspect.a001800

4. Hall, A. & Lalli, G. Rho and Ras GTPases in axon growth, guidance, and branching. *Cold Spring Harb. Perspect. Biol.* **2**, a001818 (2010).

5. Jung, H., Yoon, B. C. & Holt, C. E. Axonal mRNA localization and local protein synthesis in nervous system assembly, maintenance and repair. *Nat. Rev. Neurosci.* **13**, 308–324 (2012).

6. Battum, E. Y. Van, Brignani, S. & Pasterkamp, R. J. Axon guidance proteins in neurological disorders. *Lancet Glob. Heal.* **4422**, (2015).

7. Nugent, A. A., Kolpak, A. L. & Engle, E. C. Human disorders of axon guidance. *Curr. Opin. Neurobiol.* **22**, 837–843

8. McFadden, K. & Minshew, N. J. Evidence for dysregulation of axonal growth and guidance in the etiology of ASD. *Frontiers in Human Neuroscience* (2013). doi:10.3389/fnhum.2013.00671

9. Salussolia, C. L., Klonowska, K., Kwiatkowski, D. J. & Sahin, M. Genetic Etiologies, Diagnosis, and Treatment of Tuberous Sclerosis Complex. *Annu. Rev. Genomics Hum. Genet.* **20**, 217–240 (2019).

10. Gomez, M. R., Sampson, J. & Whittemore, V. *Tuberous Sclerosis Complex*. (Oxford University Press, 1999).

11. Van Eeghen, A. M., Black, M. E., Pulsifer, M. B., Kwiatkowski, D. J. & Thiele, E. A. Genotype and cognitive phenotype of patients with tuberous sclerosis complex. *Eur. J. Hum. Genet.* **20**, 510–515 (2012).

12. Martin, K. R. *et al.* Martin, Katie R. et al. 2017. “The Genomic Landscape of Tuberous Sclerosis Complex.” Nature Communications 8(May): 15816. http://www.nature.com/doifinder/10.1038/ncomms15816.The genomic landscape

of tuberous sclerosis complex. *Nat. Commun.* **8**, 15816 (2017).

13. Widjaja, E. *et al.* Diffusion tensor imaging identifies changes in normal-appearing white matter within the epileptogenic zone in tuberous sclerosis complex. *Epilepsy Res.* **89**, 246–53 (2010).

14. Baumer, F. M. *et al.* Longitudinal changes in diffusion properties in white matter pathways of children with tuberous sclerosis complex. *Pediatr. Neurol.* **52**, 615–623 (2015).

15. Im, K. *et al.* Altered Structural Brain Networks in Tuberous Sclerosis Complex. *Cereb. Cortex* **26**, 2046–2058 (2016).

16. Goorden, S. M. I., van Woerden, G. M., van der Weerd, L., Cheadle, J. P. & Elgersma, Y. Cognitive deficits in Tsc1+/- mice in the absence of cerebral lesions and seizures. *Ann. Neurol.* **62**, 648–55 (2007).

17. Tsai, P. & Sahin, M. Mechanisms of neurocognitive dysfunction and therapeutic considerations in tuberous sclerosis complex. *Curr. Opin. Neurol.* **24**, 106–13 (2011).

18. Nie, D. *et al.* Tsc2-Rheb signaling regulates EphA-mediated axon guidance. *Nat. Neurosci.* **13**, 163–172 (2010).

19. Ban, H. *et al.* Efficient generation of transgene-free human induced pluripotent stem cells (iPSCs) by temperature-sensitive Sendai virus vectors. *Proc. Natl. Acad. Sci. U. S. A.* **108**, 14234–14239 (2011).

20. Yang, L. *et al.* Optimization of scarless human stem cell genome editing. *Nucleic Acids Res.* **41**, 9049–61 (2013).

21. Chen, Y. *et al.* Engineering Human Stem Cell Lines with Inducible Gene Knockout using CRISPR/Cas9. *Cell Stem Cell* **17**, 233–244 (2015).

22. Doers, M. E. *et al.* iPSC-Derived Forebrain Neurons from FXS Individuals Show Defects in Initial Neurite Outgrowth. *Stem Cells Dev.* (2014). doi:10.1089/scd.2014.0030

23. Du, Z. W. *et al.* Generation and expansion of highly pure motor neuron progenitors from human pluripotent stem cells. *Nat. Commun.* (2015). doi:10.1038/ncomms7626

24. Santiago-Medina, M., Myers, J. P. & Gomez, T. M. Imaging Adhesion and Signaling Dynamics in Xenopus laevis Growth Cones. *Dev. Neurobiol.* 585–599 (2011). doi:10.1002/dneu.20886

25. Longair, M. H., Baker, D. A. & Armstrong, J. D. Simple Neurite Tracer: open source software for reconstruction, visualization and analysis of neuronal

processes. *Bioinformatics* **27**, 2453–4 (2011).

26. Schindelin, J. *et al.* Fiji: An open-source platform for biological-image analysis. *Nature Methods* **9**, 676–682 (2012).

27. Schneider, C. A., Rasband, W. S. & Eliceiri, K. W. NIH Image to ImageJ: 25 years of image analysis. *Nature Methods* **9**, 671–675 (2012).

28. Rueden, C. T. *et al.* ImageJ2: ImageJ for the next generation of scientific image data. *BMC Bioinformatics* **18**, (2017).

29. Li, K. The image stabilizer plugin for ImageJ. Available at: http://www.cs.cmu.edu/~kangli/code/Image_Stabilizer.html.

30. Basu, T. *et al.* Histone deacetylase inhibitors restore normal hippocampal synaptic plasticity and seizure threshold in a mouse model of Tuberous Sclerosis Complex. *Sci. Rep.* **9**, 1–11 (2019).

31. Kerstein, P. C. *et al.* Mechanosensitive TRPC1 channels promote calpain proteolysis of talin to regulate spinal axon outgrowth. *J. Neurosci.* **33**, 273–285 (2013).

32. Schmidt, E. K., Clavarino, G., Ceppi, M. & Pierre, P. SUnSET, a nonradioactive method to monitor protein synthesis. *Nat. Methods* **6**, 275–277 (2009).

33. Zhang, Y., Vanoli, F., LaRocque, J. R., Krawczyk, P. M. & Jasin, M. Biallelic targeting of expressed genes in mouse embryonic stem cells using the Cas9 system. *Methods* **69**, 171–178 (2014).

34. Karpova, T. & McNally, J. G. Detecting Protein-Protein Interactions with CFP-YFP FRET by Acceptor Photobleaching. in *Current Protocols in Cytometry* (John Wiley & Sons, Inc., 2006). doi:10.1002/0471142956.cy1207s35

35. Pertz, O., Hodgson, L., Klemke, R. L. & Hahn, K. M. Spatiotemporal dynamics of RhoA activity in migrating cells. *Nature* **440**, 1069–72 (2006).

36. Ferreira, T. A. *et al.* Neuronal morphometry directly from bitmap images. *Nature Methods* **11**, 982–984 (2014).

37. Zhang, S. C., Wernig, M., Duncan, I. D., Brüstle, O. & Thomson, J. A. In vitro differentiation of transplantable neural precursors from human embryonic stem cells. *Nat. Biotechnol.* **19**, 1129–1133 (2001).

38. Yuan, F. *et al.* Efficient generation of region-specific forebrain neurons from human pluripotent stem cells under highly defined condition. *Sci. Rep.* **5**, 1–11 (2015).

39. Meyuhas, O. Ribosomal Protein S6 Phosphorylation: Four Decades of Research.

Int. Rev. Cell Mol. Biol. **320**, 41–73 (2015).

40. Biever, A., Valjent, E. & Puighermanal, E. Ribosomal protein S6 phosphorylation in the nervous system: From regulation to function. *Front. Mol. Neurosci.* **8**, (2015).

41. Costa, V. *et al.* MTORC1 Inhibition Corrects Neurodevelopmental and Synaptic Alterations in a Human Stem Cell Model of Tuberous Sclerosis. *Cell Rep.* **15**, 86–95 (2016).

42. Blair, J. D., Hockemeyer, D. & Bateup, H. S. Genetically engineered human cortical spheroid models of tuberous sclerosis. *Nat. Med.* **24**, 1568–1578 (2018).

43. Chi, O. Z. *et al.* Restoration of Normal Cerebral Oxygen Consumption with Rapamycin Treatment in a Rat Model of Autism–Tuberous Sclerosis. *NeuroMolecular Med.* **17**, 305–313 (2015).

44. Sen, A., Kallos, M. S. & Behie, L. A. New tissue dissociation protocol for scaled-up production of neural stem cells in suspension bioreactors. *Tissue Eng.* **10**, 904–13

45. Jacinto, E. *et al.* Mammalian TOR complex 2 controls the actin cytoskeleton and is rapamycin insensitive. *Nat. Cell Biol.* **6**, 1122–8 (2004).

46. Thoreen, C. C. *et al.* An ATP-competitive Mammalian Target of Rapamycin Inhibitor Reveals Rapamycin-resistant Functions. *J. Biol. Chem.* **284**, 8023–8032 (2009).

47. Benavides-Serrato, A. *et al.* Specific blockade of Rictor-mTOR association inhibits mTORC2 activity and is cytotoxic in glioblastoma. *PLoS One* **12**, (2017).

48. Grabole, N. *et al.* Genomic analysis of the molecular neuropathology of tuberous sclerosis using a human stem cell model. *Genome Med.* **8**, 1–14 (2016).

49. Choi, Y. J. *et al.* Tuberous sclerosis complex proteins control axon formation. *Genes Dev.* **22**, 2485–2495 (2008).

50. Ruppe, V. *et al.* Developmental brain abnormalities in tuberous sclerosis complex: A comparative tissue analysis of cortical tubers and perituberal cortex. *Epilepsia* **55**, 539–550 (2014).

51. Nédelec, S. *et al.* Concentration-Dependent Requirement for Local Protein Synthesis in Motor Neuron Subtype-Specific Response to Axon Guidance Cues. **32**, 1496–1506 (2012).

52. Cord, B. J. *et al.* Characterization of axon guidance cue sensitivity of human embryonic stem cell-derived dopaminergic neurons. *Mol. Cell. Neurosci.* **45**, 324–34 (2010).

53. Giandomenico, S. L. *et al.* Cerebral organoids at the air–liquid interface generate diverse nerve tracts with functional output. *Nat. Neurosci.* **22**, 669–679 (2019).

54. Cioni, J. M. *et al.* Late Endosomes Act as mRNA Translation Platforms and Sustain Mitochondria in Axons. *Cell* **176**, 56-72.e15 (2019).

55. Campbell, D. S. & Holt, C. E. Chemotropic responses of retinal growth cones mediated by rapid local protein synthesis and degradation. *Neuron* **32**, 1013–1026 (2001).

56. Piper, M. *et al.* Signaling mechanisms underlying Slit2-induced collapse of Xenopus retinal growth cones. *Neuron* **49**, 215–228 (2006).

57. Gouveia Roque, C. & Holt, C. E. Growth cone tctp is dynamically regulated by guidance cues. *Front. Mol. Neurosci.* **11**, (2018).

58. Leung, K. M. *et al.* Asymmetrical β-actin mRNA translation in growth cones mediates attractive turning to netrin-1. *Nat. Neurosci.* **9**, 1247–1256 (2006).

59. Inoki, K., Zhu, T. & Guan, K.-L. TSC2 Mediates Cellular Energy Response to Control Cell Growth and Survival phosphorylation decreases the ability of TSC2 to inhibit the phosphorylation of ribosomal S6 kinase (S6K) and eukaryotic initiation factor 4E binding protein-1 (4EBP1). *Cell* **115**, 577–590 (2003).

60. Wykosky, J. *et al.* Soluble monomeric EphrinA1 is released from tumor cells and is a functional ligand for the EphA2 receptor. 7260–7273 (2008). doi:10.1038/onc.2008.328

61. Regeneron, G. *et al.* Ligands for EPH-related receptor tyrosine kinases that require membrane attachment or clustering for activity. *Science (80-.).* **266**, 816–819 (1994).

62. Lamming, D. W. *et al.* Rapamycin-induced insulin resistance is mediated by mTORC2 loss and uncoupled from longevity. *Science* **335**, 1638–43 (2012).

63. Sarbassov, D. D. *et al.* Prolonged Rapamycin Treatment Inhibits mTORC2 Assembly and Akt/PKB. *Mol. Cell* **22**, 159–168 (2006).

64. Goncharova, E., Goncharov, D., Noonan, D. & Krymskaya, V. P. TSC2 modulates actin cytoskeleton and focal adhesion through TSC1-binding domain and the Rac1 GTPase. *J. Cell Biol.* **167**, 1171–1182 (2004).

65. Goncharova, E. A., Goncharov, D. A., Lim, P. N., Noonan, D. & Krymskaya, V. P. Modulation of cell migration and invasiveness by tumor suppressor TSC2 in lymphangioleiomyomatosis. *Am. J. Respir. Cell Mol. Biol.* **34**, 473–480 (2006).

66. Woo, S. & Gomez, T. M. Rac1 and RhoA Promote Neurite Outgrowth through Formation and Stabilization of Growth Cone Point Contacts. **26**, 1418–1428

(2006).

67. Jalink, K. *et al.* Inhibition of lysophosphatidate- and thrombin-induced neurite retraction and neuronal cell rounding by ADP ribosylation of the small GTP-binding protein Rho. *J. Cell Biol.* **126**, 801–810 (1994).

68. Murray, A., Naeem, A., Barnes, S. H., Drescher, U. & Guthrie, S. Slit and Netrin-1 guide cranial motor axon pathfinding via Rho-kinase, myosin light chain kinase and myosin II. *Neural Dev.* **5**, (2010).

69. Karpova, T. S. *et al.* Fluorescence resonance energy transfer from cyan to yellow fluorescent protein detected by acceptor photobleaching using confocal microscopy and a single laser. *J. Microsc.* **209**, 56–70 (2003).

70. Burridge, K., Monaghan-Benson, E. & Graham, D. M. Mechanotransduction: From the cell surface to the nucleus via RhoA. *Philosophical Transactions of the Royal Society B: Biological Sciences* **374**, (2019).

71. Hoffman, A., Taleski, G. & Sontag, E. The protein serine/threonine phosphatases PP2A, PP1 and calcineurin: A triple threat in the regulation of the neuronal cytoskeleton. *Molecular and Cellular Neuroscience* **84**, 119–131 (2017).

72. Cotter, J. A. An update on the central nervous system manifestations of tuberous sclerosis complex. *Acta Neuropathol.* (2019). doi:10.1007/s00401-019-02003-1

73. Cioni, J.-M., Koppers, M. & Holt, C. E. Molecular control of local translation in axon development and maintenance. *Curr. Opin. Neurobiol.* **51**, 86–94 (2018).

74. Jung, H., Gkogkas, C. G., Sonenberg, N. & Holt, C. E. Remote control of gene function by local translation. *Cell* **157**, 26–40 (2014).

75. Neuman, N. A. & Henske, E. P. Non-canonical functions of the tuberous sclerosis complex-Rheb signalling axis. *EMBO Mol. Med.* **3**, 189–200 (2011).

76. Gan, B., Yoo, Y. & Guan, J. L. Association of focal adhesion kinase with tuberous sclerosis complex 2 in the regulation of S6 kinase activation and cell growth. *J. Biol. Chem.* **281**, 37321–37329 (2006).

77. Armstrong, L. C. *et al.* Heterozygous loss of TSC2 alters p53 signaling and human stem cell reprogramming. *Hum. Mol. Genet.* **26**, 4629–4641 (2017).

78. Choi, S. *et al.* Farnesylation-defective rheb increases axonal length independently of mTORC1 activity in embryonic primary neurons. *Exp. Neurobiol.* **28**, 172–182 (2019).

79. Lamb, R. F. *et al.* The TSC1 tumour suppressor hamartin regulates cell adhesion through ERM proteins and the GTPase Rho. *Nat. Cell Biol.* **2**, 281–287 (2000).

80. Astrinidis, A. *et al.* Tuberin, the tuberous sclerosis complex 2 tumor suppressor gene product, regulates Rho activation, cell adhesion and migration. *Oncogene* **21**, 8470–8476 (2002).

Figure 1: Growth cones of hFB neurons differentiated from WT and TSC2 mutant iPSCs have reduced TSC2 expression and increased mTOR signaling. **A.** hFB neuronal growth cones of indicated genotype immunolabeled for TSC2 (green) and counter-stained for F-actin (magenta) in merge. Note complete absence of TSC2 in null growth cone. **B.** Average fluorescence intensity values of TSC2 in all measured growth cones. **C.** Western blots from extracted hFB neurospheres of each genotype showed similar reduction and absence of TSC2 in heterozygous and null TSC2 lines, respectively. Western blots also showed increased phospho-S6 (p-S6), a downstream target of mTORC1, only in $TSC2^{-/-}$ neurons, while total S6 was unchanged. **D.** hFB neuronal growth cones of indicated genotype immunolabeled for p-S6 (green) and counter-stained for F-actin (magenta) in merge. Fluorescence intensity values of phospho-S6 immunofluorescence, in all measured growth cones, with average values indicated ±SEM. Note that similar to Western blot results, P-S6 was elevated only in TSC2 null growth cones.****P<0.0001. One-way ANOVA with Tukey's Multiple Comparison. Scale, 5 μm.

Figure 1

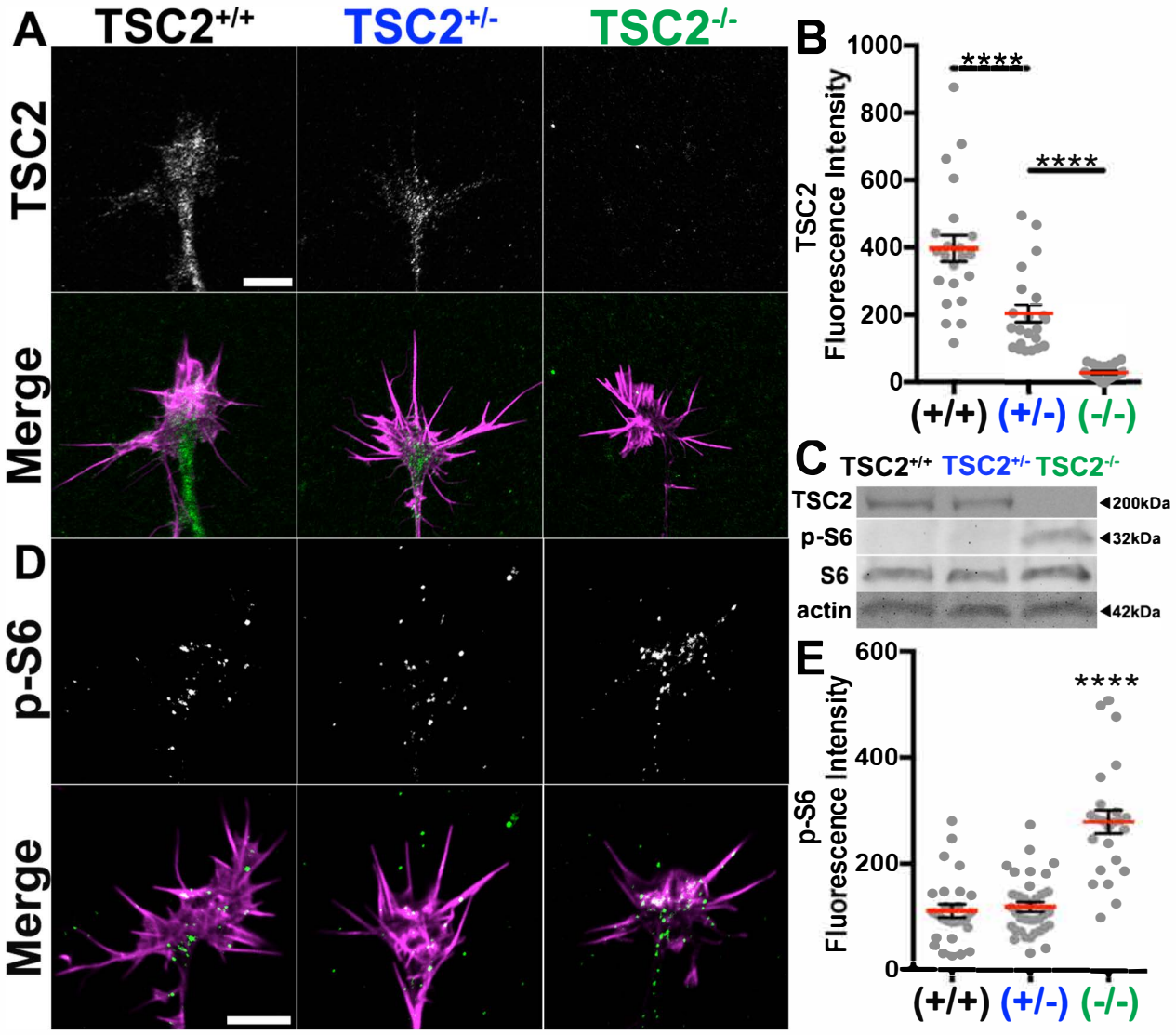
A
TSC2+/+
TSC2+/-
TSC2-/-
TSC2
Merge
D
p-S6
Merge
B
TSC2 Fluorescence Intensity
1000
800
600
400
200
0
****
****
(+/+) (+/-) (-/-)
C
TSC2+/+ TSC2+/- TSC2-/-
TSC2
p-S6
S6
actin
200kDa
32kDa
42kDa
E
p-S6 Fluorescence Intensity
600
400
200
0
****
(+/+) (+/-) (-/-)

Figure 2: TSC2 mutant hFB neurons exhibit enhanced neurite extension compared to isogenic control neurons, which is independent of mTOR. **A.** hFB neurospheres of indicated genotype after one day *in vitro* immunolabeled for Acetylated-tubulin (green) and counter-stained for F-actin (magenta). Note longer axons extend from both $TSC2^{+/-}$ and $TSC2^{-/-}$ neurospheres compared to isogenic control neurons. **B.** Average neurite lengths of 20 longest axons per neurosphere of each genotype. **C.** Live cell, differential interference contrast (DIC) imaging of growing axons from $TSC2^{+/+}$ and $TSC2^{+/-}$ hFB neurons at 15 min time intervals. **D.** Average axon extension rates show that $TSC2^{+/-}$ hFB neurites grew markedly faster compared to isogenic control neurons and TSC2 null neurons, as well as hFB neurons differentiated from unrelated control iPSCs (IMR90) and ESCs (WA09). **E,F.** Axon extension rates of $TSC2^{+/+}$ and $TSC2^{+/-}$ hFB neurons were not significantly affected by mTORC1 or mTORC2 inhibitors that were applied acutely (**E**, 1 hr) or chronically (**F**, 24 hrs or as indicated). *P<0.05, ****P<0.0001. One-way ANOVA with Tukey's Multiple Comparison. Scale, 100 μm (A), 5 μm (C).

Figure 2

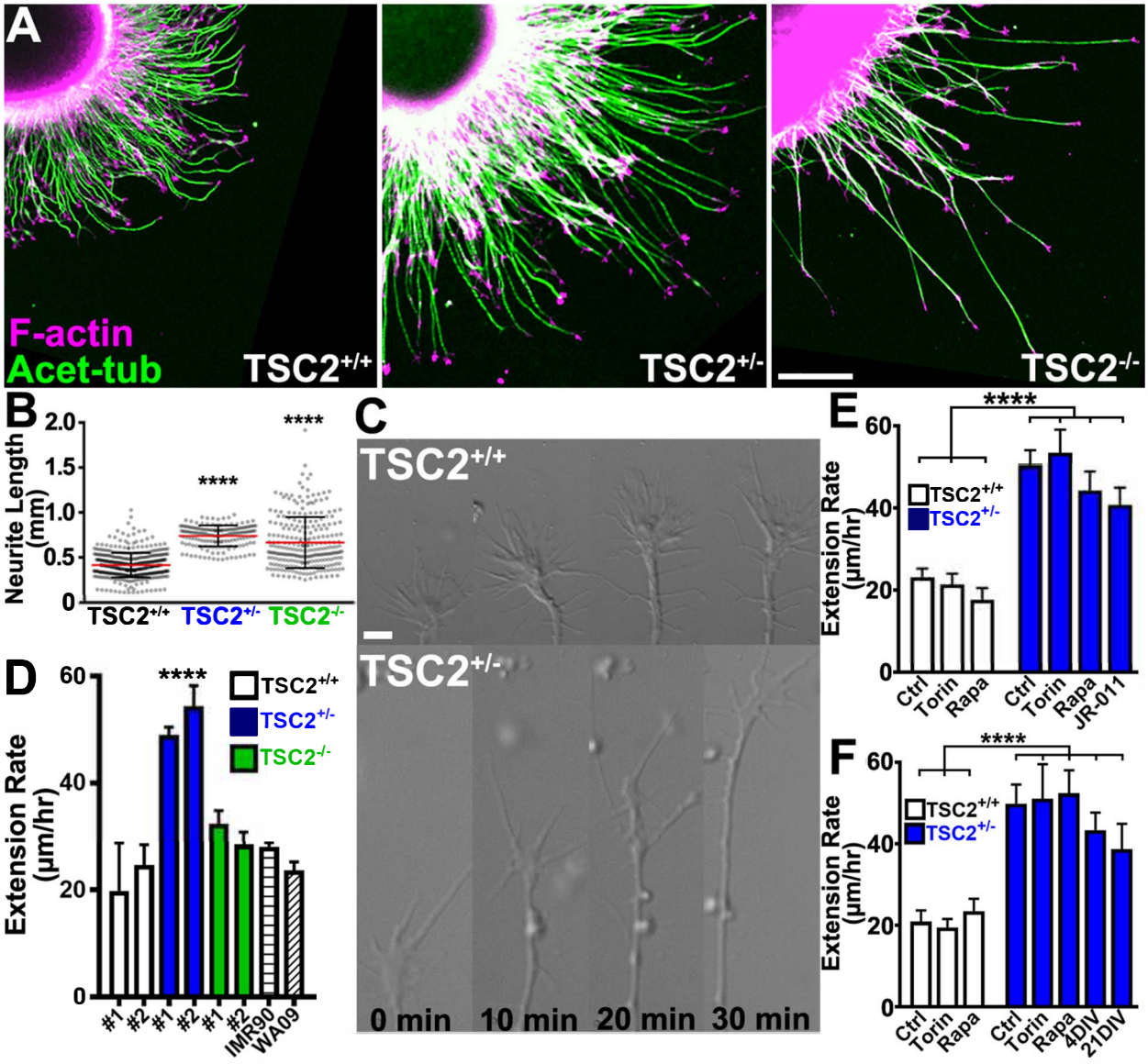
A
F-actin
Acet-tub
TSC2+/+
TSC2+/-
TSC2-/-
B
Neurite Length (mm)
2.0
1.5
1.0
0.5
0
****
****
TSC2+/+
TSC2+/-
TSC2-/-
C
TSC2+/+
TSC2+/-
0 min
10 min
20 min
30 min
D
Extension Rate (µm/hr)
60
40
20
0
****
TSC2+/+
TSC2+/-
TSC2-/-
#1
#2
#1
#2
#1
#2
IMR90
WA09
E
Extension Rate (µm/hr)
60
40
20
0
****
TSC2+/+
TSC2+/-
Ctrl
Torin
Rapa
Ctrl
Torin
Rapa
JR-011
F
Extension Rate (µm/hr)
60
40
20
0
****
TSC2+/+
TSC2+/-
Ctrl
Torin
Rapa
Ctrl
Torin
Rapa
4DIV
21DIV

Figure 3: $TSC2^{+/-}$ neurites are less sensitive to inhibitory guidance factors. A. $TSC2^{+/+}$ and $TSC2^{+/-}$ hFB neurons were acutely treated with ephrin-A1 (2µg/mL) over indicated time. Note the rapid collapse of the $TSC2^{+/+}$ growth cone, but only pausing of the $TSC2^{+/-}$ growth cone. **B-C**. Neurite extension rates normalized to pre-application extension rates for high (**B**) and low dose ephrin-A1 (**C**). In response to 2 µg/ml ephrin-A1, $TSC2^{+/+}$ neurites retracted within minutes and rarely restored outgrowth, while $TSC2^{+/-}$ neurites only transiently paused extension. In response to 0.2µg/ml ephrin-A1, $TSC2^{+/+}$ neurites slowly retracted while $TSC2^{+/-}$ neurites showed little effect. **D.** Analysis of percent growth cone collapse by $TSC2^{+/+}$ and $TSC2^{+/-}$ hFB neurons in response to ephrin-A1 and Slit2 (in µg/ml), as well as LPA (in µM). $TSC2^{+/-}$ growth cones failed to collapse in response to the repulsive cue Slit2 or to a low dose of the GPCR ligand and RhoA pathway activator lysophosphatidic acid (LPA) (100nM). A higher dose of LPA (1µM) induced collapse in $TSC2^{+/-}$ growth cones. **E.** Acute mTOR modulation with 30 min pre-incubation had no effect on collapse response of $TSC2^{+/+}$ growth cones and failed to rescue cue response in $TSC2^{+/-}$ growth cones. mTORC1 was specifically inhibited with acute rapamycin (40nM), mTORC1/C2 were both inhibited with torin-1 (100nM), and mTORC2 was specifically inhibited with JR-AB2-011 (1µM). **F.** Chronic (24hr) mTOR inhibition with rapamycin (40 nM) or torin-1 (100 nM) reduced the sensitivity of $TSC2^{+/+}$ growth cones to ephrin-A1 but did not significantly affect $TSC2^{+/-}$ growth cones. Long-term treatment with low dose rapamycin (5nM) throughout differentiation also failed to modulate the collapse response of $TSC2^{+/-}$ neurons. ** $p<0.01$, # $p<0.0001$, One-way ANOVA with Tukey's Multiple Comparison. Scale, 5 µm.

Figure 3

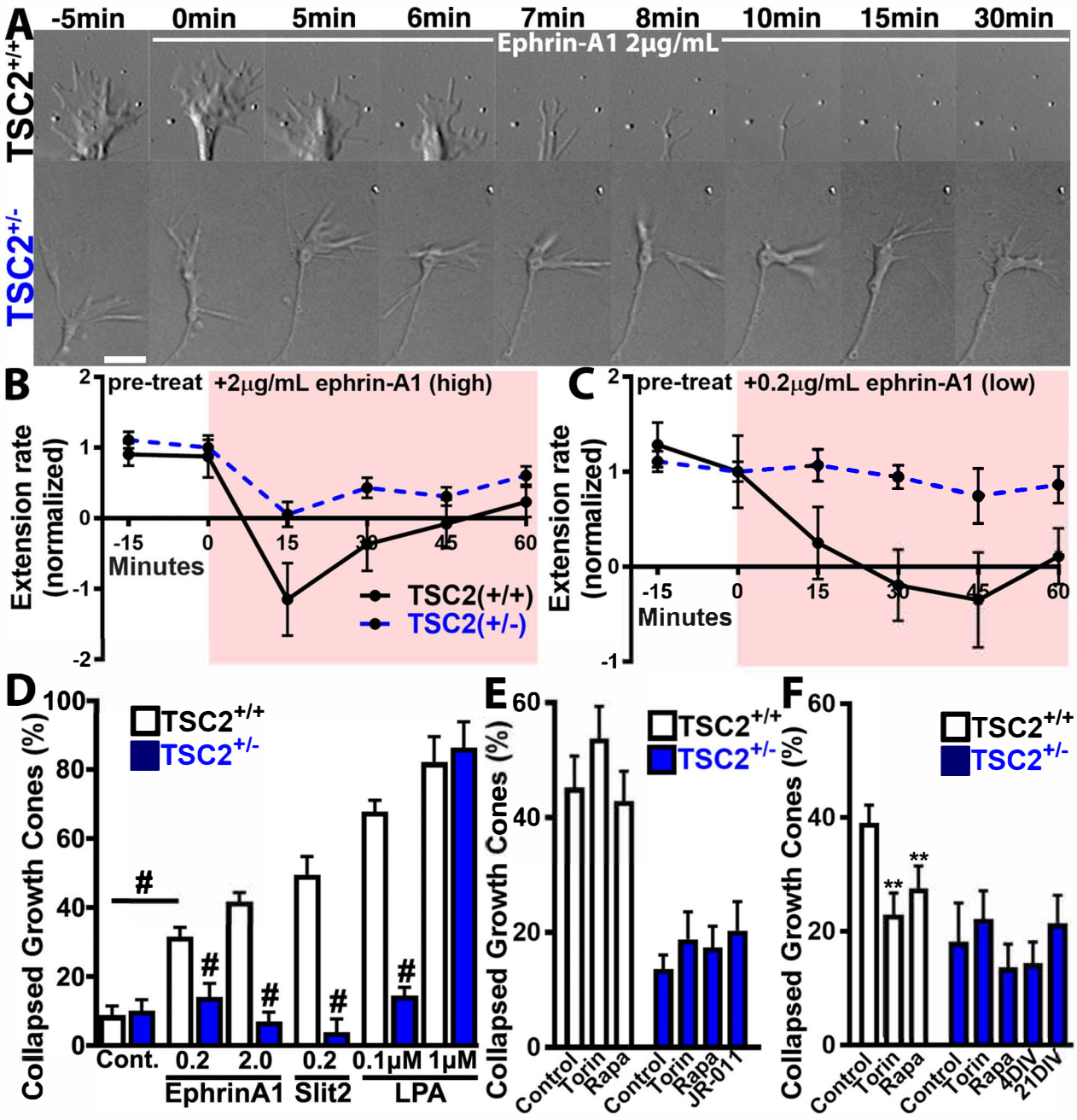
A
-5min
0min
5min
6min
7min
8min
10min
15min
30min
Ephrin-A1 2µg/mL
TSC2+/+
TSC2+/-
B
pre-treat
+2µg/mL ephrin-A1 (high)
Extension rate (normalized)
Minutes
TSC2(+/+)
TSC2(+/-)
C
pre-treat
+0.2µg/mL ephrin-A1 (low)
Extension rate (normalized)
Minutes
D
Collapsed Growth Cones (%)
TSC2+/+
TSC2+/-
Cont.
0.2
2.0
0.2
0.1µM
1µM
EphrinA1
Slit2
LPA
E
Collapsed Growth Cones (%)
TSC2+/+
TSC2+/-
Control
Torin
Rapa
Control
Torin
Rapa
JR-011
F
Collapsed Growth Cones (%)
TSC2+/+
TSC2+/-
Control
Torin
Rapa
Control
Torin
Rapa
4DIV
21DIV

Figure 4: $TSC2^{+/+}$ and $TSC2^{+/-}$ hFB growth cones modulate protein synthesis in response to cues. A. Puromycin labeled growth cones (green in merges) of indicated genotypes with and without ephrin-A1 treatment and counter-stained for F-actin (magenta in merges). Puromycin-labeled proteins were detected with anti-puromycin antibody (see methods). **B.** Normalized fluorescence intensities (to untreated control growth cones) show that basal local protein synthesis (LPS) rates were not significantly different between $TSC2^{+/+}$ and $TSC2^{+/-}$ hFB growth cones, while $TSC2^{-/-}$ growth cones show a marked increase in LPS. LPS was inhibited with 30min pre-incubation of rapamycin (40nM) or anisomycin (40nM), and rapamycin incubation restored the rate of LPS by $TSC2^{-/-}$ neurons down to control levels. **C-D.** LPS within the growth cones was significantly reduced by EphrinA1 (2µg/mL) treatment in all genotypes. **E.** Ten min. treatment with Slit2 (200ng/mL) and netrin-1 (100ng/mL) increased PS in $TSC2^{+/+}$ and $TSC2^{+/-}$ hFB growth cones. Slit2-mediated LPS was sensitive to rapamycin in both $TSC2^{+/+}$ and $TSC2^{+/-}$ hFB growth cones. One-way ANOVA with Tukey's Multiple Comparison, ****$p < .0001$ (between $TSC2^{+/+}$ and $TSC2^{-/-}$ hFB growth cones), * $p < 0.05$, *** $p<0.001$, # $p < 0.0001$. Scale, 5µm.

Figure 4

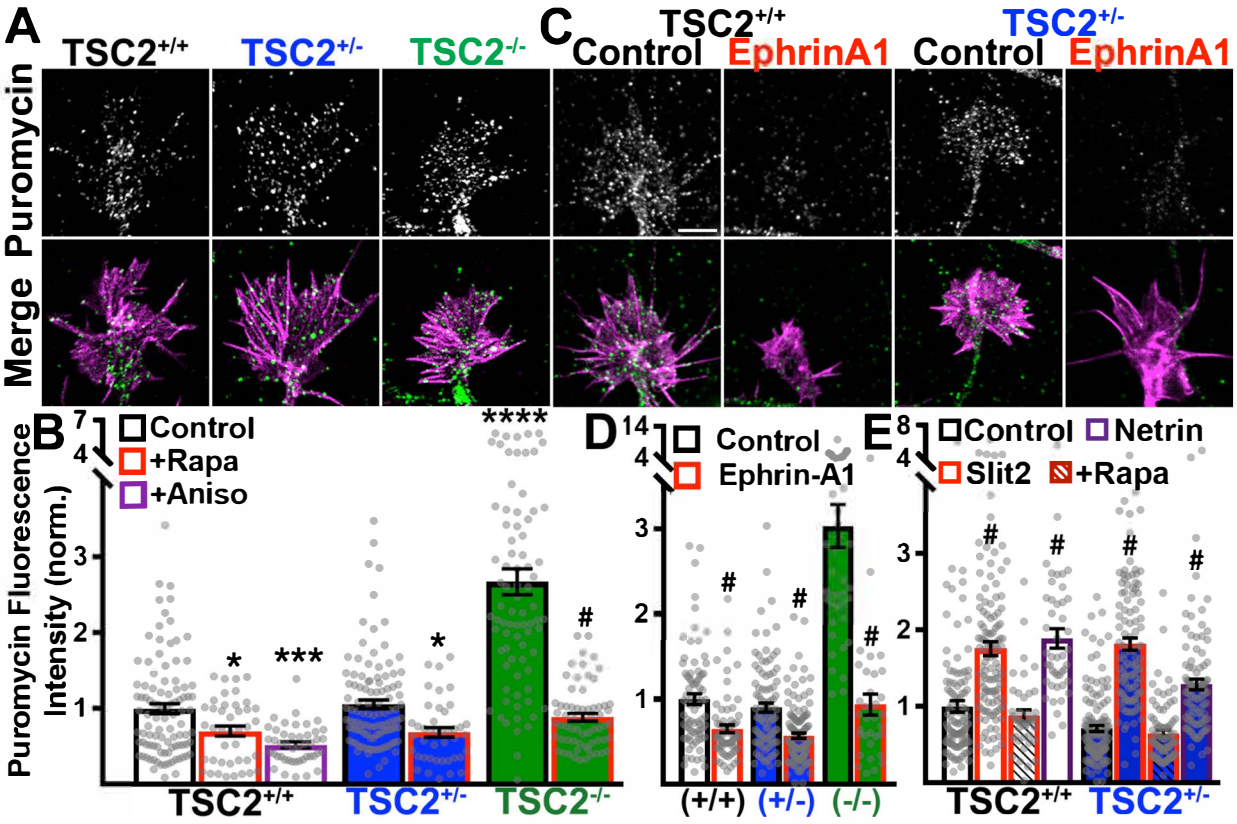
A
TSC2+/+
TSC2+/-
TSC2-/-
Puromycin
Merge
C
TSC2+/+
Control
EphrinA1
TSC2+/-
Control
EphrinA1
B
Puromycin Fluorescence Intensity (norm.)
Control
+Rapa
+Aniso
****
*
***
*
#
TSC2+/+
TSC2+/-
TSC2-/-
D
Control
Ephrin-A1
#
#
#
(+/+)
(+/-)
(-/-)
E
Control
Netrin
Slit2
+Rapa
#
#
#
#
TSC2+/+
TSC2+/-

Figure 5: Repulsive guidance of control hFB neurons by ephrinA is lost in TSC2$^{+/-}$ hFB neurons. **A.** hFB neurospheres were cultured for three days on parallel stripes of Fc-tagged ephrin-A5 and laminin (LN), then fixed and stained for anti-Fc (green in merges) and F-actin (magenta in merges). Note that anti-Fc antibody cross-reacts with neurites, making processes appear white in merge. Many TSC2$^{+/+}$ neurites extended upon LN, parallel to the pattern, while avoiding the ephrin-A5 stripes. On the other hand, TSC2$^{+/-}$ hFB neurites showed little substratum preference, crossing ephrin-containing lanes repeatedly. **B.** Modified Sholl analysis measures neurite crossings of concentric circles every 10 μm away from sphere edge, with data binned by quadrant for neurites extending parallel and perpendicular to stripes (inset). Note long TSC2$^{+/-}$ neurites extended equally well in all directions from spheres. C, D. High magnification images of LN/ephrin-A5 patterns (C) and analysis (D) of thresholded area occupied by neurites (F-actin channel) on each substratum normalized to the area of neurites growing on laminin only (see Methods). **E, F**. Similar images and analysis for LN/ephrin-A1 patterns. Note that TSC2$^{+/+}$ neurites were robustly guided by both ephrinAs, while TSC2$^{+/-}$ neurites failed to guide. **G, H.** TSC2$^{+/+}$ hFB neurites grown on unclustered ephrin-A5 controls were not guided. #$p < 0.0001$, Student's t-test. Scale, 500 μm (A), 100 μm (C-G).

Figure 5

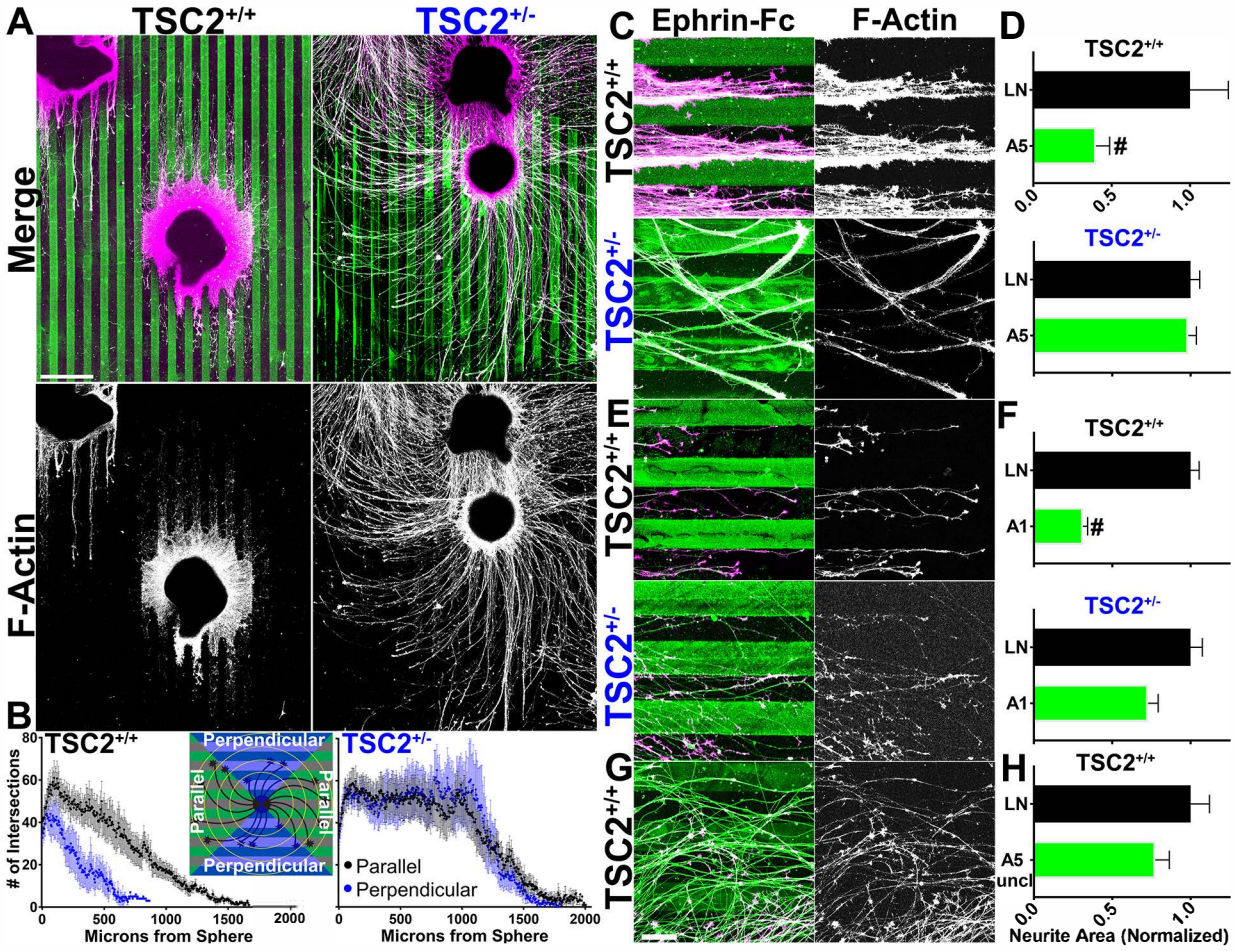
A
TSC2+/+
TSC2+/-
Merge
F-Actin
B
TSC2+/+
TSC2+/-
Perpendicular
Parallel
Parallel
Perpendicular
# of Intersections
Microns from Sphere
Parallel
Perpendicular
C
Ephrin-Fc
F-Actin
TSC2+/+
TSC2+/-
D
TSC2+/+
LN
A5
#
TSC2+/-
LN
A5
E
TSC2+/+
TSC2+/-
F
TSC2+/+
LN
A1
#
TSC2+/-
LN
A1
G
TSC2+/+
H
TSC2+/+
LN
A5
uncl
Neurite Area (Normalized)

Figure 6: Chronic mTOR inhibition prevents guidance by repulsive cues. Analysis of thresholded area occupied by neurites (F-actin channel) normalized to the area of neurites growing on laminin only for ephrin-A1 and Slit2 patterns, as described previously. **A, B.** Inhibition of mTOR with rapamycin (40nM) blocked guidance of $TSC2^{+/+}$ neurites on patterned ephrin-A1 (10µg/mL) and failed to rescue $TSC2^{+/-}$ mis-guidance. **C, D.** $TSC2^{+/+}$ hFB neurons, but not $TSC2^{+/-}$ neurons were guided by patterned LN and Slit2 (1µg/mL) . **E, F.** Guidance of $TSC2^{+/+}$ on patterned Slit2 was blocked by chronic mTOR inhibition with rapamycin and rapamycin failed to rescue $TSC2^{+/-}$ mis-guidance #$p < 0.0001$, Student's t-test. Scale, 100 µm.

Figure 6

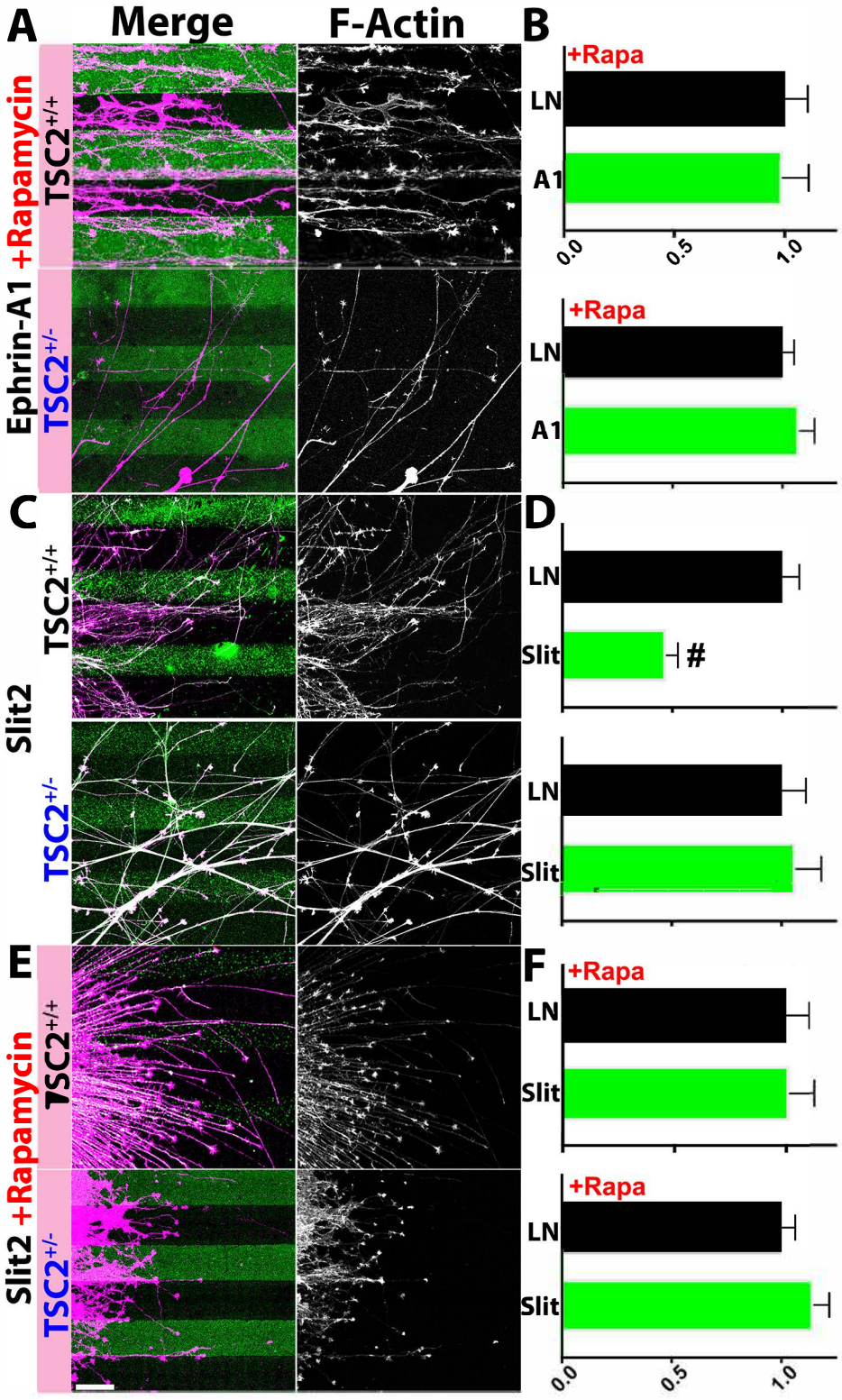
A
Merge
F-Actin
B
+Rapamycin
TSC2+/+
Ephrin-A1
TSC2+/-
+Rapa
LN
A1
0.0
0.5
1.0
C
D
Slit2
Slit
#
E
F
Slit2 +Rapamycin

Figure 7: $TSC2^{+/-}$ neurons have reduced RhoA-ROCK-MLC signaling . A. CFP (donor) fluorescent images of RhoA FRET sensor expressing control hFB growth cone before (above) and after YFP (acceptor) bleaching. **B.** Analysis of FRET efficiency in $TSC^{+/+}$ compared to $TSC^{+/-}$ growth cones. **C.** Analysis of RhoA activity by G-LISA in whole $TSC2^{+/+}$ and $TSC2^{+/-}$ neurospheres treated with Ephrin-A1. RhoA activity was normalized to untreated control neurons. Active RhoA was significantly increased in $TSC2^{+/+}$ neurons in response to Ephrin-A1 (2µg/mL) compared to$TSC2^{+/-}$ neurons. Note that basal RhoA activity also trended 20% lower in $TSC2^{+/-}$ compared to $TSC2^{+/+}$ neurospheres. N = 4-5 assays per condition. **C-E.** hFB neuronal growth cones of indicated genotype immunolabeled for p-MLC (green in merge) and counterstained for F-actin (magenta in merge) in control **(C)** and after ephrin-A1 stimulation **(D)**. Note $TSC2^{+/-}$ growth cones show significantly lower basal p-MLC labeling relative to control. .$TSC2^{+/+}$ neurons treated for 5 min with Ephrin-A1 show a robust increase in p-MLC, but $TSC2^{+/-}$ growth cones show little change in p-MLC in response to ephrin-A1. **E.** Fluorescence intensity measurements normalized to untreated control neurons for each condition. *$p < 0.05$, #$p < 0.0001$. One-way ANOVA with Tukey's Multiple Comparison. Scale, 5µm.

Figure 7

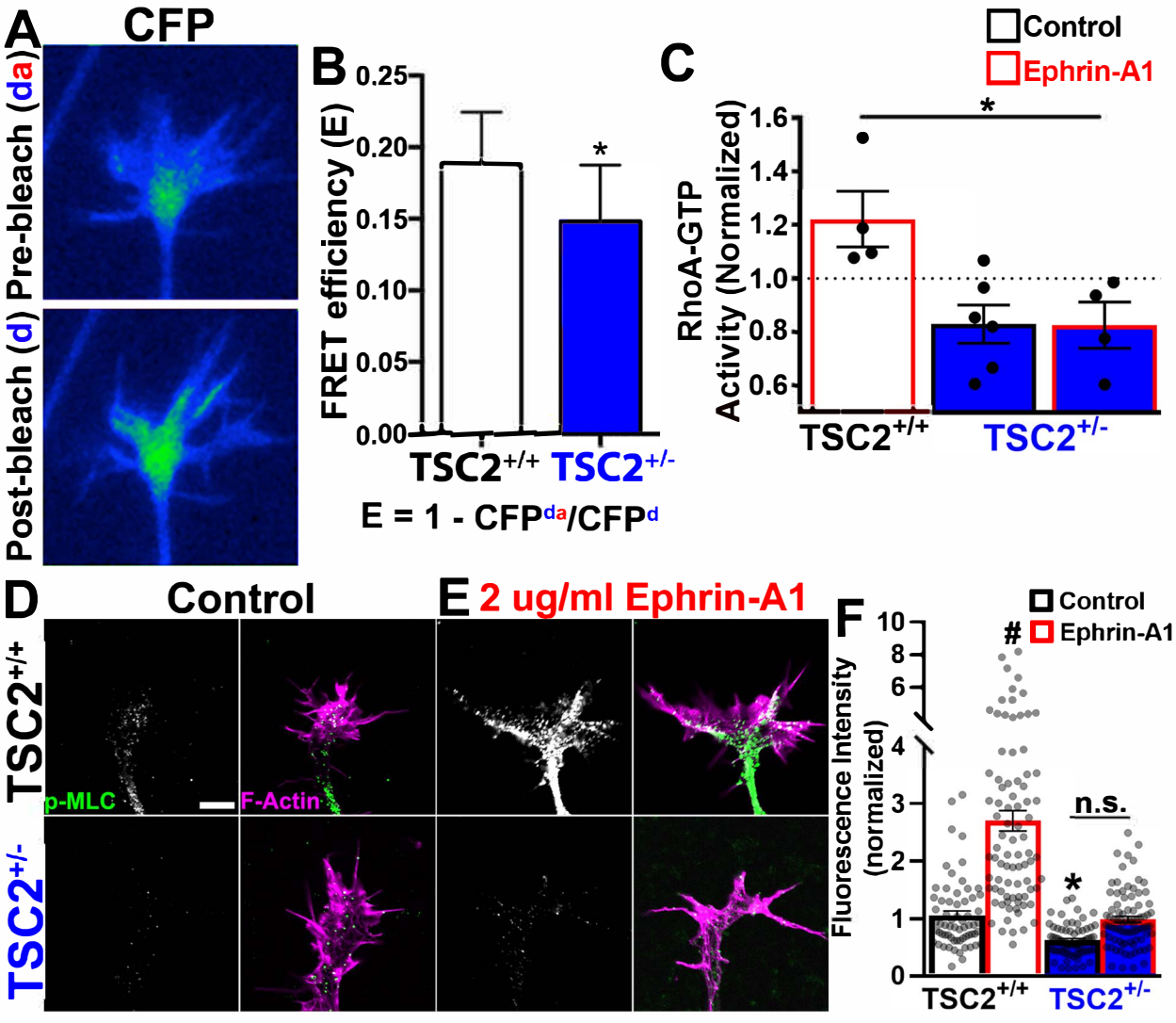
A
CFP
Post-bleach (d)
Pre-bleach (da)
B
FRET efficiency (E)
0.25
0.20
0.15
0.10
0.05
0.00
*
TSC2+/+
TSC2+/-
E = 1 - CFPda/CFPd
C
Control
Ephrin-A1
RhoA-GTP Activity (Normalized)
1.6
1.4
1.2
1.0
0.8
0.6
*
TSC2+/+
TSC2+/-
D
Control
E 2 ug/ml Ephrin-A1
TSC2+/+
TSC2+/-
p-MLC
F-Actin
F
Control
Ephrin-A1
Fluorescence Intensity (normalized)
10
8
6
4
3
2
1
0
n.s.
*
TSC2+/+
TSC2+/-

Figure 8: RhoA pathway modulation phenocopies and rescues $TSC2^{+/-}$ phenotypes

A. DIC images of growing axons from $TSC2^{+/+}$ and $TSC2^{+/-}$ hFB neurons at 5 min time intervals during treatment with ROCK inhibitor Y-27632 (10μM). Note that inhibition of ROCK increased $TSC2^{+/+}$ neurite extension rates to a level similar to $TSC2^{+/-}$ neurites, while $TSC2^{+/-}$ neurites did not respond to ROCK inhibitor. Dashed gray line indicates extension rate of control neurons before treatment, while dashed red lines indicate extension rates for $TSC2^{+/-}$ neurons (before and after treatment) and $TSC2^{+/+}$ neurons after treatment. **B.** Neurite extension rate measurements before and after inhibition of ROCK (Y-27632) and myosin-II with blebbistatin (Blebb, 50μM) in $TSC2^{+/+}$ and $TSC2^{+/-}$ neurons, shows $TSC2^{+/+}$ neurite outgrowth accelerated upon ROCK and myosin-II inhibition. Conversely, activation of MLC with the phosphatase inhibitor CalyculinA (200 pM) slowed neurite extension of both $TSC2^{+/+}$ and $TSC2^{+/-}$ neurons, slowing the latter to a rate comparable to basal $TSC2^{+/+}$ neurons. **C.** Ephrin-A1 mediated collapse of $TSC2^{+/+}$ growth cones was prevented by inhibition of RhoA (C3, 2μg/mL), myosin-II (Blebb, 50 μM), and ROCK (Y-27632, 10 μM), while no further reduction in collapse was observed by $TSC2^{+/-}$ growth cones. Conversely, activation of MLC with a low dose of calyculinA (200pM) rescued ephrin-A1 induced collapse by $TSC2^{+/-}$ growth cones. **D.** Treatment with Y-27632 blocked $TSC2^{+/+}$ axon guidance on ephrin-A1 stripes but had no additional effect on $TSC2^{+/-}$ neurons. *$p < 0.05$, #$p < 0.0001$. One-way ANOVA with Tukey's Multiple Comparison, or Student's t-test (C and I). Scale, 5μm and 100μm.

Figure 8

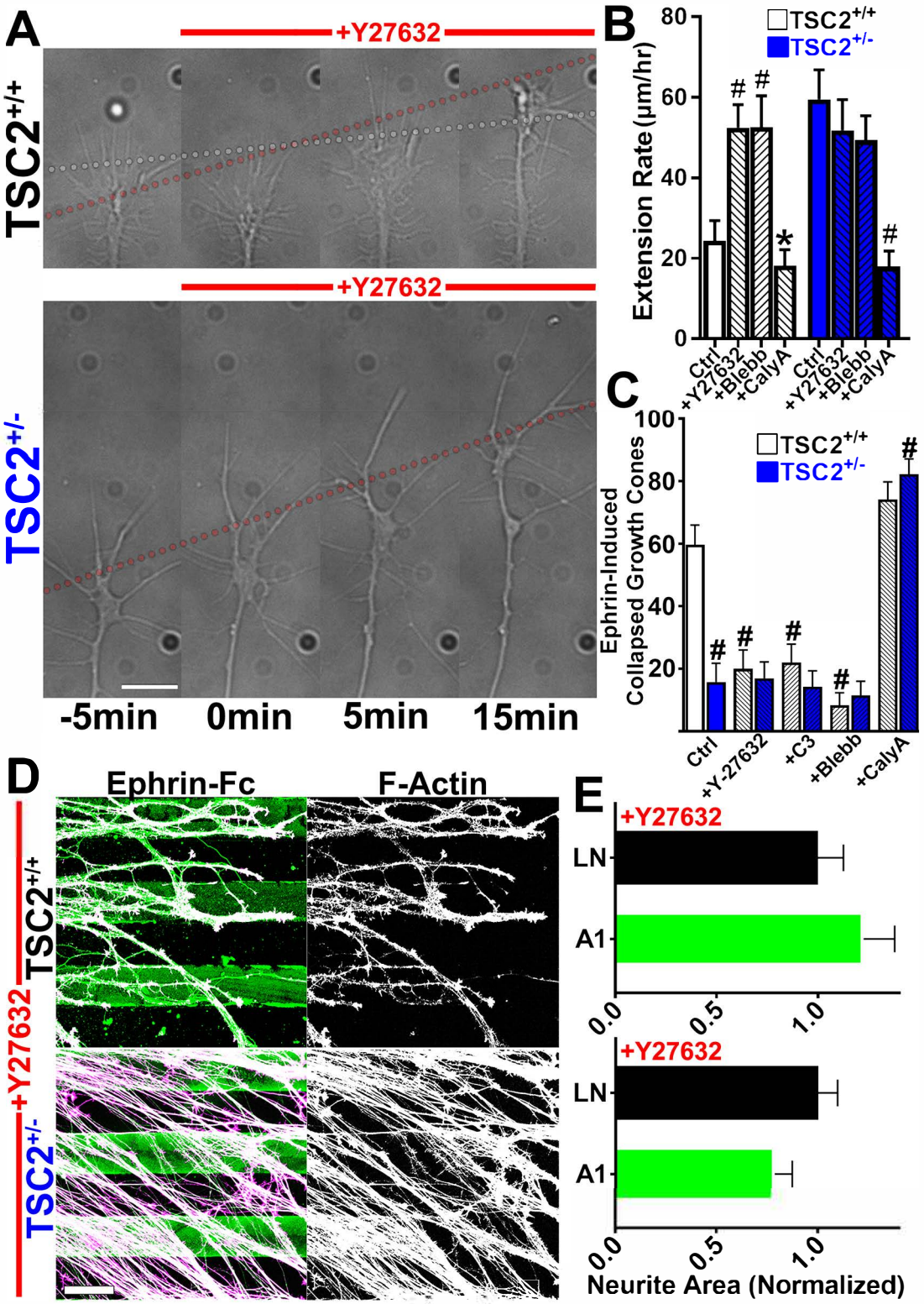
A
+Y27632
TSC2+/+
+Y27632
TSC2+/-
-5min
0min
5min
15min
B
TSC2+/+
TSC2+/-
Extension Rate (μm/hr)
0
20
40
60
80
Ctrl
+Y27632
+Blebb
+CalyA
C
TSC2+/+
TSC2+/-
Ephrin-Induced Collapsed Growth Cones
0
20
40
60
80
100
Ctrl
+Y-27632
+C3
+Blebb
+CalyA
D
Ephrin-Fc
F-Actin
TSC2+/+
TSC2+/-
+Y27632
E
+Y27632
LN
A1
0.0
0.5
1.0
+Y27632
LN
A1
0.0
0.5
1.0
Neurite Area (Normalized)

Supplemental Figure 1: TSC2 mutant iPSCs and neurons express normal cell fate markers. A. Sanger sequencing of $TSC2^{+/-}$ iPSCs showed a nonsense mutation at bp 972 near the boundary between exon 8 and exon 9. **B.** Reprogrammed iPSCs from patient lines as well as CRISPR/Cas9 corrected $TSC2^{+/+}$ and $TSC2^{-/-}$ cells showed normal morphology and similar growth rates. **C-E.** Immunofluorescence for neuroprogenitor and neural stem cell fates show appropriate neural differentiation in various cell lines. **F.** TSC2-patient and isogenic control lines show dorsal forebrain fates via FoxG1 immunofluorescence. Scale, 100 μm (B, D-E) and 200 μm (F).

Supplementary Figure 1

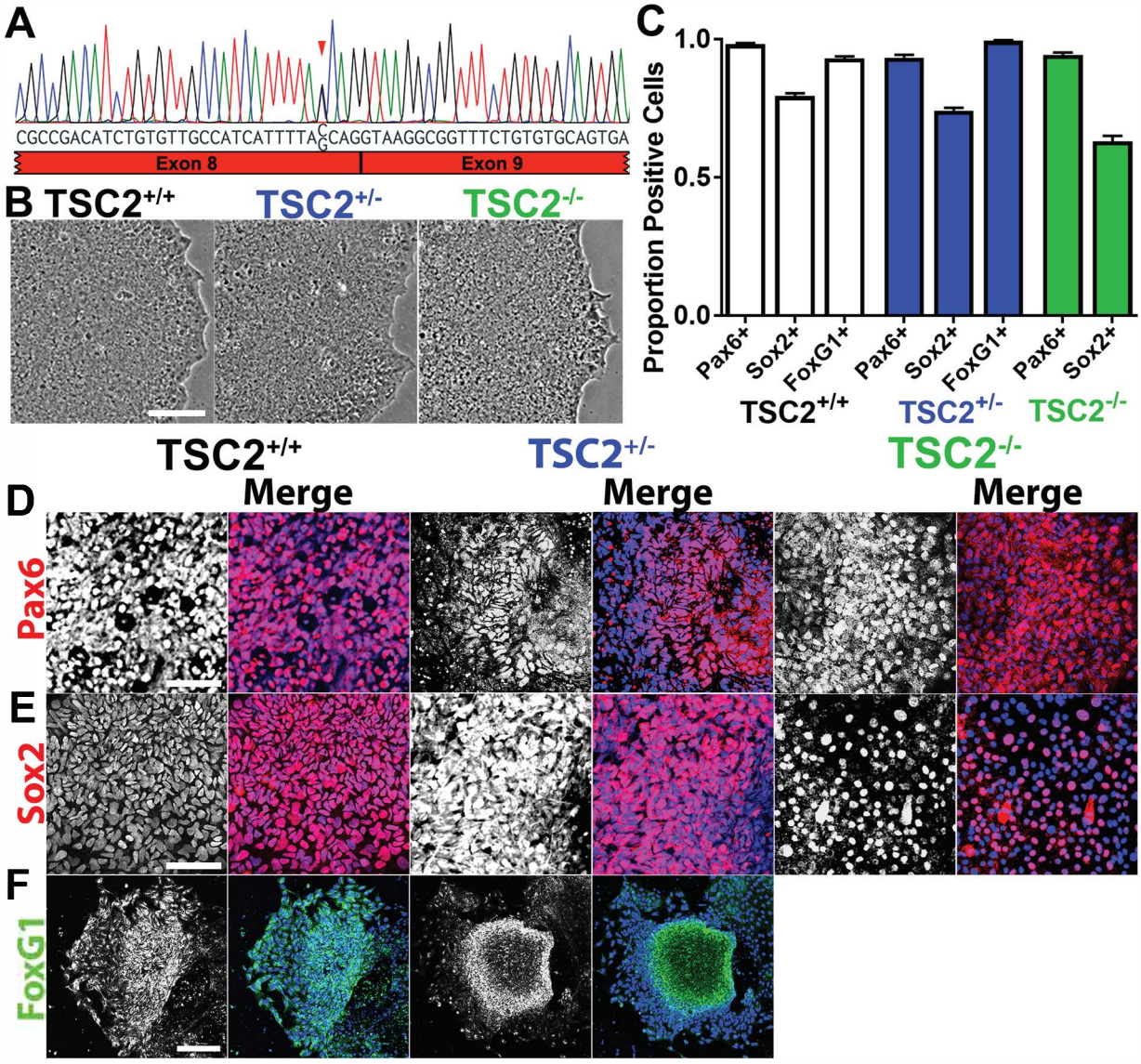

Supplemental Figure 2: $TSC2^{+/-}$ human motor neurons exhibit enhanced neurite extension compared to isogenic control neurons. A, B. hMN neurospheres of indicated genotype after two days *in vitro* immunolabeled for acetylated-tubulin (green) and counter-stained for F-actin (red). Note longer axons extend from $TSC2^{+/-}$ neurospheres compared to isogenic control neurons. **C.** Average neurite lengths of 12 longest axons per neurosphere of each genotype. **D.** Average axon extension rates show that $TSC2^{+/-}$ hMN neurites grew markedly faster compared to isogenic control neurons. **E.** Analysis of percent growth cone collapse by $TSC2^{+/+}$ and $TSC2^{+/-}$ hMNs in response to Sema-3F and ephrin-A1. For MN experiments, ephrin-A1 was pre-clustered prior to application. #$P < 0.0001$. Scale, 150 μm.

Supplementary Figure 2

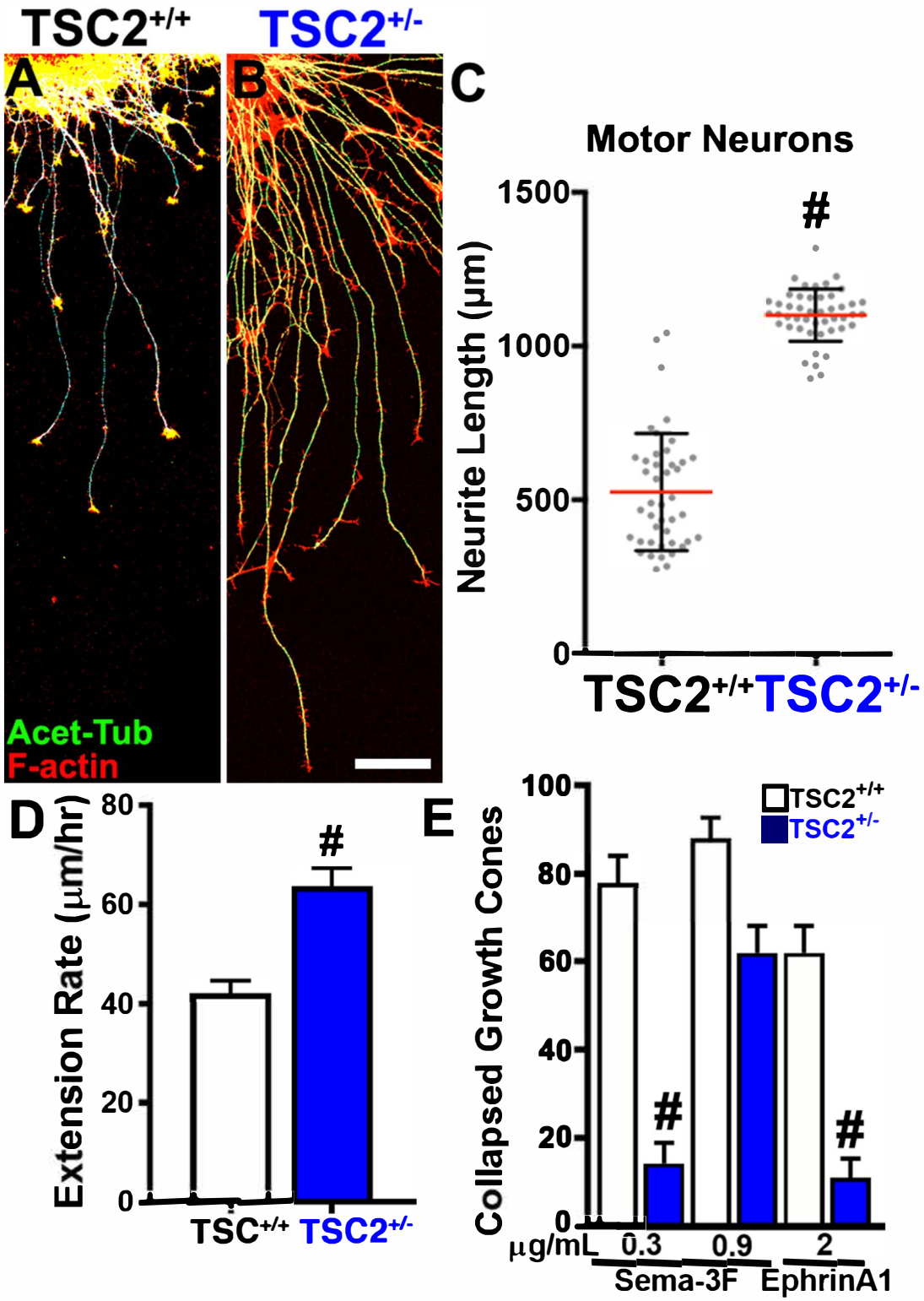

Supplemental Figure 3: Pharmacological inhibitors effectively block mTORC1 and mTORC2 function. hFB neurons were treated with mTOR inhibitors for 30 min then fixed and immunolabeled for p-S6 and p-Akt473, which are mTORC1 and mTORC2 specific targets, respectively. Fluorescence intensity measurements were made within growth cones and normalized to untreated control neurons. #P < 0.0001.

Supplementary Figure 3

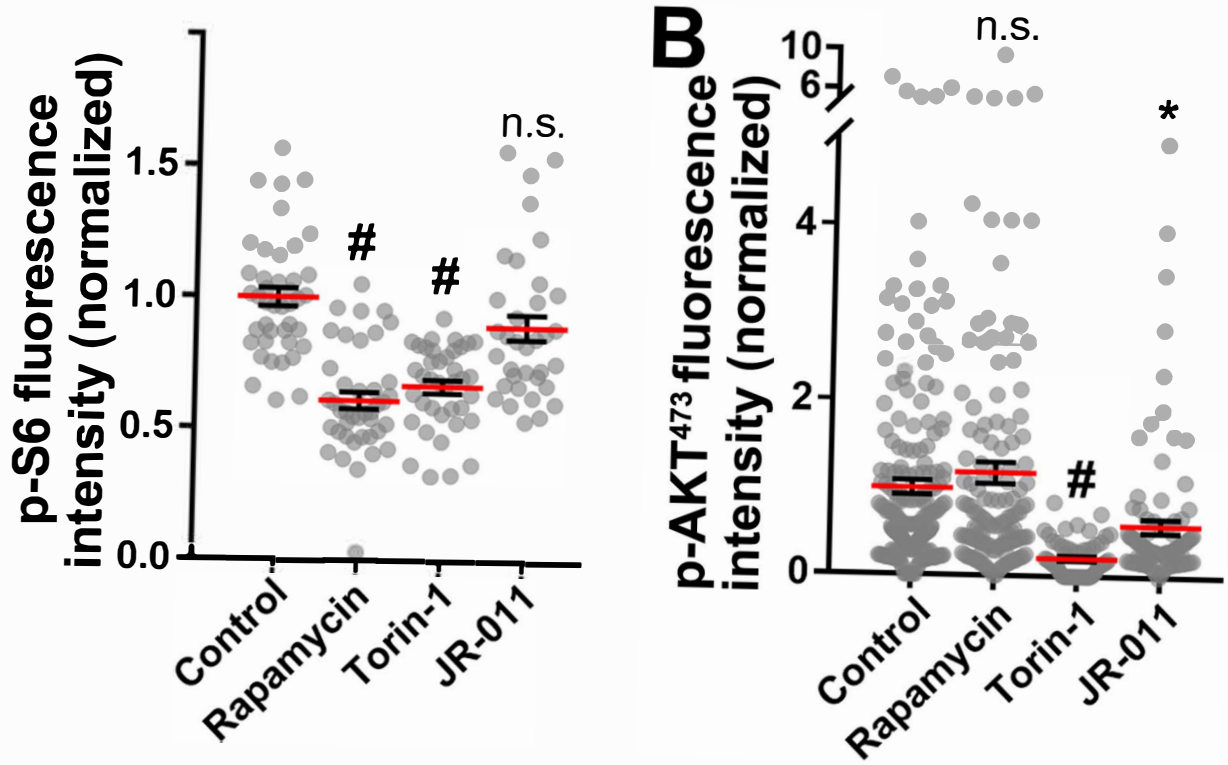

Supplemental Figure 4: $TSC2^{+/+}$ and $TSC2^{+/-}$ hFB neuronal growth cones express EphA4 and EphA2 receptors. **A.** hFB neurons were fixed and immunolabeled for EphA4 receptors (green in merge) and counterstained with phalloidin to label F-actin (magenta in merge). **B.** Fluorescence intensity measurements were made within growth cones and no significant difference was observed between $TSC2^{+/+}$ and $TSC2^{+/-}$ neurons. **C.** hFB neurons were fixed and immunolabeled for EphA2 receptors (green in merge) and counterstained with phalloidin to label F-actin (magenta in merge). **D.** Fluorescence intensity measurements were made within growth cones and no significant difference was observed between $TSC2^{+/+}$ and $TSC2^{+/-}$ neurons. Scale, 5 μm.

Supplementary Figure 4

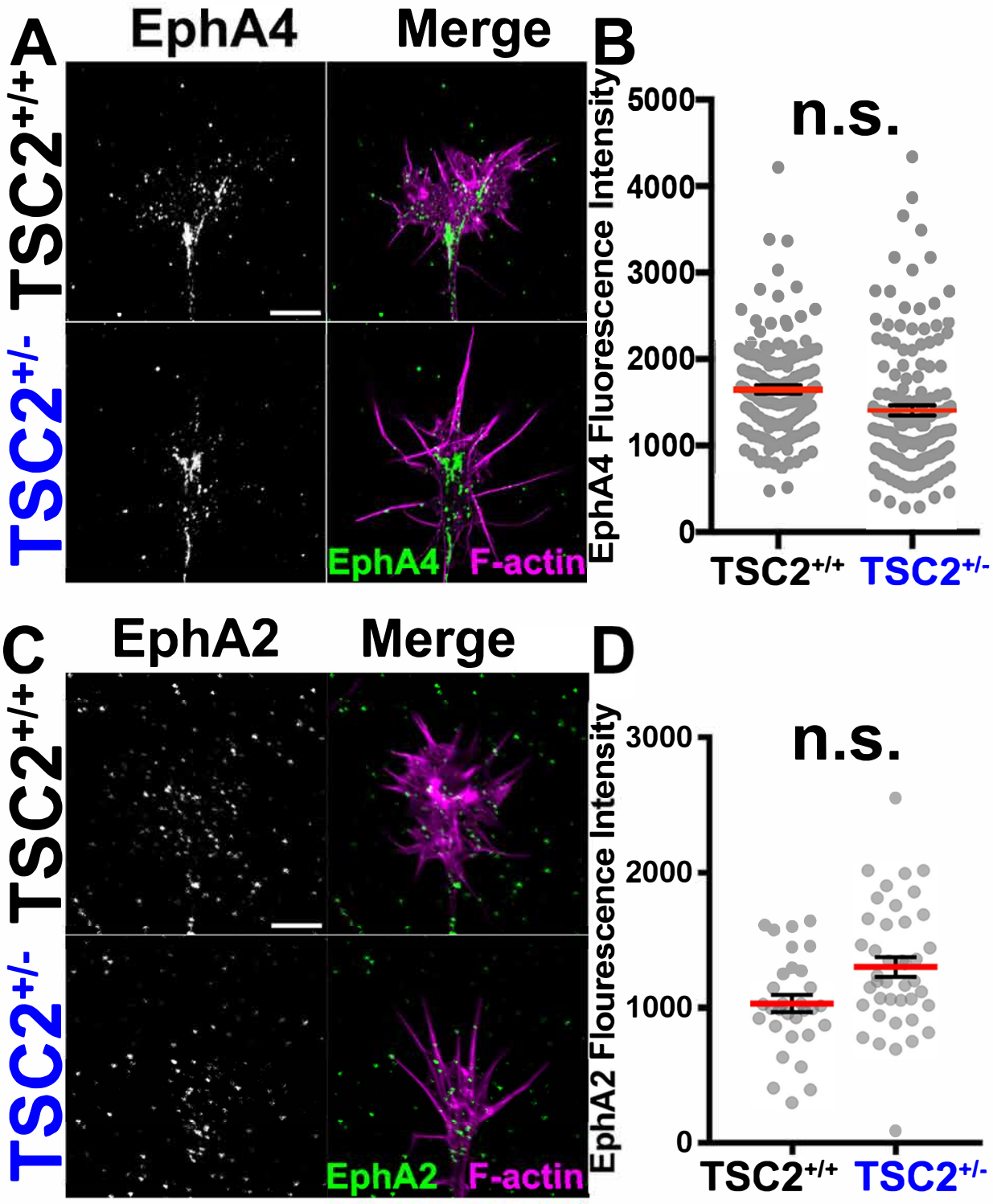

Supplemental Figure 5: Control hFB neurons differentiated from iPSC (IMR90) and ESC (WA09) lines are sensitive to inhibitory guidance cues. The percentage of collapsed hFB neuron growth cones was measured in before and after 15 min treatment with ephrin-A1 (2 μg/ml) or Slit2 (0.2 μg/ml) in neurosphere cultures. #P < 0.0001.

Supplementary Figure 5

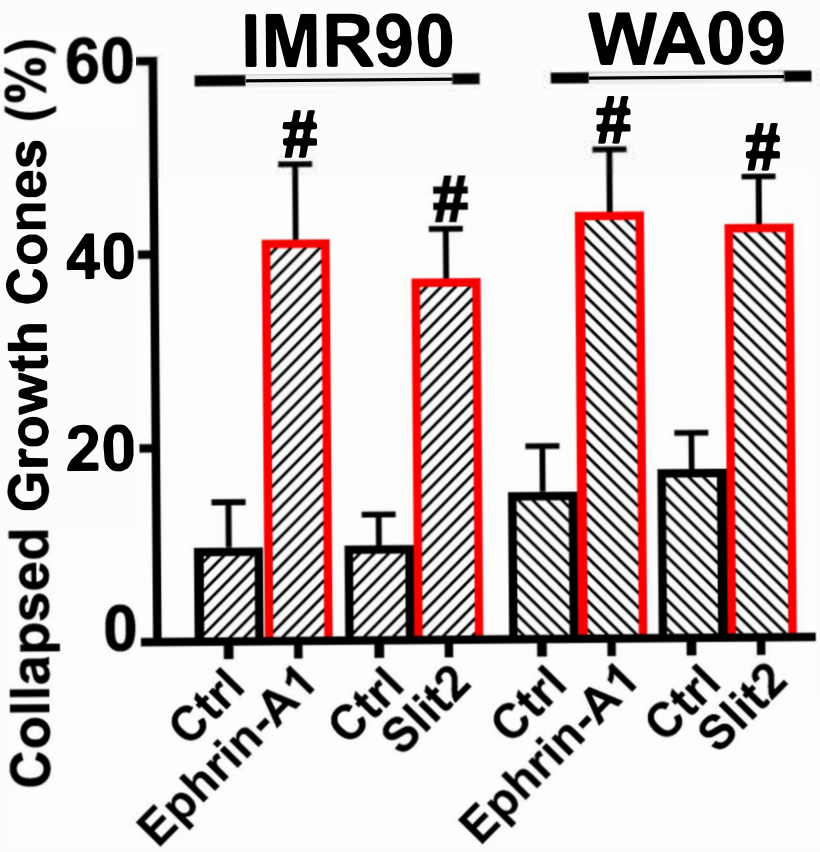

Supplemental Figure 6: Slit2 and Netrin activate protein synthesis in $TSC2^{+/+}$ and $TSC2^{+/-}$ hFB growth cones. A, B. Puromycin labeled $TSC2^{+/+}$ (A) and $TSC2^{+/-}$ (B) hFB neuron growth cones (green in merges) counter-stained for F-actin (magenta in merges). Puromycin-labeled proteins were detected with anti-puromycin antibody (see methods). Note increased labeling in response to Slit2 is blocked by pre-treatment with Rapamycin. Netrin treatment also increases puromycin incorporation. Scale, 5 μm.

Supplementary Figure 6

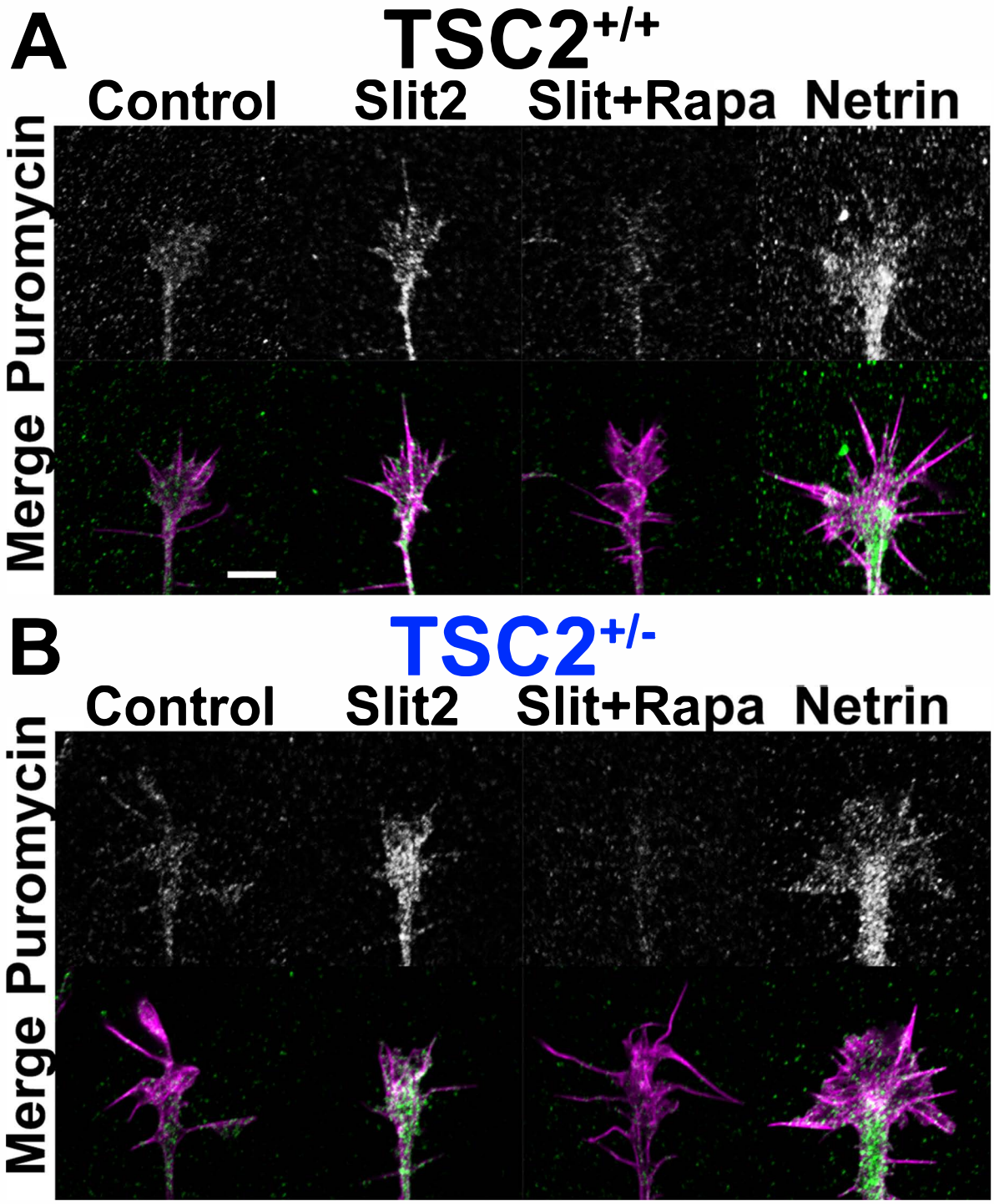

Supplemental Figure 7: Activation of p-MLC with calyculinA in growth cones. hFB neurons were treated with low dose of calyculinA (200pM) for 15 min then fixed and immunolabeled for p-MLC. Fluorescence intensity was measured within $TSC2^{+/+}$ and $TSC2^{+/-}$ growth cones and normalized to untreated control neurons. CalyA activates p-MLC in both $TSC2^{+/+}$ and $TSC2^{+/-}$ growth cones. *P < 0.05, **P < 0.01.

Supplementary Figure 7

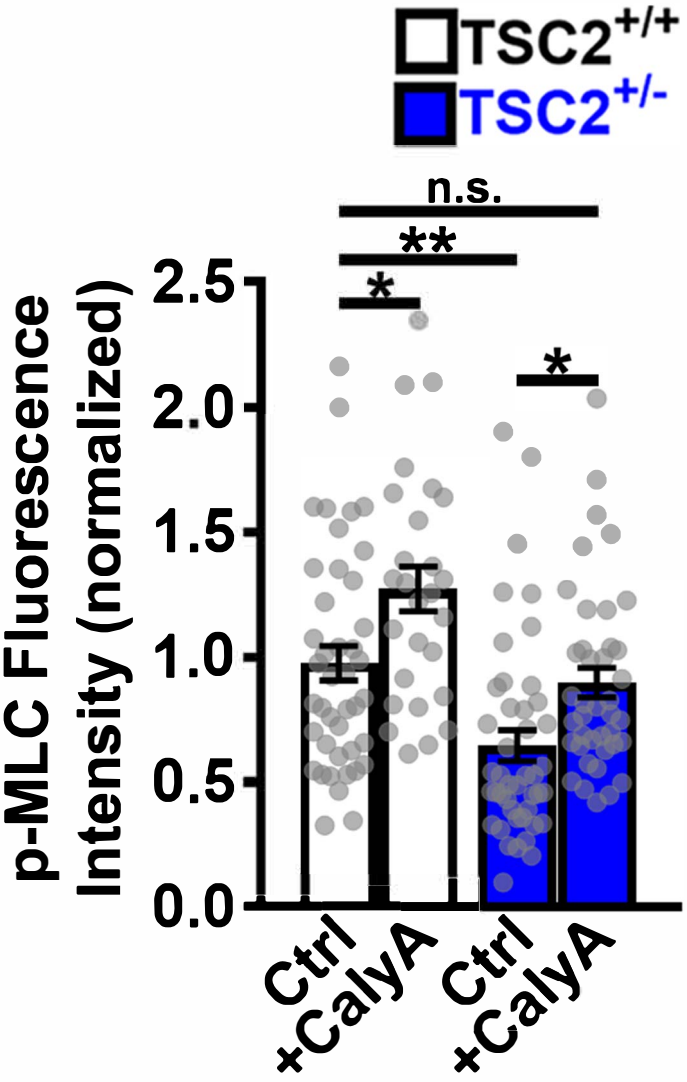

Supplementary Figure 8: RhoA/ROCK/myosin modulation downstream of TSC2 leads to axon guidance defects TSC2 haploinsufficiency appears to be sufficient to regulate mTORC1 signaling and mTOR-dependent LPS within hFBs. In this model, $TSC2^{+/-}$ within growth cones suppresses RhoA signaling and decreases myosin activity upstream of cytoskeletal actin dynamics. Decreased contractility downstream of myosin increases outgrowth rates and decrease the ability of growth cones to sufficiently contract to trigger growth cone collapse. Increasing basal myosin activity is sufficient to restore growth cone outgrowth rates and collapse.

Supplementary Figure 8

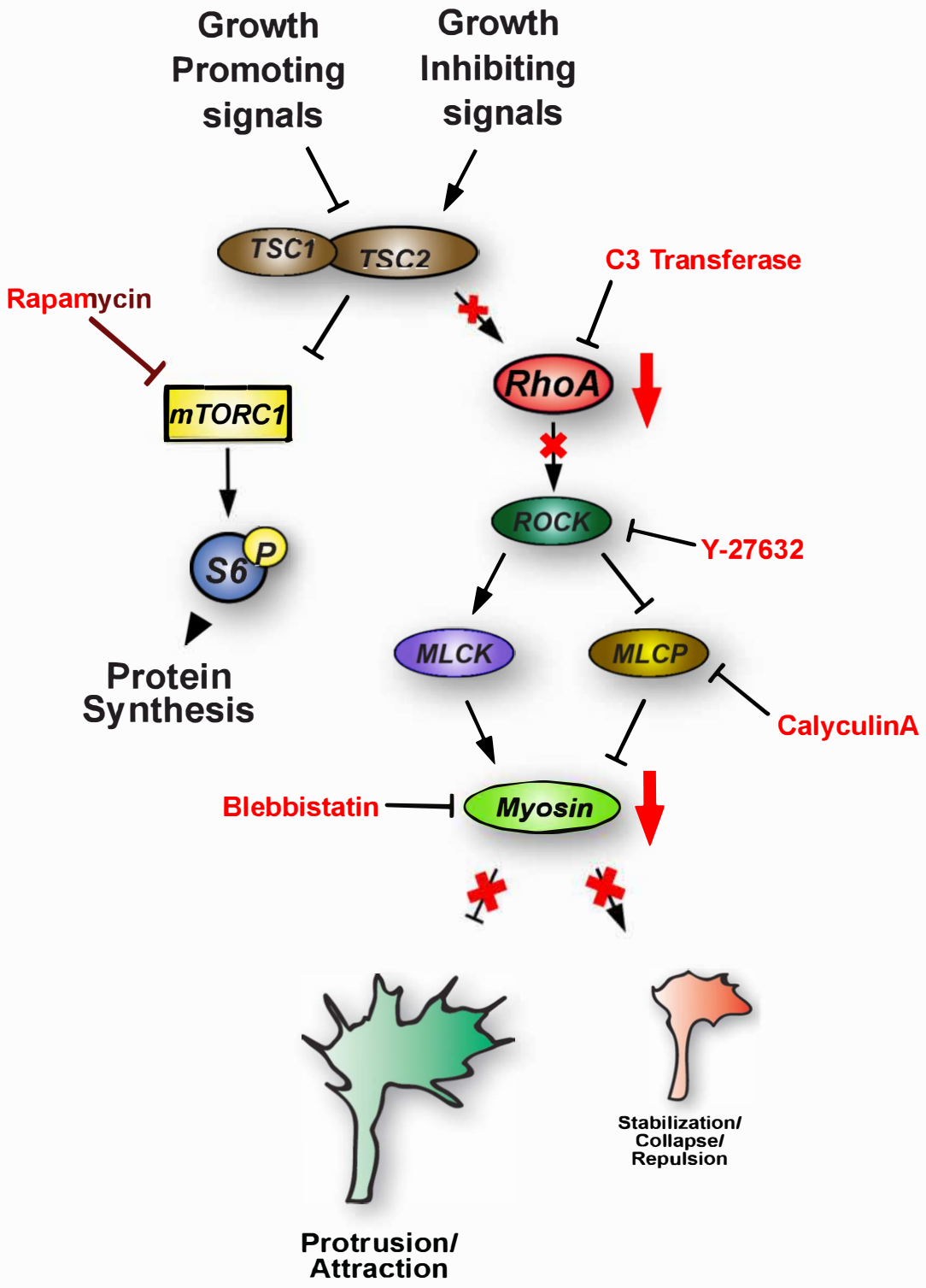

Chapter 3: HDAC6 inhibition rescues guidance defects in human Tuberous Sclerosis neurons

---

Timothy Catlett designed and performed the research, analyzed the data, and wrote the chapter.

Abstract

Evidence suggests that patients with Tuberous Sclerosis Complex (TSC), like other neurodevelopmental disorders, have miswiring of neuronal connections that form during development. These defects in neuronal connectivity likely contribute to symptoms of TSC including intellectual disabilities, autism, and epilepsy. In previous work, we showed that axon guidance by human neurons was defective in a heterozygous human stem cell model of TSC. Surprisingly, suppression of the canonical TSC-target, mTOR, was unable to rescue TSC phenotypes, which were responsive to modulation of RhoA/ROCK/myosin pathways. We showed that basal RhoA pathways are suppressed in human forebrain growth cones and fail to activate in response to canonical guidance cues. Similarly, histone deacetylase complexes (HDACs) have been shown to be altered in heterozygous TSC brains and suppression rescued phenotypes in a mouse model of TSC. Here, I examined cytoplasmic HDAC6, finding it substantially upregulated in $TSC2^{+/-}$ growth cones. Modulation of HDAC6 with specific inhibition partially rescued $TSC2^{+/-}$ phenotypes, including neurite guidance response to the repulsive cue ephrin-A5. I also observed substantial downregulation of microtubule acetylation within growth cones. Given the mTOR resistance of TSC2 phenoypes of axonal development, this work potentially suggests new targets for TSC2 modulation, and further research may lead to a fuller understanding of the pathways underlying TSC pathology.

Introduction

Developing axons must elongate throughout the organism and accurately assemble its neural circuits. Synaptic partners are reached via cues, chemical and mechanical in nature and patterned in soluble and substratum-bound fashion to guide the tip of the axon, the growth cone, to its target. Each growth cone carries a complement of receptors activated by various cues and integrates their cumulative signal into the underlying cytoskeleton to ultimately effect extension and guidance[1–3]. Defects in this guidance cue-cytoskeleton signaling axis have been linked to abnormal neural network wiring in animal models, yet few human neural development disorders have been attributed to specific growth cone signaling abnormalities[4–6]. As guidance pathways involve molecular players with roles in a variety of developmental processes, it is difficult to parse post hoc the relative contributions of events such as axon guidance or synaptogenesis to disease. The arrival of induced pluripotent stem cell (iPS) technology therefore promises the opportunity to isolate the effects of genetic mutations on individual neurodevelopmental events *in vitro* in a targeted manner not before possible in human subjects.

Tuberous Sclerosis (TSC) is a complex neurodevelopmental disorder presenting with a high incidence of ASD (50%), mental disability (50%), and epilepsy (85%)[7]. A multi-system syndrome characterized by benign tumors historically referred to as tubers or hamartomas, most cases have been isolated to mutations in one of two Tuberous Sclerosis Complex genes, the eponymous TSC1 or TSC2[8,9]. As a monogenic disorder, TSC is a powerful tool for studying ASD particularly, as the latter is predominantly idiopathic[10]. These proteins together with TBC1D7 constitute the Tuberous Sclerosis Complex, a negative regulator of mTOR signaling and linked to protein synthesis,

autophagy, and cell growth and proliferation regulation. TSC1 stabilizes TSC2 as the latter's GTPase-activating (GAP) domain negatively regulates mTOR via its upstream activator, the GTPase Rheb. TSC1/2 thus serves as a hub of nutrient and cell stress signaling, as well as growth-promoting and -inhibiting pathways, and mTOR activation has been implicated in axon guidance pathways via its control of local protein synthesis[11]. TSC1/2 have also been linked to cytoskeletal rearrangements upstream of the Rho GTPases RhoA and Rac1 in mTOR-dependent and independent pathways, although these are as yet poorly understood[12–15]. With links to Rho GTPase signaling and local protein synthesis, TSC1/2 are promising candidates in axon guidance signaling modulation.

TSC has been previously linked with axon guidance specifically via animal model studies. A heterozygous mouse model of TSC showed significant aberrant retinogeniculate-mapping errors and reduced *in vitro* sensitivity to the guidance cues ephrin-A1 and ephrin-A5[16]. Work in *D. melanogaster* demonstrated rapamycin-resistant retinal guidance abnormalities in a TSC1 knockout model[17]. TSC-patient axon tracts, as measured by white matter diffusivity via diffusion tensor imaging (DTI), also show significant differences from patient controls[18–20].

In our previous work, we examined signal transduction within human TSC patient-derived growth cones; specifically, the contribution of mTOR-dependent local protein synthesis and RhoGTPase regulation in this neurodevelopmental disorder (Chapter 2). We found that TSC heterozygous cortical growth cones exhibited exuberant outgrowth and resistance to canonical repulsive guidance cues via both collapse and guidance assays. We also found the surprising result that substantial *in vitro* guidance abnormalities within

TSC were mTOR-independent, but that long term mTOR inhibition via rapamycin suppressed the ability of human growth cones to respond to guidance cues.

HDAC6 is a cytoplasmic deacetylase highly expressed in developing neurites, and has previously been implicated in cell motility, axon outgrowth, and neurological disease[21–23]. Commonly associated with microtubule deacetylation, the protein possesses deacetylase activity as well as ubiquitin-binding activity, implicating it in cargo trafficking and autophagy/degradation pathways. While HDAC6 is associated with microtubule deacetylation, studies have shown it also implicated in post-translational modification of over thirty targets, including other proteins important for neurite growth and guidance such as Akt[24], cortactin[25], miro1[26], and HSP90[27]. Recent work has also shown HDACs to be upregulated in hippocampi of a heterozygous mouse model of TSC and contributing to rapamycin resistance to a long term depression phenotype[28].

Here we show that HDAC6 is upregulated in human TSC2$^{+/-}$ cortical growth cones. HDAC inhibition also rescues TSC phenotypes of aberrant outgrowth and response to the repulsive guidance cue ephrin-A1. These results shed light on rapamycin-resistant TSC phenotypes *in vitro* and importantly suggest a new targetable locus in treatment of Tuberous Sclerosis.

METHODS

IPSC generation, characterization, and maintenance

Reprogramming and validation was performed as in Chapter 2. iPSCs and WA09 (H9) cells were cultured on feeder-free substrate vitronectin (Thermofisher) with Essential 8 Flex media (ThermoFisher) as described (https://assets.thermofisher.com/TFS-Assets/LSG/manuals/Essential_8_Flex_Medium_UG.pdf), or on mTeSR and Matrigel.

Neural differentiation and culture

hFBs were differentiated as previously described in Doers et al., 2014 and Chapter 2. Following differentiation, neurons were cultured as neurospheres on acid-washed coverslips coated with poly-D-lysine (PDL, 50µg/mL; Sigma-Aldrich) and laminin (LN, 25µg/mL; Sigma-Aldrich) in Neurobasal (ThermoFisher) media with B27 supplement and Glutamax (NB) for 1- 3DIV with half media changes every third day as needed. Pharmacological agents (Trichostatin A, Sigma, Tubacin, Cayman Chemical) were bath applied for 15-60 minutes prior to treatment with guidance cues (ephrin-A1-Fc, R&D).

Live and fixed immunofluorescent cell imaging

For live phase contrast or differential interference contrast (DIC) microscopy, images were acquired using either a 10x/0.3, 20x/0.5, or 40x/1.3 numerical aperture (NA) objective lens on a Nikon TE2000 inverted microscope with a Coolsnap HQ2 camera (Roper Scientific) with no binning (pixel size = 155 nm). Fixed immunostained images were acquired using a 63x/1.4 NA objective lens at 2-2.5x zoom on a Zeiss LSM800 Airy-disc scanning confocal system mounted on an Axio Observer Inverted Microscope. Live images of fluorescent neurons were acquired using the Nikon TE2000 or Zeiss microscopes.

Immunofluorescence staining and outgrowth analyses

Immunofluorescence (IF) staining was performed as previously described[30]. Measurements of fluorescence intensity of proteins of interest were made within growth cones by creating an image mask from a thresholded F-actin (AlexaFluor (AF)-phalloidin, ThermoFisher) channel and measuring the average pixel intensity of immunolabeling

within the selected area. Measurements of fixed neurite lengths were made by tracing from the end of the neurite as determined by acetylated-tubulin (Sigma-Aldrich) labeling to the edge of the neurosphere using the Simple Neurite Tracer plug-in[31] and Fiji/ImageJ[32–34]. Image stacks of live neurons were stabilized as needed prior to analysis using the ImageStabilizer plug-in[35].

Live DIC outgrowth analysis was performed by taking consecutive measurements at the furthest edge of the growth cone lamellipodia opposite the central domain; retraction distances were capped at three times growth cone length or 30 microns to account for skewing of single very large retractions. Collapse was quantified via disassembly of the lamellipodial veil and ≤ 2 filopodia of <10 microns in length.

All other data analysis was performed on raw images; the Unsharp Mask filter (ImageJ) was utilized in some instances for display purposes only. Gaussian blur background subtraction was similarly utilized in DIC images as needed for background shading correction for display purposes.

iPSC nucleofection protocol

IPSC neurons were transfected as described in the Amaxa Primary Mammalian Neuron protocol (https://bioscience.lonza.com/lonza_bs/US/en/download/product/asset/21464) using whole or dissociated neurospheres, as described above. Cells were immersed in transfection solution with 1-5μg of plasmid DNA and transfected using an Amaxa Nucleofector II, program settings B-016 for neurospheres (kit VPI-1003, Amaxa). We utilized a lab prepared solution[36]. Cells were allowed to recover in suspension for 24 hrs before culturing on PDL-LN coated coverslips or on stripes (below).

Stripe Guidance assay

Stripe molds were utilized as described in Chapter 2. Briefly, acid washed coverslips were pre-coated with PDL. Molds were affixed and a solution of ephrin-A1 (10µg/mL), fluorescent-conjugated dextran, and laminin were vacuum fed through the mold and incubated for one hour at RT. After removal of the mold and rinsing, coverslips were incubated in a laminin solution and then rinsed in PBS before culturing. Neurons on patterned cues were labeled AF-Phalloidin and neurite orientation and length within quadrants were quantified using a Sholl analysis plug-in[37].

RESULTS

TSC2$^{+/-}$ abnormal neurite outgrowth is rescued by HDAC inhibition

TSC2$^{+/-}$ patient lines and isogenic controls were generated and validated as previously described in Chapter 2. Excitatory glutamatergic dorsal human forebrain neurons (hFB) of each genotype were differentiated using established protocols[38,39], validated as shown in Chapter 2. As previously shown, despite haploinsufficiency of TSC2 at the protein level, basal mTOR activity was not significantly different in TSC2$^{+/+}$ versus TSC2$^{+/-}$ growth cones (Chapter 2). Upon culturing each genotype as neurospheres for 24 hrs, cells were fixed and stained for acetylated tubulin and F-actin. Neurite lengths were significantly increased in TSC2$^{+/-}$ neurons (Figure 1A & Chapter 2 Figure 2B). Interestingly, acetylated tubulin intensity was decreased at the tips of TSC2$^{+/-}$ neurites (Figure 1B-C). We also confirmed these differences by a ratio of acetylated to total alpha-tubulin (Supplemental Figure 1A). As HDAC6 is a primary negative regulator of microtubule acetylation in growth cones[40], we utilized IF to assay the presence of HDAC6 within fixed growth cones at

higher magnification and found that HDAC6 is indeed constitutively upregulated in $TSC2^{+/-}$ growth cones (Figure 1D-E). Since HDAC6 has been implicated in neurite outgrowth and development[41], we next sought to determine if its upregulation in $TSC2^{+/-}$ neurites was significant to the defects in outgrowth and guidance we observed in Chapter 2, Figure 2. To examine the acute effects of HDAC modulation on neurite outgrowth, we performed live DIC imaging of $TSC2^{+/-}$ neurites in the presence and absence of HDAC inhibitors (Figure 2). The general HDAC inhibitor trichostatin A (TsA) decreased $TSC2^{+/-}$ neurite extension rates to levels indistinguishable from isogenic control (Figure 2). Pan-HDAC inhibition has been linked to transcriptional changes in neurons modulating neurite outgrowth and cue response[42], making the acute and HDAC6-specific pharmacological applications important to confirm lack of nuclear involvement. While the acute timing of TsA dosing suggests little nuclear involvement from other canonical HDACs, we also utilized tubacin (Tbn), a more specific inhibitor of HDAC6, which also slowed neurites to control extension rates (Figure 2). We confirmed the effects of both pharmacological agents on acetylation via incubation of neurites in the presence of each followed by fixation and staining of acetylated and total alpha-tubulin. Acetylation increases were robust (Supplemental Figure 1B-C). This data suggests that increased HDAC6 expression within $TSC2^{+/-}$ growth cones may play a role in enhanced outgrowth phenotypes.

HDAC inhibition rescues $TSC2^{+/-}$ resistance to repulsive guidance cue

In our previous work, we showed resistance of $TSC2^{+/-}$ growth cones to repulsive guidance cues in collapse assays and the failure of mTOR pathway manipulation to rescue these phenotypes (Figure 3C, Chapter 2 Figure 3). In order to assess whether

increased HDAC6 expression was playing a role in $TSC2^{+/-}$ growth cone insensitivity, we stimulated growing neurites with ephrin-A1 in the presence of HDAC inhibitors. As previously shown, isogenic control growth cones respond robustly to ephrin-A1 via retraction and collapse; however, $TSC2^{+/-}$ growth cones were insensitive (Figure 3A, C). In the presence of general HDAC inhibition (TsA) or HDAC6-specific inhibition (Tbn), growth cone sensitivity to ephrin-A1 was restored to $TSC2^{+/+}$ collapse levels, suggesting that increased HDAC6 activity may be contributing to guidance cue insensitivity in $TSC2^{+/-}$ neurons (Figure 3B-C).

$TSC2^{+/-}$ guidance defects rescued by HDAC6 inhibition

We previously showed that $TSC2^{+/-}$ neurites fail to respond to a variety of guidance cues in guidance assays (Chapter 2 Figure 5). To test the role of HDAC6 in chronic $TSC2^{+/-}$ neurite guidance defects, we plated neurospheres on striped carpets of ephrin-A1 in the presence of Tbn. In contrast to the media only condition in which $TSC2^{+/-}$ neurites largely ignore boundaries of ephrin-A1 and laminin, incubation in Tbn significantly improve guidance along these borders, suggesting HDAC6 is inhibiting appropriate axon guidance in $TSC2^{+/-}$ neurons (Figure 4A-B).

Discussion

In this work we demonstrated that constitutive HDAC6 upregulation is playing a role in $TSC2^{+/-}$ neurite phenotypes. Tubulin acetylation is decreased in growing $TSC2^{+/-}$ neurites, and HDAC6 is increased in these growth cones over isogenic control growth cones. Our previous work showed that $TSC2^{+/-}$ neurites grew significantly faster than isogenic or other control neurites, and that TSC2 haploinsufficiency was also associated with

resistance to guidance cues in an mTOR-independent manner. Modulation of HDAC6 via pan- or specific pharmacological inhibition rescued these defects.

Acetylation is associated with microtubule stability and preferential association of specific trafficking proteins. The site of microtubule acetylation assayed here, K40, resides within the microtubule lumen and the mode of accessibility by acetyltransferases and HDACs is yet undetermined[43]. Some researchers think that microtubule acetylation may contribute to the flexibility of individual microtubules, facilitating the repair of small breaks in the tubulin network along the lattice to prevent wholesale microtubule disassembly. Motor proteins shuttle cargo in and out of the growth cone via microtubules, and both kinesin-1 and dynein processivity is positively correlated with microtubule acetylation, though the mechanism is yet under investigation[43–45]. Microtubule motor proteins shuttle individual cargoes and membrane to and from the outer plasma membrane, facilitating cue sensitivity and directionality[46]. Dysregulation of microtubule acetylation at the neurite periphery may disrupt cue signaling in a variety of ways. Motor proteins bind microtubules and generate sliding forces which may overcome the retrograde flow of the cortical actin network and promote selective microtubule invasion of the periphery, facilitating turning[47,48]. For example, while acetylation itself is more often associated with processivity rather than binding affinities, dynein stability within the shaft of unipolar microtubules may facilitate sliding into the peripheral domain. These events are difficult to disentangle from microtubule polymerization dynamics, which have also been associated with HDAC6[49]. Downstream of ligand-receptor binding and endocytosis, cargoes are shuttled via the endosomal pathway to lysosomes within the central domain for degradation. This process is interwoven with receptor activation and modulates the intensity of downstream

signaling[50]. Ubiquitination of ligand-bound eph receptors and the ubiquitin-binding domain of HDAC6 make this mechanism an attractive avenue of investigation. For example, in $TSC2^{+/-}$ growth cones, overactive HDAC6 may bind the ubiquitinated ephA receptor and facilitate its premature degradation in lysosomes, attenuating the ephrin-A1-ephA signaling pathway and preventing collapse. Alternatively, a single study in mouse hippocampal neurons noted that overexpression of SIRT2, the only other cytoplasmic HDAC known to de-acetylate microtubules at K40, also blocked ephrin-A5 mediated collapse[51]. Alterations in microtubule PTMs may thus interfere with trafficking-dependent downstream signal transduction. Endosomal cargo or macropinocytosis downstream of ephrin signaling may inappropriately re-merge with the outer plasma membrane, or signaling may be otherwise attenuated by aberrant endosomal sorting complexes. A microtubule-binding Rho GEF, GEF-H1, facilitates RhoA activation upon its release from microtubules, although evidence for its activity in axons is yet limited[52]. Potential microtubule-mediated mechanisms thus remain to be investigated.

While microtubules are the best studied de-acetylation targets of HDAC6, other targets have also been identified. HDAC6 knockdown was shown to increase acetylation of the actin-polymerizing protein cortactin, which decreased its actin-binding affinity and led to its nuclear localization[25]. It is plausible that enhanced de-acetylation activity in the growth cone may lead to an increase in cortactin association and enhanced neurite speeds and loss of sensitivity to cues[53,54]. However, while an increase in cortactin activity cannot be completely ruled out, preliminary results indicated no significant difference in total cortactin within $TSC2^{+/-}$ versus isogenic control growth cones (Supplemental Figure 2A). A recent report showed HDAC6-dependent miro-1 deacetylation was responsible for a

decrease in the availability of mitochondria at the growth cone periphery on inhibitory substrates[26]. Miro-1 is an adaptor protein linking mitochondria to microtubule motors, and inhibiting HDAC6 increased mitochondrial transport to the periphery and growth cone motility on inhibitory substrates. Intriguingly, the Sahin group also reported mitochondrial transport defects in an iPS model of TSC, although the majority of their defects were observed in $TSC2^{-/-}$ neurons and were rapamycin sensitive[55]. Clearly, HDAC6 modulation affects motor protein activity and transport of relevant cargoes, either through modulation of microtubules or other substrates.

Especially promising was the rescue of long-term guidance defects by the HDAC6 inhibitor tubacin, because the mTOR pathway was grossly normal in $TSC2^{+/-}$ growth cones, and long-term rapamycin treatment decreased the ability of control neurites to guide without rescuing $TSC2^{+/-}$ neurite phenotypes (Chapter 2). This suggested the possibility that early rapamycin treatment *in vivo* may have deleterious effects on the ability of normal neurons to guide appropriately. While TSC-related giant cells and dysplastic cells within tubers both have an outsized effect on brain development and are often responsive to rapamycin derivatives, the vast majority of neurons in a patient brain are heterozygous and exhibit grossly normal mTOR activity. By isolating the pathways that lead to a decreased ability of developing cells to guide appropriately, more targeted approaches can be developed to minimize potential side effects of pharmacological mTOR manipulations. This is more crucial than ever as the need for early intervention in TSC is becoming more clear.

References

1. Gallo, G. & Letourneau, P. C. Regulation of Growth Cone Actin Filaments by Guidance Cues. *J. Neurobiol.* **58**, 92–102 (2004).
2. Lowery, L. A. & Vactor, D. Van. The trip of the tip : understanding the growth cone machinery. **10**, (2009).
3. Dent, E. W. *et al.* The Growth Cone Cytoskeleton in Axon. (2011). doi:10.1101/cshperspect.a001800
4. Battum, E. Y. Van, Brignani, S. & Pasterkamp, R. J. Axon guidance proteins in neurological disorders. *Lancet Glob. Heal.* **4422**, (2015).
5. Nugent, A. A., Kolpak, A. L. & Engle, E. C. Human disorders of axon guidance. *Curr. Opin. Neurobiol.* **22**, 837–843
6. McFadden, K. & Minshew, N. J. Evidence for dysregulation of axonal growth and guidance in the etiology of ASD. *Frontiers in Human Neuroscience* (2013). doi:10.3389/fnhum.2013.00671
7. Salussolia, C. L., Klonowska, K., Kwiatkowski, D. J. & Sahin, M. Genetic Etiologies, Diagnosis, and Treatment of Tuberous Sclerosis Complex. *Annu. Rev. Genomics Hum. Genet.* **20**, 217–240 (2019).
8. Gomez, M. R., Sampson, J. & Whittemore, V. *Tuberous Sclerosis Complex*. (Oxford University Press, 1999).
9. Van Eeghen, A. M., Black, M. E., Pulsifer, M. B., Kwiatkowski, D. J. & Thiele, E. A. Genotype and cognitive phenotype of patients with tuberous sclerosis complex. *Eur. J. Hum. Genet.* **20**, 510–515 (2012).
10. Lai, M. *et al.* Autism. *Lancet (London, England)* **383**, 1–5 (2014).
11. Jung, H., Yoon, B. C. & Holt, C. E. Axonal mRNA localization and local protein synthesis in nervous system assembly, maintenance and repair. *Nat. Rev. Neurosci.* **13**, 308–324 (2012).
12. Lamb, R. F. *et al.* The TSC1 tumour suppressor hamartin regulates cell adhesion through ERM proteins and the GTPase Rho. *Nat. Cell Biol.* **2**, 281–287 (2000).
13. Astrinidis, A. *et al.* Tuberin, the tuberous sclerosis complex 2 tumor suppressor gene product, regulates Rho activation, cell adhesion and migration. *Oncogene* **21**, 8470–8476 (2002).
14. Goncharova, E. A., James, M. L., Kudryashova, T. V., Goncharov, D. A. & Krymskaya, V. P. Tumor suppressors TSC1 and TSC2 differentially modulate actin cytoskeleton and motility of mouse embryonic fibroblasts. *PLoS One* **9**, 1–10 (2014).
15. Goncharova, E., Goncharov, D., Noonan, D. & Krymskaya, V. P. TSC2 modulates actin cytoskeleton and focal adhesion through TSC1-binding domain and the

Rac1 GTPase. *J. Cell Biol.* **167**, 1171–1182 (2004).

16. Nie, D. *et al.* Tsc2-Rheb signaling regulates EphA-mediated axon guidance. *Nat. Neurosci.* **13**, 163–172 (2010).

17. Knox, S. *et al.* Mechanisms of TSC-mediated Control of Synapse Assembly and Axon Guidance. *PLoS One* **2**, e375 (2007).

18. Widjaja, E. *et al.* Diffusion tensor imaging identifies changes in normal-appearing white matter within the epileptogenic zone in tuberous sclerosis complex. *Epilepsy Res.* **89**, 246–53 (2010).

19. Baumer, F. M. *et al.* Longitudinal changes in diffusion properties in white matter pathways of children with tuberous sclerosis complex. *Pediatr. Neurol.* **52**, 615–623 (2015).

20. Im, K. *et al.* Altered Structural Brain Networks in Tuberous Sclerosis Complex. *Cereb. Cortex* **26**, 2046–2058 (2016).

21. Fiesel, F. C., Schurr, C., Weber, S. S. & Kahle, P. J. TDP-43 knockdown impairs neurite outgrowth dependent on its target histone deacetylase 6. *Mol. Neurodegener.* **6**, (2011).

22. Valenzuela-Fernández, A., Cabrero, J. R., Serrador, J. M. & Sánchez-Madrid, F. HDAC6: a key regulator of cytoskeleton, cell migration and cell-cell interactions. *Trends in Cell Biology* **18**, 291–297 (2008).

23. Iaconelli, J., Xuan, L. & Karmacharya, R. HDAC6 modulates signaling pathways relevant to synaptic biology and neuronal differentiation in human stem cell-derived neurons. *International Journal of Molecular Sciences* **20**, (2019).

24. Iaconelli, J. *et al.* Lysine Deacetylation by HDAC6 Regulates the Kinase Activity of AKT in Human Neural Progenitor Cells. *ACS Chem. Biol.* **12**, 2139–2148 (2017).

25. Zhang, X. *et al.* HDAC6 Modulates Cell Motility by Altering the Acetylation Level of Cortactin. *Mol. Cell* **27**, 197–213 (2007).

26. Kalinski, A. L. *et al.* Deacetylation of Miro1 by HDAC6 blocks mitochondrial transport and mediates axon growth inhibition. *J. Cell Biol.* **218**, 1871–1890 (2019).

27. Quintá, H. R., Maschi, D., Gomez-Sanchez, C., Piwien-Pilipuk, G. & Galigniana, M. D. Subcellular rearrangement of hsp90-binding immunophilins accompanies neuronal differentiation and neurite outgrowth. *J. Neurochem.* **115**, 716–734 (2010).

28. Basu, T. *et al.* Histone deacetylase inhibitors restore normal hippocampal synaptic plasticity and seizure threshold in a mouse model of Tuberous Sclerosis Complex. *Sci. Rep.* **9**, 1–11 (2019).

29. Doers, M. E. *et al.* iPSC-Derived Forebrain Neurons from FXS Individuals Show Defects in Initial Neurite Outgrowth. *Stem Cells Dev.* (2014).

doi:10.1089/scd.2014.0030

30. Santiago-Medina, M., Myers, J. P. & Gomez, T. M. Imaging Adhesion and Signaling Dynamics in Xenopus laevis Growth Cones. *Dev. Neurobiol.* 585–599 (2011). doi:10.1002/dneu.20886

31. Longair, M. H., Baker, D. A. & Armstrong, J. D. Simple Neurite Tracer: open source software for reconstruction, visualization and analysis of neuronal processes. *Bioinformatics* **27**, 2453–4 (2011).

32. Schindelin, J. *et al.* Fiji: An open-source platform for biological-image analysis. *Nature Methods* **9**, 676–682 (2012).

33. Schneider, C. A., Rasband, W. S. & Eliceiri, K. W. NIH Image to ImageJ: 25 years of image analysis. *Nature Methods* **9**, 671–675 (2012).

34. Rueden, C. T. *et al.* ImageJ2: ImageJ for the next generation of scientific image data. *BMC Bioinformatics* **18**, (2017).

35. Li, K. The image stabilizer plugin for ImageJ. Available at: http://www.cs.cmu.edu/~kangli/code/Image_Stabilizer.html.

36. Zhang, Y., Vanoli, F., LaRocque, J. R., Krawczyk, P. M. & Jasin, M. Biallelic targeting of expressed genes in mouse embryonic stem cells using the Cas9 system. *Methods* **69**, 171–178 (2014).

37. Ferreira, T. A. *et al.* Neuronal morphometry directly from bitmap images. *Nature Methods* **11**, 982–984 (2014).

38. Zhang, S. C., Wernig, M., Duncan, I. D., Brüstle, O. & Thomson, J. A. In vitro differentiation of transplantable neural precursors from human embryonic stem cells. *Nat. Biotechnol.* **19**, 1129–1133 (2001).

39. Yuan, F. *et al.* Efficient generation of region-specific forebrain neurons from human pluripotent stem cells under highly defined condition. *Sci. Rep.* **5**, 1–11 (2015).

40. Cho, Y. & Cavalli, V. HDAC signaling in neuronal development and axon regeneration. *Current Opinion in Neurobiology* **27**, 118–126 (2014).

41. Tapia, M., Wandosell, F. & Garrido, J. J. Impaired Function of HDAC6 Slows Down Axonal Growth and Interferes with Axon Initial Segment Development. *PLoS One* **5**, e12908 (2010).

42. Gaub, P. *et al.* HDAC inhibition promotes neuronal outgrowth and counteracts growth cone collapse through CBP/p300 and P/CAF-dependent p53 acetylation. *Cell Death Differ.* **17**, 1392–1408 (2010).

43. Janke, C. & Montagnac, G. Causes and Consequences of Microtubule Acetylation. *Current Biology* **27**, R1287–R1292 (2017).

44. Alper, J. D., Decker, F., Agana, B. & Howard, J. The Motility of Axonemal Dynein Is Regulated by the Tubulin Code. *Biophys. J.* **107**, 2872–2880 (2014).

45. Reed, N. A. *et al.* Microtubule Acetylation Promotes Kinesin-1 Binding and Transport. *Curr. Biol.* **16**, 2166–2172 (2006).

46. Liu, G. & Dwyer, T. Microtubule dynamics in axon guidance. *Neuroscience Bulletin* **30**, 569–583 (2014).

47. Burnette, D. T. *et al.* Myosin II Activity Facilitates Microtubule Bundling in the Neuronal Growth Cone Neck. *Dev. Cell* **15**, 163–169 (2008).

48. Schaefer, A. W. *et al.* Coordination of Actin Filament and Microtubule Dynamics during Neurite Outgrowth. *Dev. Cell* **15**, 146–162 (2008).

49. Matsuyama, A. *et al.* In vivo destabilization of dynamic microtubules by HDAC6-mediated deacetylation. *EMBO J.* **21**, 6820–6831 (2002).

50. Sabet, O. *et al.* Ubiquitination switches EphA2 vesicular traffic from a continuous safeguard to a finite signalling mode. *Nat. Commun.* **6**, (2015).

51. Harting, K. & Knöll, B. SIRT2-mediated protein deacetylation: An emerging key regulator in brain physiology and pathology. *European Journal of Cell Biology* **89**, 262–269 (2010).

52. Conde, C. *et al.* Evidence for the involvement of Lfc and Tctex-1 in axon formation. *J. Neurosci.* **30**, 6793–6800 (2010).

53. Kubo, Y. *et al.* Shootin1-cortactin interaction mediates signal-force transduction for axon outgrowth. *J. Cell Biol.* **210**, 663–676 (2015).

54. He, Y. *et al.* Src and cortactin promote lamellipodia protrusion and filopodia formation and stability in growth cones. *Mol. Biol. Cell* **26**, 3229–3244 (2015).

55. Ebrahimi-Fakhari, D. *et al.* Impaired Mitochondrial Dynamics and Mitophagy in Neuronal Models of Tuberous Sclerosis Complex. *Cell Rep.* **17**, 1053–1070 (2016).

Figure 1: TSC2 mutant hFB neurons exhibit enhanced neurite length and reduced tubulin acetylation compared to isogenic control neurons. A. hFB neurospheres of indicated genotype after one day *in vitro* immunolabeled for acetylated-tubulin (green) and counter-stained for F-actin (magenta). Note longer axons extend from $TSC2^{+/-}$ neurospheres compared to isogenic control neurons (quantified in Ch2 Figure 2B). **B.** Inset from A, note the decreased acetylated tubulin staining at the tips of the neurites in the $TSC2^{+/-}$ neurospheres (examples at arrowheads). **C.** Average fluorescence intensity values of acetylated tubulin in all measured growth cones. **D.** hFB neuronal growth cones of indicated genotype immunolabeled for HDAC6 (green), acetylated-tubulin (red) and counter-stained for F-actin (magenta) in merge. Note increased expression of HDAC6 in the $TSC2^{+/-}$ growth cone. **E.** Average fluorescence intensity values of HDAC6 in all measured growth cones. (** $P<0.01$, # $P<0.0001$, Student's T-Test)

Figure 1

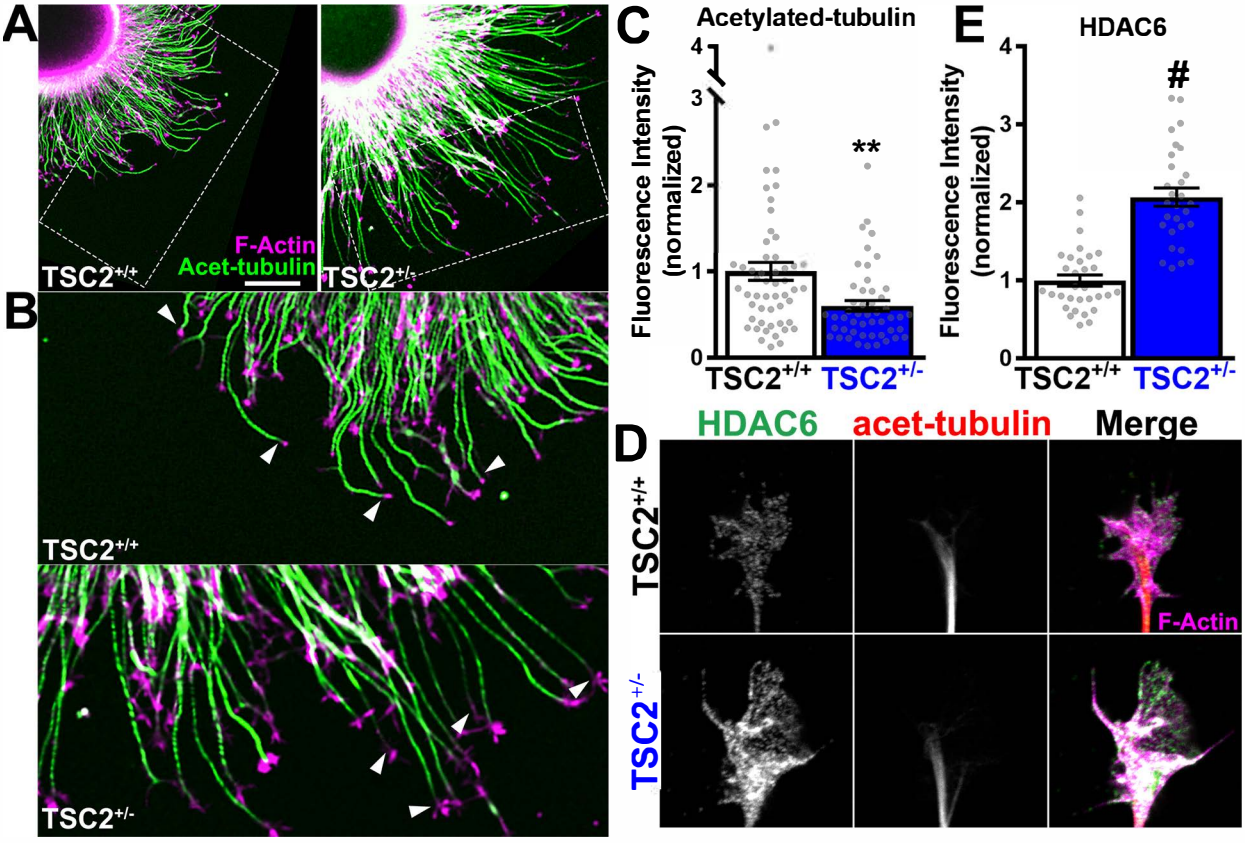
A
F-Actin
Acet-tubulin
TSC2+/+
TSC2+/-
B
TSC2+/+
TSC2+/-
C
Acetylated-tubulin
Fluorescence Intensity (normalized)
**
TSC2+/+
TSC2+/-
E
HDAC6
#
Fluorescence Intensity (normalized)
TSC2+/+
TSC2+/-
D
HDAC6
acet-tubulin
Merge
TSC2+/+
TSC2+/-
F-Actin

Figure 2: HDAC6 inhibition restores TSC2 mutant hFB neuron extension rate

A. Average axon extension rates show that $TSC2^{+/-}$ hFB neurites grew markedly faster compared to isogenic control neurons, and extension rates were slowed by incubation with TsA (1μM) or Tbn (10μM). (# $P<0.0001$, One way ANOVA w/ Tukey's Multiple Comparison)

Figure 2

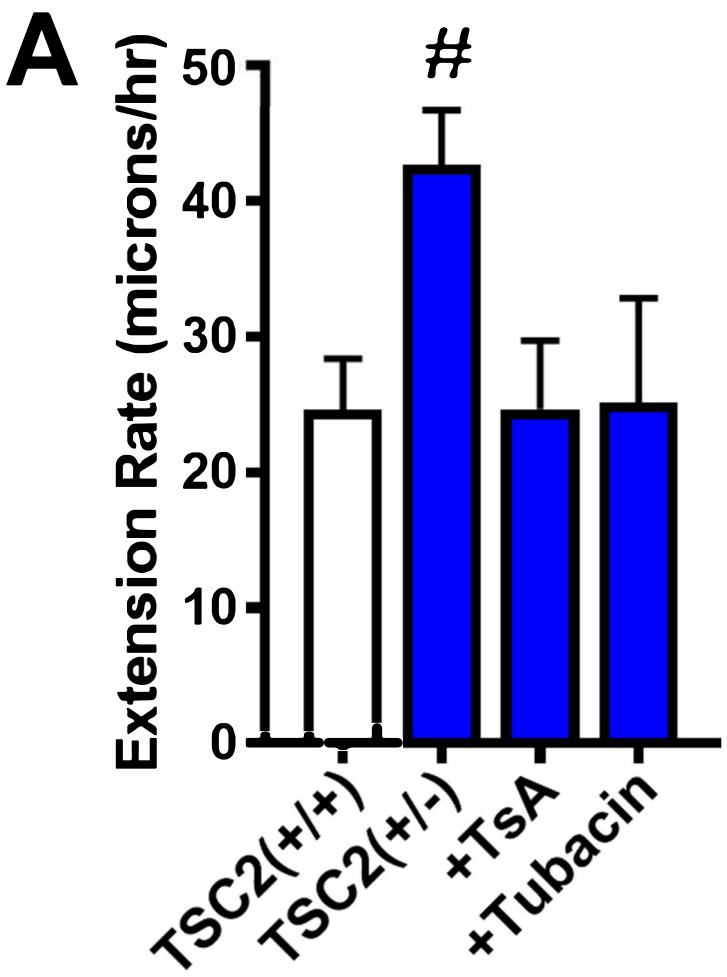
A
Extension Rate (microns/hr)
50
40
30
20
10
0
#
TSC2(+/+)
TSC2(+/-)
+TsA
+Tubacin

Figure 3: $TSC2^{+/-}$ neurite sensitivity to ephrin-A1 is enhanced by HDAC inhibition

A-B. A. In response to 2 µg/ml ephrin-A1, $TSC2^{+/+}$ neurites collapsed within 30 minutes (see Ch2 Figure 3), while $TSC2^{+/-}$ neurites resisted collapse. Pre-incubation with TsA (1µM) restored sensitivity of $TSC2^{+/-}$ neurites to ephrin. **B.** Quantification of collapse 30 minutes after ephrin-A1 exposure in $TSC2^{+/+}$ and $TSC2^{+/-}$ hFB growth cones. Note restoration of collapse in $TSC2^{+/-}$ growth cones by incubation with Tbn or TsA. (# $P<0.0001$, One way ANOVA w/ Tukey's Multiple Comparison)

Figure 3

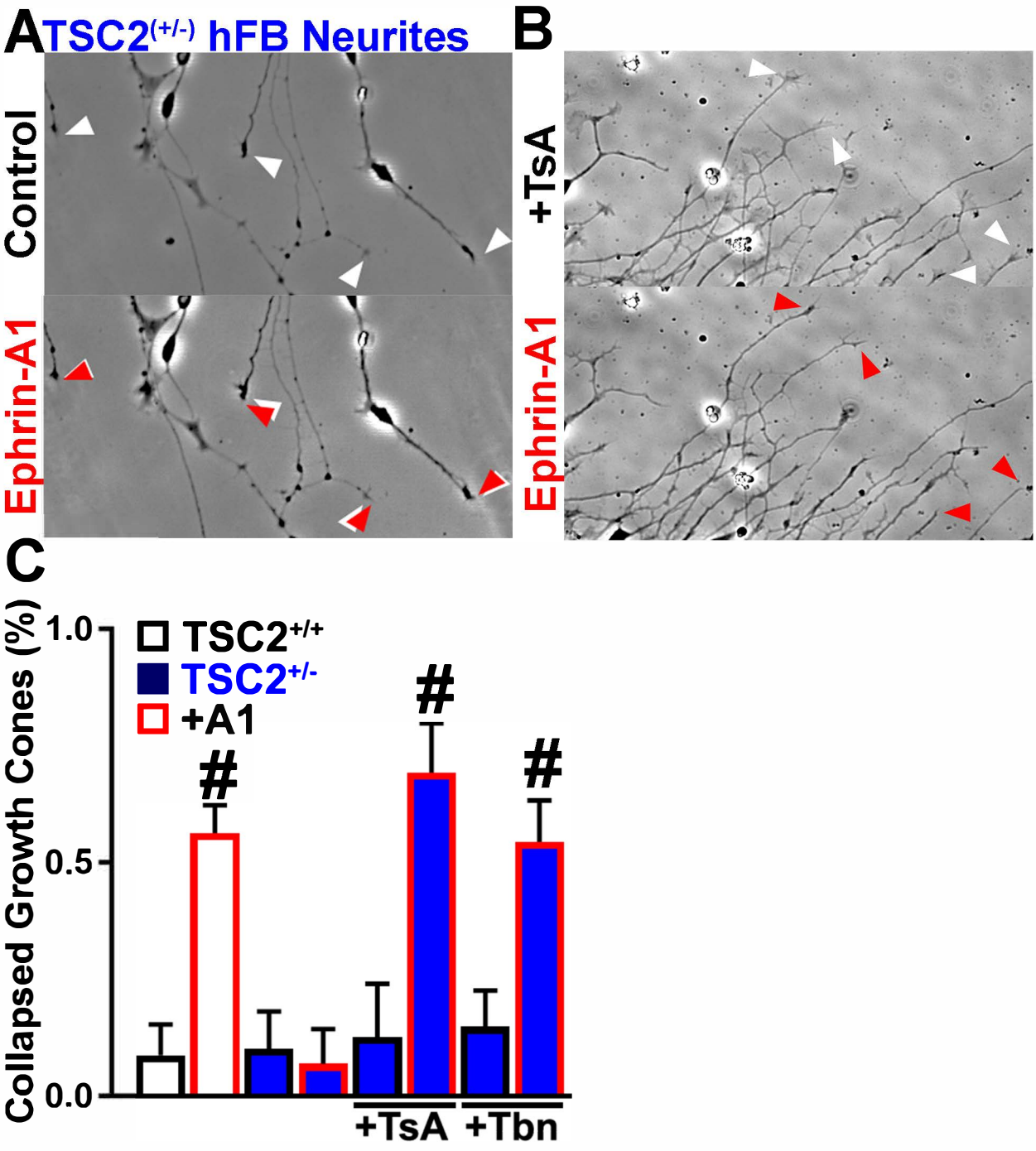
A
TSC2(+/-) hFB Neurites
Control
Ephrin-A1
B
+TsA
Ephrin-A1
C
Collapsed Growth Cones (%)
1.0
0.5
0.0
TSC2+/+
TSC2+/-
+A1
#
#
#
+TsA
+Tbn

Figure 4: HDAC inhibition restores repulsive guidance in TSC2$^{+/-}$ hFB neurons. A. hFB neurospheres were cultured for three days on parallel stripes of Fc-tagged ephrin-A1 and laminin (LN), then fixed and stained for anti-Fc (green in merges) and F-actin (magenta in merges). Many TSC2$^{+/+}$ neurites extended upon LN, parallel to the pattern, while avoiding the ephrin-A5 stripes. On the other hand, TSC2$^{+/-}$ hFB neurites showed little substratum preference, crossing ephrin-containing lanes repeatedly. **B.** Co-incubation of TSC2$^{+/-}$ neurospheres with Tbn increased their sensitivity to ephrin-A1. (** $P<0.01$, Student's T-Test)

Figure 4

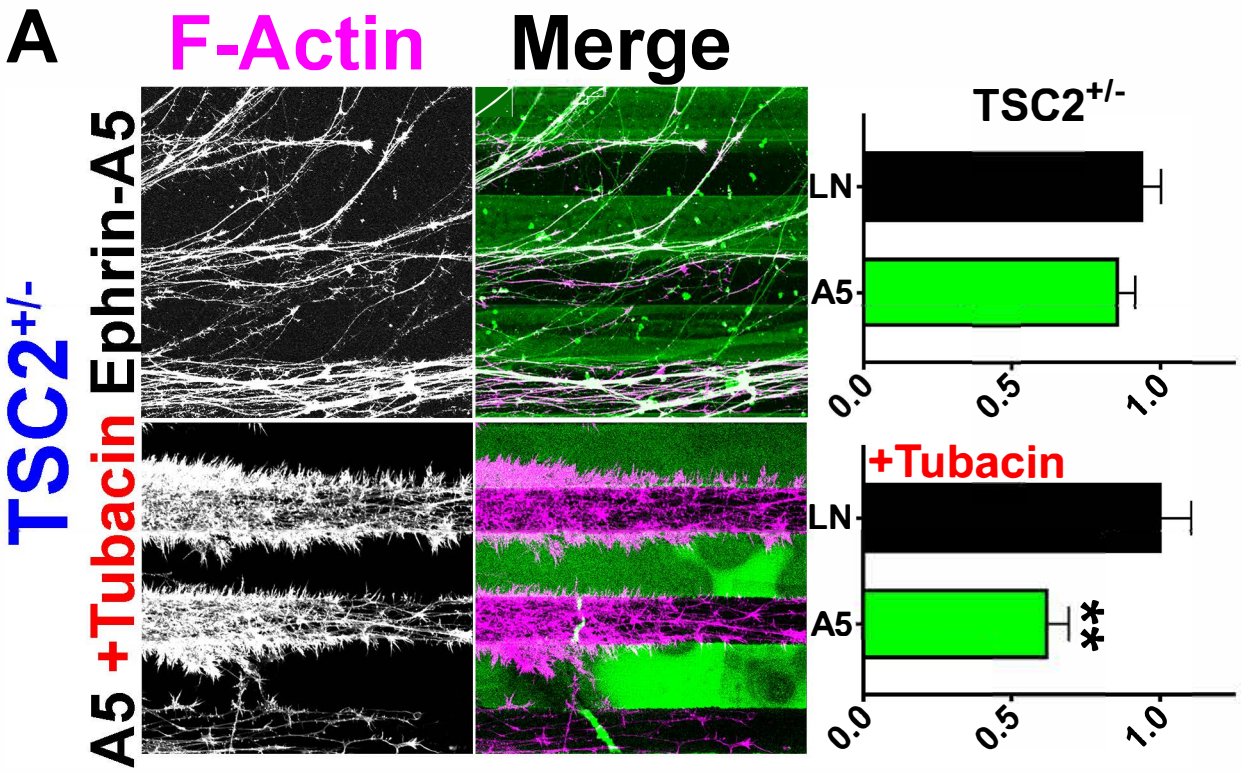
A
F-Actin
Merge
TSC2+/- Ephrin-A5
TSC2+/- A5 +Tubacin
TSC2+/-
LN
A5
0.0
0.5
1.0
+Tubacin
LN
A5
**
0.0
0.5
1.0

Supplemental Figure 1: HDAC inhibitors increase microtubule acetylation in hFB neurites. A. Acetylated tubulin normalized to total alpha tubulin within growth cones show similar decreases in the proportion of acetylation within $TSC2^{+/-}$ neurites. **B.** Neurospheres of each genotype were fixed and immunolabeled for acetylated tubulin and F-actin. Pan-inhibition of HDACs with TsA (1μM) show increases in $TSC2^{+/+}$ and $TSC2^{+/-}$ hFB growth cones. C. Quantification showing that TsA incubation or HDAC6-specific inhibition with Tbn (10μM) for 60 minutes show similar increases in tubulin acetylation. (* $P<0.05$, Student's T-Test; # $P<0.0001$, One way ANOVA w/ Tukey's Multiple Comparison)

Supplemental Figure 1

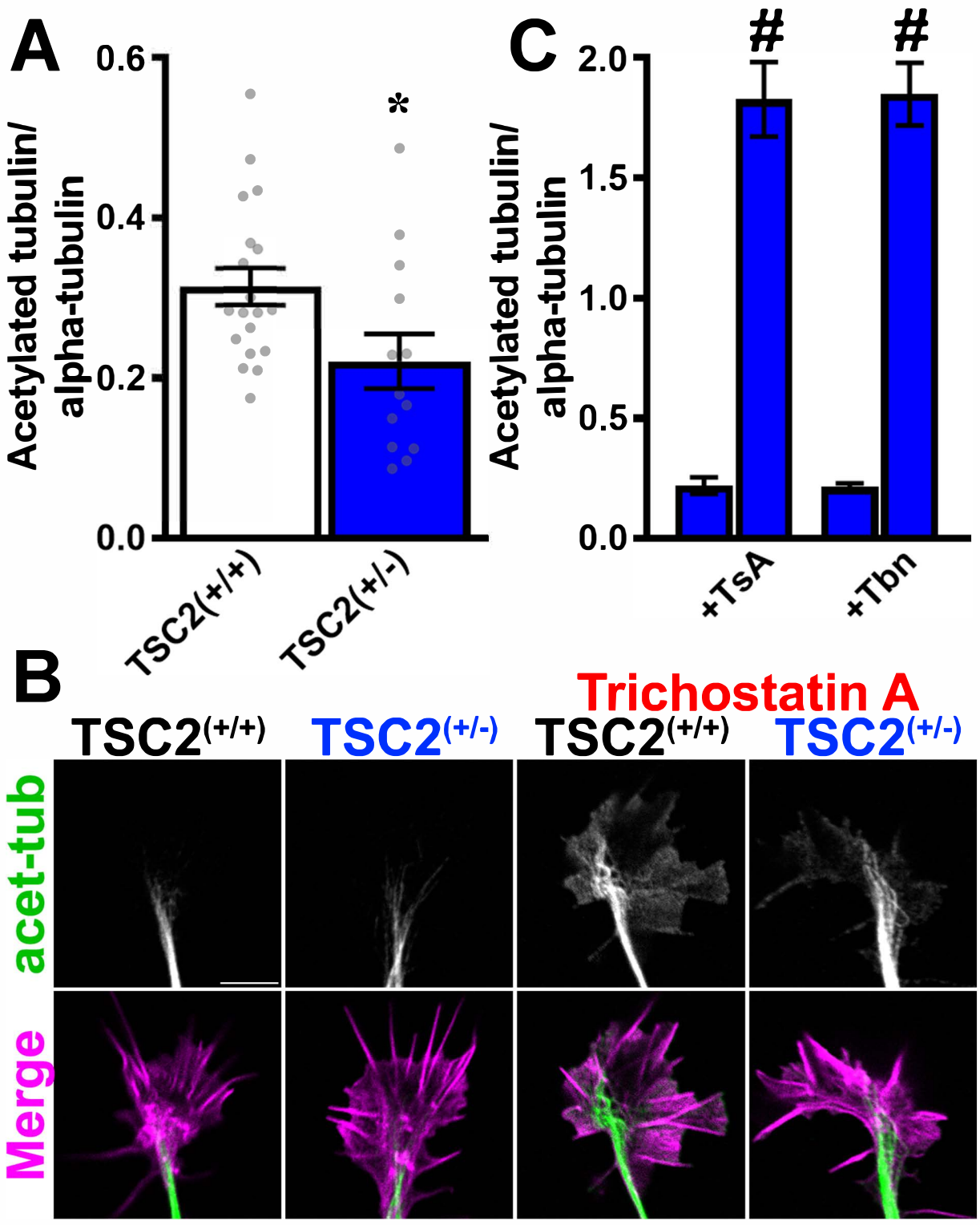

Supplemental Figure 2: Cortactin is not increased in TSC2$^{+/-}$ hFB neurons

Neurospheres of each genotype were fixed and growth cones were immunolabeled for cortactin and counterstained with F-actin. Total cortactin intensity within the growth cone was not increased in TSC2$^{+/-}$ hFB growth cones.

Supplemental Figure 2

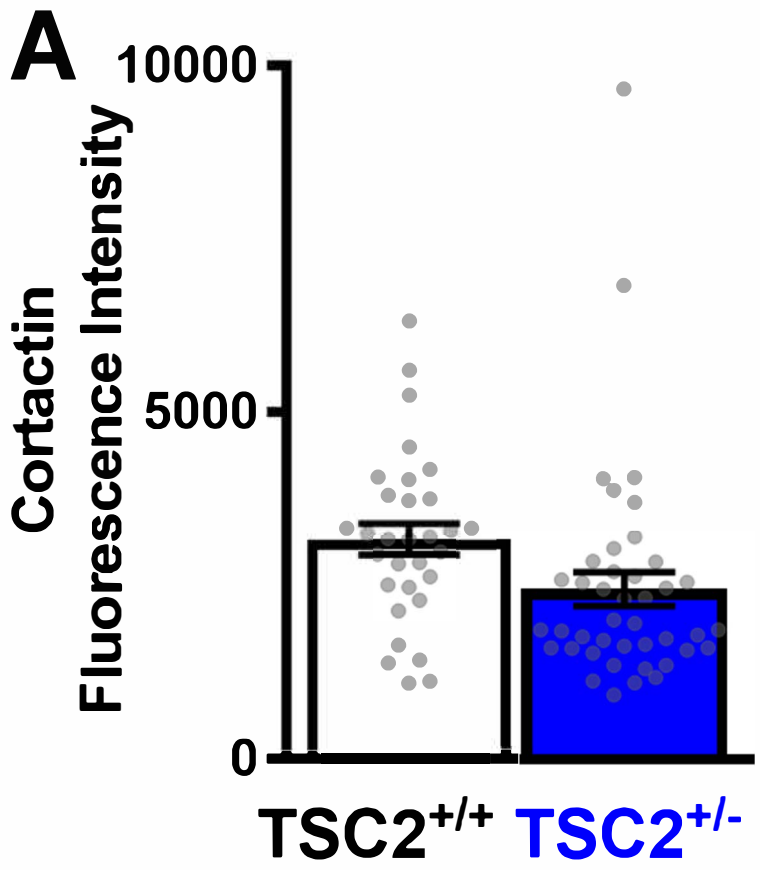

Chapter 4: Conclusions & Future Directions

Timothy Catlett designed and performed the research, analyzed the data, and wrote the chapter.

Conclusions and Future Directions

The scope of this work was two-fold. First, I wanted to establish human ES and iPS cells as a compelling in vitro model for axon guidance. Second, I wanted to test with human neurons a disease model known to intersect with axon guidance pathways to see what I could learn from stimulating those pathways with guidance cues. We hypothesized that because TSC proteins are defective in patients[1], and TSC proteins are known modulators of the mTOR pathway which controls local protein synthesis in response to cues[2], that local protein synthesis within growth cones would be aberrant and growth cones would not guide appropriately. So I hypothesized and found that cue response and guidance were perturbed in TSC2 derived neurons (Chapter 2, Figure 3-4). What I didn't expect to find was the integrity of the mTOR pathway and local protein synthesis downstream of guidance cues in the face of substantial guidance abnormalities in our heterozygous TSC2 model (Chapter 2, Figure 5). Furthermore, acute mTOR suppression failed to influence growth cone cue response to a variety of cues (Chapter 2, Figure 3, 6), suggesting that in our model, local mTOR modulation may be dispensable for axon guidance. This was also surprising because of previous reports showing a requirement for local protein synthesis in responses to netrin[3], slit2[4], and semaphorins[5,6]. A decrease in LPS has also been associated with ephrin response, which is unique amongst the canonical cues[7].

LPS in human axon guidance in vitro

There are many mechanisms which may explain the discrepancies between our in vitro experiments and some previously published reports. A few possibilities are outlined below.

1a) *LPS modulation is required for cue response, but TSC > mTOR is not necessary for this modulation.* Within WT growth cones, LPS was decreased in response to the mTOR inhibitor rapamycin, but decreased still further in response to the more potent translation inhibitor anisomycin, in agreement with previous studies and suggesting that mTOR suppression incompletely silences LPS[7]. mTOR-dependent LPS was shown to be important for Slit2-mediated collapse in one well-cited study of Xenopus retinal ganglion cells[4], and I also found that protein synthesis was transiently increased in human neurons in a rapamycin sensitive manner (Chapter 2, Figure E). However, inhibiting the Slit2-dependent LPS increase via rapamycin, or general protein synthesis inhibitors anisomycin and cycloheximide (Figure 1C) did not inhibit the WT response to Slit2, suggesting that while LPS is modulated, it is not necessary for human growth cone response in the neurons we tested. In response to ephrin bath application, LPS decreased significantly in all TSC genotypes (Chapter 2, Figure D). It cannot be ruled out that mTOR suppression is required for appropriate ephrin response, but the failure of TSC mutant growth cones to collapse in the presence of rapamycin, together with their ability to downregulate LPS in the absence of rapamycin indicates that this suppression is not sufficient. Future experiments should examine the impact of pan-synthesis inhibitors such as anisomycin on mutant TSC collapse response, although this standard experimental protocol is not without its own caveats as detailed below. Interestingly, ephrin treatment had a similar effect as rapamycin in $TSC2^{-/-}$ growth cone LPS, suggesting that whether or not LPS is modulated through mTOR in response to ephrin, it is not TSC2 dependent. This evidence also points towards a separate role for TSC2 in effecting the ephrin-dependent collapse response.

1b) *mTOR modulation is key to these phenotypes, but our assays are not sensitive enough to capture it.* Many studies of TSC > mTOR signaling utilize TSC knockout models, which are well known to cause mTOR hyperactivity[8,9]. In these models, rapamycin substantially suppresses mTOR and often corrects the phenotype of interest[10]. However, many $TSC^{+/-}$ studies do not show mTOR hyperactivation[11–13], and one study even found a decrease in global protein synthesis in a $TSC2^{+/-}$ rodent model brain[14]. Low doses of rapamycin and its derivatives tend to substantially downregulate mTOR signaling in $TSC2^{+/-}$ cells below WT levels in serum replete conditions as evidenced by p-S6 protein assays[8], which plausibly may lead to greater signaling abnormalities than TSC protein haploinsufficiency. In Tuberous Sclerosis, doses of rapamycin which have positive benefit in the few but highly impactful $TSC2^{-/-}$ cells, likely are substantially downregulating mTOR activity in the patient's $TSC2^{+/+}$ or $TSC2^{+/-}$ cells.

Another possibility is that some of our phenotypes are attributable to rapamycin-resistant mTOR activity. Work from Scott Selleck's lab showed a TSC1 knockout axon guidance abnormality that was resistant to rapamycin, but rescued by Tor deficiency[15]. Similarly, Vera Krymskaya's group showed mTOR sensitive, but rapamycin and raptor knockout insensitive migration dysfunction in TSC2-/- MEFs[16]. Kinase dead or attenuated mTOR transfection paired with TSC2 GAP mutations may resolve non-canonical mTOR input in our phenotypes. We attempted to partially control for this by using the dual inhibitor torin-1, which has been shown in some cell types to decrease mTORC1 activity more robustly than rapamycin[17], but while this inhibitor did decrease outputs of mTORC1 and mTORC2 (Chapter 2, Supplemental Figure 4), it did not

substantial impact our phenotypes (Chapter 2, Figure 2-3, 6). The dual-inhibition of torin-1 to mTORC2 upstream of cytoskeletal rearrangement may have obscured some differences. Furthermore, we performed the LPS puromycin experiments with rapamycin but did not test torin-1 for effects on LPS. mTORC2 is little studied, and rictor mutant mice show significant neurological abnormalities[18], but to our knowledge there are no other studies of mTORC2 activity in growth cones.

1c) *Off-target effects of pharmacological protein synthesis inhibition.* Cycloheximide, anisomycin, emetine, and puromycin have all been used to block LPS in axon guidance studies[5,19,20], and each of these drugs carry substantial off-target effects. I assayed the effects of anisomycin on human growth cones and found, similar to other cell studies[21,22], substantial impacts on the p38 and p44/42 MAPK pathways, which are proteins not only impacting signaling effects in general, but are also involved in the same signal transduction pathways as guidance cues, muddying the interpretation of these assays (Figure 1A-B). Some studies have used these in combination with transcriptional inhibitors such as amanitin for short term experiments to argue for lack of transcriptional regulation[23,24]; however, many transcriptional inhibitors require several hours incubation to suppress transcription, which was not generally accounted for in these studies[25]. Axotomy experiments and microfluidic isolation are preferable and standard in the field, but localized, selective, acute protein synthesis modulation has not been demonstrated. In the future, optogenetic approaches[26] such as LOV domain conjugation to S6 and putative areas of local translation (e.g. the plasma membrane on the side of the cue) or away from translation (e.g. mitochondria) at the growth cone would allow for a rigorous study of these mechanisms. Work in the

Christine Holt and James Zheng labs showed asymmetrical β-actin translation in response to cues[3,27], and targeting polyribosomes to the plasma membrane in a directional manner would test for the necessity and sufficiency of cue directed local translation more directly, and eliminate the input of off-target MAPK regulation.

2) *Neurosphere-specific effects* Neurospheres are an advantageous system for neural cell culture for several reasons. They provide an environment that is arguably more representative of the in vivo environment, in its three-dimensional arrangement full of supporting cells. It has long been appreciated that neurosphere cultures produce increased numbers of process-producing neurons of increased length[28]. Furthermore, the dissociation of tissues lead to tearing off of the processes of many growing neurons, making subsequent neurite growth more akin to a regenerative event. The accelerated growth rates make axons comparatively easy to assay, as they can grow over one millimeter in a single day (Chapter 2, Figure 2). This allows collapse assays to be performed more reliably in the following ways: 1) limits the population of growth cones to the axonal variety, 2) measures retraction without cell body interactions, 3) limits the contribution of soma signaling events in acute stimulation, and 4) permits axotomy experiments. However, there are also compromises in neurosphere culture. 3) The cellular environment of neuronal somas is not easily assayed, and some heterogeneity is to be expected between two somas in the same neurosphere. 2) Paracrine effects from surrounding cells may influence motility in unknown ways and impact comparisons between these assays and those using dissociated cells. Future conditioned media experiments can provide some insight into paracrine effects[29]. 3) A minority of neurosphere cultures yield optic vesicles, which yield different cell

populations[30]. In my work, limited assays were performed with dissociated WT neurosphere cultures to corroborate guidance results (not shown), but much remains to be done to provide comparisons to published work with dissociated cultures, including outgrowth, cell fate, and protein synthesis inhibition studies.

4) *Serum and mTOR.* Many studies of mTOR signaling in TSC knockout cells, especially fibroblasts and HEK293 cells, make use of serum free media, in which mTOR activity is suppressed and pathway activation in response to growth factors, amino acids, or guidance cues is more easily seen[31,32]. Neuronal cell culture infrequently uses serum, but standard media formulations include various amino acids in addition to N2, B27, BDNF, and other compounds known to impact mTOR signaling. Our puromycin studies show clear mTOR activation and suppression in response to various cues or mTOR-inhibitors, but it is possible that differences between our media preparations and those of other groups could contribute to differences in outcomes.

5) *Animal model and cell type.* LPS is clearly important for neuronal development. Growing axonal and dendritic growth cones are full of a variety of mRNAs and translational machinery, and many studies have shown in vitro roles for translation in classic assays of neurodevelopment[33]. Axonal LPS is still an area of intense study, yielding new insights as techniques improve. Elegant work earlier this year by Poulopoulos and colleagues used a combination of growth cone isolation and FACS-sorting of rodent pre- and post-crossing callosal projection neurons to detect compartment-specific mRNA populations[34]. To support their findings, they then used shRNA knockdown of a plexin adaptor protein downstream of semaphorins, finding a decrease in crossing projections. As noted above, slit2 is commonly cited as an LPS

dependent guidance cue, based on studies in Xenopus retinal ganglion cells, with cofilin posited as a target of LPS[4,35]. As I was not able to replicate this result in human forebrain neurons, suggesting other mechanisms may also play a role in slit2-dependent guidance in neurodevelopment. While there is undoubtedly conservation of many signaling pathways in axon guidance which have been valuable in our candidate-based approaches in human neurons, discrepancies amongst published work in the field are abundant. For example, Paul Letourneau's lab published work showing little effect of protein synthesis inhibition on chick and mouse guidance in response to netrin, semaphorin-3a, and neurotrophins[36]. Follow-up work by multiple labs suggested that semaphorin collapse may be protein synthesis dependent at low concentrations in chick DRG and mouse motor neurons[37,38], although validation of the protein synthesis-dependence of pharmacological inhibition results was not undertaken. In a rat DRG model, the Rho GTPase RHOA was reported to be locally translated downstream of semaphorin[6] in an mTOR-dependent manner, although it remains to be investigated why this mechanism is not necessary for RHOA-dependent collapse responses to other cues in our studies or others.

6) Neural cell culture is not yet a mature discipline, and work from our own lab and others have demonstrated that neuronal responses are acutely sensitive to substrates[39,40]. Cell fate is also an often overlooked aspect of in vitro assays, as in primary cells the mechanisms of isolation, dissociation and time in vitro may profoundly affect cell fates and cue response[41,42]. Embryonic and induced pluripotent stem cell differentiation is not exempt from these challenges. Regarding ES and iPS culture, currently many in the field have defaulted to WA09 (i.e. H9) ES lines because

of their superior performance in ectodermal and subsequent neuronal differentiation[43]. iPS cell differentiation is more variable by line and more troubleshooting is often involved, for reasons that are yet largely opaque[43]. RNA sequencing to identify cell populations of interest is improving replicability, but the field is yet in infancy[44]. How differentiating iPS cells into glutamatergic projection neurons positive for deep layer cortex actually mirrors a primary mouse cortical culture of a given age and time in vitro is an open question, and much work remains to be done.

What is the role of TSC in growth cones?

Given TSC's canonical role in negatively regulating mTOR, paired with limited information on homologous domains in TSC1 and TSC2, investigating other functions is challenging. TSC2 is present in growth cones and displays heterozygous haploinsufficiency (Chapter 2, Figure 1), and S6 activity and LPS within growth cones show that it is 1) is negatively regulating mTOR (Chapter 2, Figures 1, 5) and 2) this regulation does not explain guidance defects (Chapter 2, Figures 2-3, 6). Many open questions remain.

TSC2 local growth cone function

Work by Brendan Manning's group and others have demonstrated that, in HEK293 and mouse embryonic fibroblasts (MEFs), TSC2 localizes to lysosomes and interferes with mTORC1 function in an amino acid and growth factor dependent manner[45,46]. A recent report also places LPS within the sphere of mTOR-lysosomal recruitment[47]. I attempted to replicate these experiments in growth cones with B27 withdrawal experiments but failed to find significant localization of TSC2 with the lysosomal marker LAMP1 in the presence or absence of B27 supplement (not shown). Given that ribosomal protein S6

phosphorylation is decreased in these withdrawal experiments, there may be other mechanisms of mTOR activation downstream of growth factors, and lyosomal-independent mTOR activation has been reported[45,48]. Whether late endosomes/lysosomes are important scaffolds for LPS-dependent signaling in human growth cones remains to be seen.

In Chapter 2, Figures 7-8, I investigated RhoA signaling in $TSC2^{+/-}$ neurons. These proteins have been linked before, originally in Alan Hall's group[49–51], and Rho GTPase activation failures through decreases in local TSC protein are an attractive hypothesis for insensitivity in TSC-deficient cells. First, RhoA pathway activity is inversely linked to neurite extension, and $TSC2^{+/-}$ neurites exhibited markedly faster extension rates. Although $TSC2^{+/+}$ neurites extended much faster via ROCK or myosin-2 inhibition, mutant neurites were insensitive to further increases; this suggests either that the RhoA pathway was already maximally inhibited or that neurites were already travelling at maximum rates and further RhoA inhibition was inconsequential. We demonstrated via G-LISA assays that RhoA activation downstream of ephrin-A1 was defective in $TSC2^{+/-}$ neurons, and mild activation of myosin-2 via calyculinA downstream of ephrin-A1 was sufficient to restore mutant extension rates and growth cone collapse. Whether the same mechanism drives both reduced RhoA activity in the basal extension rate differences and the failure to sufficiently upregulate RhoA to effect collapse is unknown and warrants further investigation.

Further investigation of RHOA-dependent pathways

TSC2 haploinsufficiency may reduce its ability to locally regulate signaling at the growth cone in an mTOR-independent manner. In preliminary experiments, RhoA signaling is

aberrant, but more work remains to be done. Time course fluorescence resonance energy transfer (FRET) assays for RhoA activity downstream of multiple guidance cues will inform whether RhoA activation is aberrant more generally. Preliminary studies also suggest Rac1 activity may be increased in $TSC2^{+/-}$ growth cones, although whether this is upstream or downstream of RhoA is unknown. Preliminary results suggest that acute full length TSC2 transfection can rescue $TSC2^{-/-}$ mTOR activity as measured by p-S6 and neurite lengths (not shown). Future work will test exogenous fluorescent-tagged TSC2 for its ability to rescue cue response and guidance deficits, and make use of GAP-dead TSC2 and variants of TSC1-binding domains in TSC2 to determine if GAP activity is necessary upstream of Rho GTPase activity. The significant phenotypes seen in haploinsufficient-TSC2 cells makes controlling for TSC2 levels a significant concern in these studies. Indeed, preliminary studies showed that exogenous TSC significantly decreased WT neurite lengths (not shown). Accordingly, future experiments will incorporate Tet-On systems to tune TSC2 expression to doxycycline. Tagged-TSC2 permits assaying its localization within growth cones. As noted above, TSC2 is reported to inhibit mTOR at lysosomes, but this has been demonstrated in only a few cell types. Rho GTPases are active at the plasma membrane, as are other proteins linked to TSC such as the ERM proteins. Combined with conflicting reports of cytosolic mTOR activation and TSC1/2 localization, it will be informative to examine TSC1/2 activity in live growth cones to determine its locus of activity downstream of growth factors and guidance cues. The necessity of TSC protein localization to its function may be examined by optogenetic approaches to target TSC proteins to mitochondria, lysosomes, or the outer plasma membrane.

Signaling cascades and collapse phenotypes

The collapse pathway may yield clues as to the source of the growth cone dysfunction. Considering growth cone collapse as a temporal cascade of events from initial repulsive ligand-receptor interactions through to actin depolymerization and reorganization, adhesion loss, enhanced endocytosis, and increased retraction, comparing intracellular activity of known players in this cascade between genotypes may reveal where signaling is failing. To this end, we have performed experiments at several points in these pathways, determining that 1) EphA2 and EphA4 receptors are expressed at similar levels in $TSC2^{+/+}$ and $TSC2^{+/-}$ growth cones (Chapter 2, Supplemental Figure 5); 2) ephrin-EphA4 binding and internalization is similar in both groups (not shown); 3) tyrosine phosphorylation is attenuated in $TSC2^{+/-}$ growth cones at 2 minutes post-treatment (not shown); 4) LPS downstream of ephrin-A1 and other cues is similar between groups (not shown); 5) macropinocytosis, actin depolymerization, and myosin-2 activation (Chapter 2, Figure 8 and not shown) are attenuated in $TSC2^{+/-}$ growth cones. TSC2 activation is modulated via phosphorylation of unique sites downstream of Akt, ERK, GSK3β, and AMPK. Many phospho-TSC2 antibodies are reported to specifically bind TSC2 phosphorylation sites for immunofluorescence quantification. We tested three commercial phospho-antibodies and all robustly immunostained $TSC2^{-/-}$ growth cones, highlighting the importance of independently validating these antibodies. Results from TSC1 immunofluorescence assays have also been unconvincing in our hands. Future studies will make use of western blotting to attempt to confirm TSC2 activation states in response to cues.

It is also possible that chronic, rapamycin-insensitive mechanisms underlie mutant neuron phenotypes. Multiple groups have reported mild transcriptional and translational differences between WT and heterozygous TSC neurons which are only partially responsive to rapamycin. TSC2 contains DNA-binding domains and has been reported in the nucleus[52], where transcription factors are often implicated in haploinsufficiency phenotypes[53]. As noted above, rapamycin and ribosomal protein S6 phosphorylation may be too crude a readout of total mTOR activity, which may be involved in an as-yet undescribed, rapamycin-insensitive manner. Rapamycin-insensitive Rheb GTPase involvement in TSC phenotypes has been reported[54,55], often making use of farnesylation inhibitors, as this PTM is known to be important for Rheb's mTOR activity.

Tuberous Sclerosis is a complex disease with a corresponding complex etiology. Discovery that mTOR is downstream of TSC proteins fifteen years ago led to clinical trials with rapamycin analogues, which have greatly improved the quality of life for patients and their families. However, rapamycin is not a cure, and as we and others have shown, some phenotypes of TSC are still resistant to rapamycin analogue treatment, and substantial side effects remain. I hope that these modest studies inform understanding of TSC protein pathways, and that more work will lead to the design of new treatments to improve outcomes.

References

1. Van Eeghen, A. M., Black, M. E., Pulsifer, M. B., Kwiatkowski, D. J. & Thiele, E. A. Genotype and cognitive phenotype of patients with tuberous sclerosis complex. *Eur. J. Hum. Genet.* **20**, 510–515 (2012).

2. Jung, H., Yoon, B. C. & Holt, C. E. Axonal mRNA localization and local protein synthesis in nervous system assembly, maintenance and repair. *Nat. Rev. Neurosci.* **13**, 308–324 (2012).

3. Leung, K. M. *et al.* Asymmetrical β-actin mRNA translation in growth cones mediates attractive turning to netrin-1. *Nat. Neurosci.* **9**, 1247–1256 (2006).

4. Piper, M. *et al.* Signaling mechanisms underlying Slit2-induced collapse of Xenopus retinal growth cones. *Neuron* **49**, 215–228 (2006).

5. Campbell, D. S. & Holt, C. E. Chemotropic responses of retinal growth cones mediated by rapid local protein synthesis and degradation. *Neuron* **32**, 1013–1026 (2001).

6. Wu, K. Y. *et al.* Local translation of RhoA regulates growth cone collapse. *Nature* **436**, 1020–1024 (2005).

7. Nie, D. *et al.* Tsc2-Rheb signaling regulates EphA-mediated axon guidance. *Nat. Neurosci.* **13**, 163–172 (2010).

8. Kwiatkowski, D. J. A mouse model of TSC1 reveals sex-dependent lethality from liver hemangiomas, and up-regulation of p70S6 kinase activity in Tsc1 null cells. *Hum. Mol. Genet.* **11**, 525–534 (2002).

9. Goncharova, E. A. *et al.* Tuberin regulates p70 S6 kinase activation and ribosomal protein S6 phosphorylation: A role for the TSC2 tumor suppressor gene in pulmonary lymphangioleiomyomatosis (LAM). *J. Biol. Chem.* **277**, 30958–30967 (2002).

10. Ehninger, D. & Silva, A. J. Rapamycin for treating Tuberous sclerosis and Autism spectrum disorders. *Trends Mol. Med.* **17**, 78–87 (2011).

11. Costa, V. *et al.* MTORC1 Inhibition Corrects Neurodevelopmental and Synaptic Alterations in a Human Stem Cell Model of Tuberous Sclerosis. *Cell Rep.* **15**, 86–95 (2016).

12. Blair, J. D., Hockemeyer, D. & Bateup, H. S. Genetically engineered human cortical spheroid models of tuberous sclerosis. *Nat. Med.* **24**, 1568–1578 (2018).

13. Chi, O. Z. *et al.* Restoration of Normal Cerebral Oxygen Consumption with Rapamycin Treatment in a Rat Model of Autism–Tuberous Sclerosis. *NeuroMolecular Med.* **17**, 305–313 (2015).

14. Auerbach, B. D., Osterweil, E. K. & Bear, M. F. Mutations causing syndromic autism define an axis of synaptic pathophysiology. *Nature* **480**, 63–68 (2011).

15. Knox, S. *et al.* Mechanisms of TSC-mediated Control of Synapse Assembly and Axon Guidance. *PLoS One* **2**, e375 (2007).

16. Goncharova, E. A., James, M. L., Kudryashova, T. V., Goncharov, D. A. & Krymskaya, V. P. Tumor suppressors TSC1 and TSC2 differentially modulate actin cytoskeleton and motility of mouse embryonic fibroblasts. *PLoS One* **9**, 1–10 (2014).

17. Thoreen, C. C. *et al.* An ATP-competitive Mammalian Target of Rapamycin Inhibitor Reveals Rapamycin-resistant Functions. *J. Biol. Chem.* **284**, 8023–8032 (2009).

18. Carson, R. P., Fu, C., Winzenburger, P. & Ess, K. C. Deletion of Rictor in neural progenitor cells reveals contributions of mTORC2 signaling to tuberous sclerosis complex. **22**, 140–152 (2013).

19. Ming, G. L. *et al.* Adaptation in the chemotactic guidance of nerve growth cones. *Nature* **417**, 411–418 (2002).

20. Eng, H., Lund, K. & Campenot, R. B. Synthesis of ɴʟ-Tubulin , Actin , and Other Proteins in Axons of Sympathetic Neurons in Compartmented Cultures. **19**, 1–9 (1999).

21. Törocsik, B., Szeberényi, J., Töro"csik, B. & Szeberényi, J. *Anisomycin uses multiple mechanisms to stimulate mitogen-activated protein kinases and gene expression and to inhibit neuronal differentiation in PC12 phaeochromocytoma cells*. *European Journal of Neuroscience* **12**, 527–532 (2000).

22. Shifrin, V. I. & Anderson, P. Trichothecene mycotoxins trigger a ribotoxic stress response that activates c-Jun N-terminal kinase and p38 mitogen-activated protein kinase and induces apoptosis. *J. Biol. Chem.* **274**, 13985–13992 (1999).

23. Leung, L. C. *et al.* Coupling of NF-protocadherin signaling to axon guidance by cue-induced translation. *Nat. Neurosci.* **16**, 166–173 (2013).

24. Brunet, I. *et al.* The transcription factor Engrailed-2 guides retinal axons. *Nature* **438**, 94–98 (2005).

25. Bensaude, O. Inhibiting eukaryotic transcription. Which compound to choose? How to evaluate its activity? *Transcription* **2**, 103–108 (2011).

26. Van Bergeijk, P., Adrian, M., Hoogenraad, C. C. & Kapitein, L. C. Optogenetic control of organelle transport and positioning. *Nature* **518**, 111–114 (2015).

27. Yao, J., Sasaki, Y., Wen, Z., Bassell, G. J. & Zheng, J. Q. An essential role for β-actin mRNA localization and translation in Ca2+-dependent growth cone guidance.

Nat. Neurosci. **9**, 1265–1273 (2006).

28. Sen, A., Kallos, M. S. & Behie, L. A. New tissue dissociation protocol for scaled-up production of neural stem cells in suspension bioreactors. *Tissue Eng.* **10**, 904–13

29. Geranmayeh, M. H. *et al.* Paracrine neuroprotective effects of neural stem cells on glutamate-induced cortical neuronal cell excitotoxicity. *Adv. Pharm. Bull.* **5**, 515–521 (2015).

30. Meyer, J. S. *et al.* Modeling early retinal development with human embryonic and induced pluripotent stem cells. *Proc. Natl. Acad. Sci. U. S. A.* **106**, 16698–16703 (2009).

31. Huang, J., Dibble, C. C., Matsuzaki, M. & Manning, B. D. The TSC1-TSC2 Complex Is Required for Proper Activation of mTOR Complex 2. *Mol. Cell. Biol.* **28**, 4104–4115 (2008).

32. Sancak, Y. *et al.* The rag GTPases bind raptor and mediate amino acid signaling to mTORC1. *Science (80-.).* **320**, 1496–1501 (2008).

33. Jung, H., Gkogkas, C. G., Sonenberg, N. & Holt, C. E. Remote control of gene function by local translation. *Cell* **157**, 26–40 (2014).

34. Poulopoulos, A. *et al.* Subcellular transcriptomes and proteomes of developing axon projections in the cerebral cortex. *Nature* **565**, 356–360 (2019).

35. Bellon, A. *et al.* miR-182 Regulates Slit2-Mediated Axon Guidance by Modulating the Local Translation of a Specific mRNA. *Cell Rep.* **18**, (2017).

36. Roche, F. K., Marsick, B. M. & Letourneau, P. C. Protein Synthesis in Distal Axons Is Not Required for Growth Cone Responses to Guidance Cues. *J. Neurosci.* **29**, 638–652 (2009).

37. Manns, R. P. C., Cook, G. M. W., Holt, C. E. & Keynes, R. J. Differing Semaphorin 3A Concentrations Trigger Distinct Signaling Mechanisms in Growth Cone Collapse. *J. Neurosci.* **32**, 8554–8559 (2012).

38. Nédelec, S. *et al.* Concentration-Dependent Requirement for Local Protein Synthesis in Motor Neuron Subtype-Specific Response to Axon Guidance Cues. **32**, 1496–1506 (2012).

39. Gomez, T. M., Robles, E., Poo, M. & Spitzer, N. C. Filopodial Calcium Transients Promote Substrate-Dependent Growth Cone Turning. **291**, 1983–1988 (2001).

40. Kerstein, P. C., Iv, R. H. N. & Gomez, T. M. Mechanochemical regulation of growth cone motility. **9**, 1–16 (2015).

41. Machon, O., Backman, M., Krauss, S. & Kozmik, Z. The cellular fate of cortical

progenitors is not maintained in neurosphere cultures. *Mol. Cell. Neurosci.* **30**, 388–397 (2005).

42. Campbell, D. S. *et al.* Semaphorin 3A Elicits Stage-Dependent Collapse, Turning, and Branching in Xenopus Retinal Growth Cones . *J. Neurosci.* **21**, 8538–8547 (2018).

43. Bock, C. *et al.* Reference maps of human es and ips cell variation enable high-throughput characterization of pluripotent cell lines. *Cell* **144**, 439–452 (2011).

44. Griffiths, J. A., Scialdone, A. & Marioni, J. C. Using single-cell genomics to understand developmental processes and cell fate decisions. *Mol. Syst. Biol.* **14**, (2018).

45. Zhou, X. *et al.* Dynamic Visualization of mTORC1 Activity in Living Cells. *Cell Rep.* **10**, 1767–1777 (2015).

46. Demetriades, C., Plescher, M. & Teleman, A. A. Lysosomal recruitment of TSC2 is a universal response to cellular stress. *Nat. Commun.* **7**, 1–14 (2016).

47. Cioni, J. M. *et al.* Late Endosomes Act as mRNA Translation Platforms and Sustain Mitochondria in Axons. *Cell* **176**, 56-72.e15 (2019).

48. Averous, J. *et al.* Requirement for lysosomal localization of mTOR for its activation differs between leucine and other amino acids. *Cell. Signal.* **26**, 1918–1927 (2014).

49. Lamb, R. F. *et al.* The TSC1 tumour suppressor hamartin regulates cell adhesion through ERM proteins and the GTPase Rho. *Nat. Cell Biol.* **2**, 281–287 (2000).

50. Astrinidis, A. *et al.* Tuberin, the tuberous sclerosis complex 2 tumor suppressor gene product, regulates Rho activation, cell adhesion and migration. *Oncogene* **21**, 8470–8476 (2002).

51. Goncharova, E., Goncharov, D., Noonan, D. & Krymskaya, V. P. TSC2 modulates actin cytoskeleton and focal adhesion through TSC1-binding domain and the Rac1 GTPase. *J. Cell Biol.* **167**, 1171–1182 (2004).

52. Lou, D., Griffith, N. & Noonan, D. J. The tuberous sclerosis 2 gene product can localize to nuclei in a phosphorylation-dependent manner. *Mol. Cell Biol. Res. Commun.* **4**, 374–380 (2001).

53. Seidman, J. G. & Seidman, C. Transcription factor haploinsufficiency: when half a loaf is not enough. *J. Clin. Invest.* **109**, 451–455 (2002).

54. Choi, S. *et al.* Farnesylation-defective rheb increases axonal length independently of mTORC1 activity in embryonic primary neurons. *Exp. Neurobiol.* **28**, 172–182 (2019).

55. Sugiura, H. *et al.* Rheb activation disrupts spine synapse formation through accumulation of syntenin in tuberous sclerosis complex. *Nat. Commun.* **6**, (2015).

56. Alenghat, F. J. & Ingber, D. E. Mechanotransduction: all signals point to cytoskeleton, matrix, and integrins. *Science's STKE : signal transduction knowledge environment* **2002**, (2002).

Figure 1: Control growth cones collapse in response to Slit2 in a protein synthesis-independent manner, despite MAPK off-target effects C. In response to 0.2 µg/ml Slit2, $TSC2^{+/+}$ neurites collapsed within 15 minutes. Pre-incubation with anisomycin (40µM) or cycloheximide (CHX, 100µM) did not significantly impact sensitivity to Slit2. **A-B.** Quantification of immunofluorescence intensity showed marked increases in p38 (A) and p42/44 (B) activation in the presence of anisomycin. (****P<0.0001, Student's T-test (A-B) or One-Way ANOVA with Tukey's Multiple Comparison (C)

Figure 1

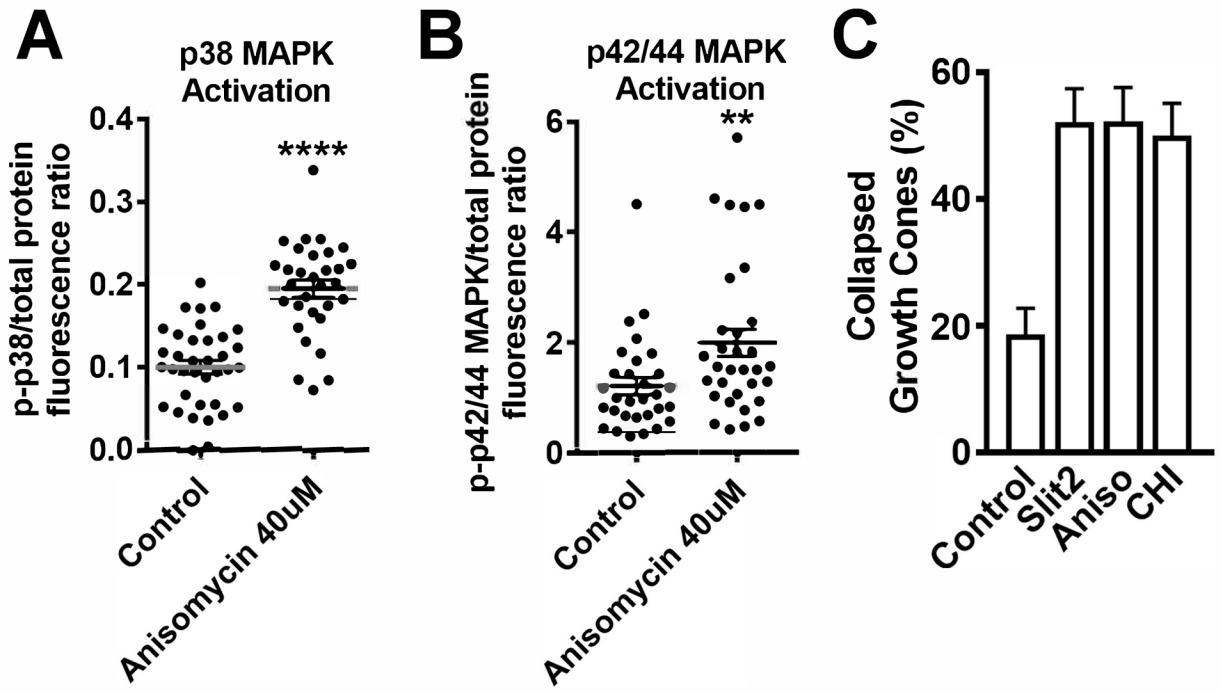
A
p38 MAPK Activation
p-p38/total protein fluorescence ratio
0.4
0.3
0.2
0.1
0.0
****
Control
Anisomycin 40uM
B
p42/44 MAPK Activation
p-p42/44 MAPK/total protein fluorescence ratio
6
4
2
0
**
Control
Anisomycin 40uM
C
Collapsed Growth Cones (%)
60
40
20
0
Control
Slit2
Aniso
CHI